# Analysis of hygrothermal simulation software and the effect of convective heat and moisture transport on hygrothermal risk assessment

van Rooijen, Daan

*Award date:*
2021

July 2021

# Analysis of hygrothermal simulation software and the effect of convective heat and moisture transport on hygrothermal risk assessment

Master thesis – 45 ECTS

Author:
D.j. van Rooijen
Student number:
1248677

*I declare that my Master's thesis has been carried out in accordance with the rules of the TU/e Code of Scientific Conduct.*

Department of the Built environment
Unit Building Physics and Services
Eindhoven University of Technology

Supervisors:
H. L. Schellen
L. C. Havinga
H. Montazeri

## Abstract

In the Netherlands, hygrothermal risk assessment is currently performed using static heat conduction simulations. While this method is designed for newly built buildings, in practice it is also used for refurbished buildings. Air transport is one of the factors that is not considered in this method of hygrothermal risk assessment which may lead to inaccurate assessment. Especially for refurbished buildings as air tightness can be harder to achieve than for newly built buildings and the air transport through leaks may lead to additional moisture transport. A literature review has been performed to assess hygrothermal simulation programs and their capabilities. The results showed that not many studies included convective air transport or 3D models in hygrothermal risk assessment. Even though the current capabilities of hygrothermal simulation programs allow for more complex risk assessment, it is not often utilized. A case study of a wooden frame wall was simulated using Delphin to assess the effect of convective moisture transport. In this wall, holes were drilled through the internal sheathing and air barrier. The simulation results could not be fully validated as there were some deviations from the laboratory results. This might have been caused by the simplification of the 2D model and/or limited material properties. This emphasizes the necessity to model air leakages in 3D in order to ensure that the results are reliable. The simulation results from this study have also been compared to a study that used COMSOL to simulate the same wall from the case study. The results were comparable, but both the simulation results from Delphin and COMSOL were not fully in line with the laboratory results. Some differences between the COMSOL and Delphin simulation could be noticed. The COMSOL study used static boundary conditions which reduced the accuracy of the results. Also, the total pressure in the construction was different comparing the COMSOL and Delphin simulations. A sensitivity analysis was performed to determine the influence of convective moisture transport and pressure differences across the structure. It was found that convection drastically improves the accuracy of hygrothermal simulation results near the air gaps. It was also found that small pressure differences can have a large impact on the absolute humidity in the structure and a gradual increase of pressure over the structure has a decreasing effect on the convective moisture transport the further it increases.

# Table of contents

## Notations

| Symbol | Description | Unit |
|---|---|---|
| ρ | Density | [ kg/m$^3$ ] |
| υ | Specific internal energy | [ J/kg ] |
| h | Specific enthalpy | [ J/kg ] |
| λ | Thermal conductivity | [ W/mK ] |
| T | Temperature | [ K ] |
| θ | Porosity / volume fraction | [ - ] |
| K | Permeability of pas / conductivity of liquid | [ kg/(msPa) ] |
| p | Pressure | [ Pa ] |
| g | Gravity | [ m/s$^2$ ] |
| R | Gas constant | [ J/kgK ] |
| $D_{v;air}$ | Vapor diffusivity in free air | [ m$^2$/s ] |
| μ | Water vapor diffusion resistance | [ - ] |
| $d_a$ | Damping or mass coefficient | [ s$^2$/m$^2$ ] |
| c | Diffusion coefficient | [ - ] |
| β | Convection coefficient | [ 1/m ] |
| C | Specific heat capacity | [ J/kgK ] |
| w | Water content | [ kg/m$^3$ ] |
| RH | Relative humidity | [ % ] |
| δ | Water vapor diffusion coefficient | [ kg/msPa ] |
| v | Vapor content of air | [ kg/m$^3$ ] |
| M | Molar mass | [ kg/mol ] |
| k | Permeability | [ m$^2$ ] |
| μ | Dynamic viscosity | [ Pa s ] |
| F | Volume force | [ kg/(m$^2$s$^2$) ] |

## Terminology

| Terminology | Abbreviation | Explanation |
|---|---|---|
| Heat air and moisture | HAM | Used to describe all the factors for hygrothermal assessment |
| Dimension | 1D/2D/3D | Amount of geometric axis used in a model |
| Volatile organic compounds | VOC | Organic chemicals responsible for scents and pollution in water or air |
| Hygrothermal | | Combination of moisture and temperature physics |
| Convection (forced / natural) | | The forced flow of a liquid or gas caused by an external cause / Flow of a liquid or gas caused by a difference in density |
| Diffusion | | The effect that causes gas molecules to move to create an equilibrium between different concentrations |
| Capillary transport | | The transport of moisture within small pores due to surface tension forces |
| Static | | Conditions remain the same over time |
| Dynamic | | Conditions continuously change over time |
| Moisture buffering | | The occurrence of moisture storage in objects which reduces the overall moisture load in a room |
| Air barrier | | A small layer at the internal side of the wall with the function to prevent air flow through the structure |
| Darcy's law | | An equation to describe a flow through porous materials |
| Permeability | | Determines the capacity of a material to let gas or liquid flow through it |
| Internal under pressure | | State where the pressure inside of the building is less than the outdoor pressure which forces an air flow from the outside to the inside |
| Internal over pressure | | State where the pressure inside of the building is higher than the outdoor pressure which forces an air flow from the inside to the outside |
| No pressure | | State where the pressure inside of the building is equal to the outdoor pressure |

# I: Introduction

## I – I Background information

An important objective in the Netherlands is to refurbish dwellings on a large scale. Especially with refurbishments hygrothermal risks should be assessed. If one does not account for moisture, retrofitting might affect building components and cause mold growth which can be harmful to the occupants' health and the durability of the construction. In the Netherlands hygrothermal risks are regulated in the Dutch Building Decree [46]. One of these regulations is the temperature ratio. This is a ratio for the relation between the indoor and outdoor air temperature and the minimum indoor surface temperature. The general consensus is that when this minimum ratio is satisfied, the hygrothermal risk caused by thermal bridges is accounted for. The Standard NEN 2778 [47] describes how the temperature ratio should be calculated. For this calculation a steady state heat conduction model is used. Depending on the complexity of the component either 1D, 2D or 3D geometry can be used. All the materials in the geometry are modelled using the respective thermal conductivities and dimensions. At the end the minimum indoor surface temperature is calculated and this is used to assess the hygrothermal risk. As this method only considers conductive heat transport internal condensation and air tightness are not considered. In order to assess the consequences of these aspects additional tests are needed.

## I - II Problem

The current assessment of hygrothermal risks is generally aimed at newly built buildings. The regulation for refurbishments is less strict and often lower temperature ratios are also accepted. Furthermore, some aspects which affect hygrothermal performance are not considered in this hygrothermal risk assessment. Air-tightness and internal condensation are two factors that should be included in a general hygrothermal risk assessment. Currently, these factors are assessed separately which may lead to inaccurate assessment. Especially for refurbished buildings as air tightness can be harder to achieve than for newly built buildings and may lead to additional moisture transport. The effect of convective air transport on hygrothermal risk assessment is also not clear. This raises the question of whether or not the current method of hygrothermal risk assessment is sufficient for refurbished buildings when only steady state heat conduction is assessed. Even though there are a lot of different hygrothermal simulation programs available, they are not often used and it can be difficult to decide which one should be used.

## I - III Research questions

Main question

Can hygrothermal risks be accurately assessed using dynamic heat and moisture (HAM) transfer models which include a dynamic indoor climate and convective HAM transport?

Sub Questions

- What heat and moisture transfer software is currently used in literature for hygrothermal risk assessment and what are the capabilities of these programs?
- Which of the currently available dynamic HAM transfer software is suited to accurately evaluate hygrothermal risks of refurbished buildings?
- Can a hygrothermal risk be accurately simulated using a HAM transfer model with a dynamic indoor climate and convective HAM transport?
- What is the difference in accuracy when convective moisture transport is considered compared to a simulation without air transport?

# II: Methodology

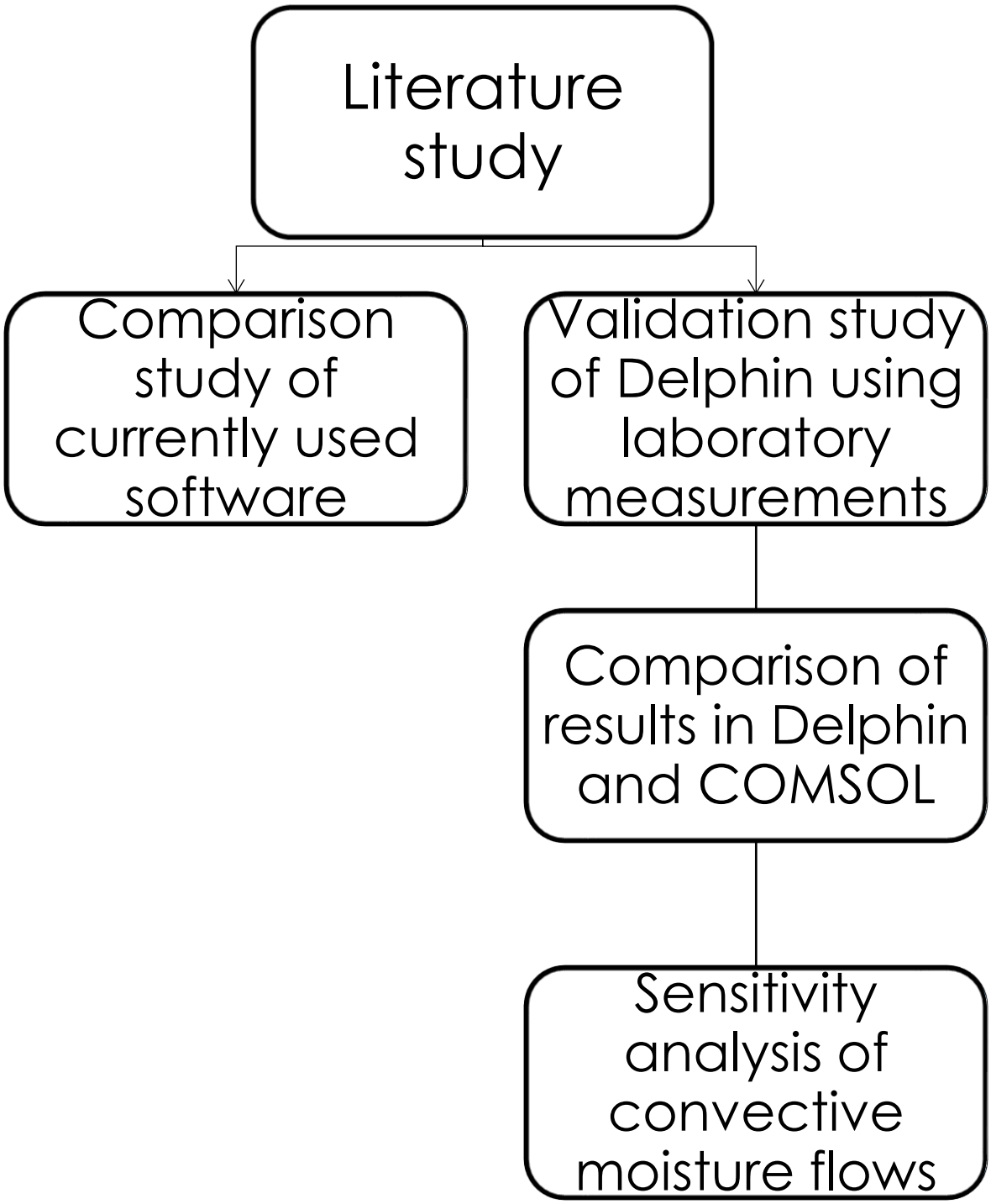

# III: Literature study

## III – I Search strategy

A literature study has been carried out to find hygrothermal software that is currently used in studies to examine hygrothermal risks. The database that was used in this literature study is ScienceDirect. The search combinations that were used can be found in Table 1. All of the 6 combinations were searched for in the database. Category 2 shows the search words dynamic and convection. These two search words are used as the current hygrothermal risk assessment is based on static heat conduction simulation, and the aim of the literature study is to find more advanced software which include dynamic and convective HAM transport.

| Category 1 | Category 2 | Category 3 |
|---|---|---|
| Hygrothermal | Dynamic | Refurbish |
| | Convection | Retrofit |
| | | Renovation |

*Table 1 Search combinations*

In addition to these search combinations some exclusion criteria were used. The goal of this literature review is to assess heat transfer software that can be used for the current hygrothermal assessment of refurbished buildings. Only studies after 2010 are used as studies before this time are far less likely to have used advanced HAM transfer software. Books were excluded as the aim is to find recent studies which used advanced software. Only studies published in English were used.

## III – II Data extraction

In Table 2 the results of the literature search are shown. In the data extraction only studies which included heat and moisture transport were examined. Also studies which performed hygrothermal risk assessment with a method other than simulation were excluded.

| Database | Unique hits | Usable hits |
|---|---|---|
| ScienceDirect | 359 | 45 |

*Table 2 Database hits*

## III – III Assessment criteria

For this literature study certain criteria are chosen to assess the used software in the literature. The following criteria were assessed:

- Included heat transfer methods
- Included moisture transfer methods
- Dimension of the model
- Moisture buffering in rooms
- Coupling with a whole building model
- Moisture analysis
- Method of risk assessment

## III – IV Results

The results from the literature review are presented below. First of all, the results for the HAM transfer methods that were used in each of the studies are shown in Table 3. Table 4 and 5 show the used HAM transfer methods that were used for every study. Furthermore, Table 6 shows the used dimensions in combination with the different simulation software. Finally, Table 7 shows the methods of hygrothermal risk assessment in each of the studies. The entire overview of the literature search can be found in Appendix 1.

| HAM transfer software | Number of studies | Articles |
|---|---|---|
| WUFI plus | 3 | [1] [26] [45] |
| WUFI pro | 13 | [2] [10] [11] [13] [17] [20] [21] [24] [28] [31] [33] [35] [38] |
| WUFI 2D | 5 | [4] [9] [13] [30] [34] |
| COMSOL | 9 | [3] [9] [16] [27] [30] [34] [39] [40] [43] |
| Delphin (version not specified) | 7 | [14] [19] [23] [29] [37] [42] [44] |
| Delphin 5 | 2 | [8] [32] |
| Delphin 5.8 | 7 | [5] [6] [12] [18] [25] [36] [41] |
| Delphin 6 | 1 | [15] |
| Bsim | 1 | [7] |
| HAM4D_VIE | 1 | [22] |

*Table 3 Used HAM transfer software*

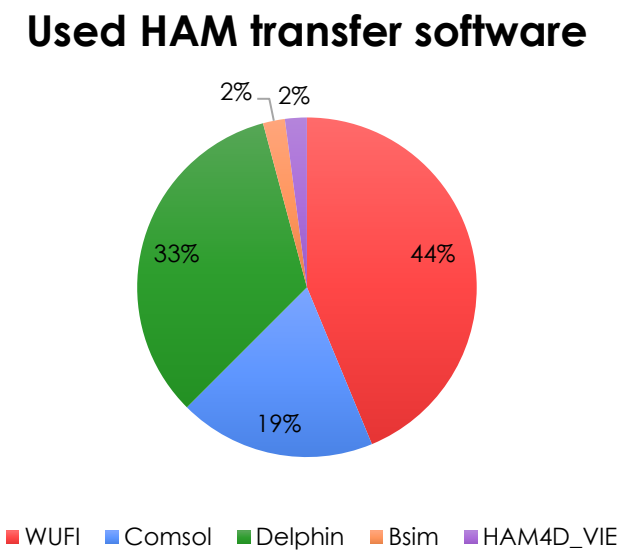


*Figure 1 HAM transfer software pie chart*

**Heat transfer method**

| Hygrothermal software | | Conduction | Convection | Radiation |
|---|---|---|---|---|
| | **WUFI** | *13* | *-* | *6* |
| | **COMSOL** | *5* | *4* | *3* |
| | **Delphin** | *17* | *2* | *3* |
| | **Bsim** | *-* | *-* | *-* |
| | **HAM4D_VIE** | *-* | *-* | *1* |

*Table 4 Heat transfer methods of examined studies*

**Moisture transfer method**

| Hygrothermal software | | Convection | Diffusion | Capillary | Driving rain |
|---|---|---|---|---|---|
| | **WUFI** | *-* | *14* | *3* | *10* |
| | **COMSOL** | *4* | *4* | *4* | *3* |
| | **Delphin** | *2* | *16* | *8* | *10* |
| | **Bsim** | *-* | *1* | *-* | *-* |
| | **HAM4D_VIE** | *1* | *-* | *-* | *-* |

*Table 5 Moisture transfer methods of examined studies*

**Dimension**

| Hygrothermal software | | 1D | 2D | 3D |
|---|---|---|---|---|
| | **WUFI** | *15* | *6* | *-* |
| | **COMSOL** | *3* | *2* | *3* |
| | **Delphin** | *10* | *9* | *1* |
| | **Bsim** | *1* | *-* | *-* |
| | **HAM4D_VIE** | *-* | *-* | *1* |

*Table 6 Model dimension of examined studies*

| Method of risk assessment | Number of studies | Articles |
|---|---|---|
| Mold growth model | 7 | [1] [3] [4] [11] [13] [14] [20] |
| Occurrence of condensation | 5 | [2] [3] [6] [17] [20] |
| Based on relative humidity and temperature (mold index) | 22 | [7] [15] [18] [19] [20] [21] [22] [24] [25] [26] [27] [29] [31] [32] [33] [34] [35] [38] [39] [41] [42] [44] |
| Occurrence of moisture accumulation | 5 | [9] [10] [24] [28] [36] |
| Freeze-thaw assessment | 4 | [12] [14] [30] [44] |
| Time of Wetness | 1 | [13] |
| Corrosion propagation model | 1 | [23] |
| Not reported in study | 7 | [5] [8] [16] [37] [40] [43] [45] |

*Table 7 Risk assessment considered in the studies*

## III – V Interesting findings literature review

From the 45 studies examined in the literature review, almost all performed hygrothermal risk assessments using Delphin, COMSOL or WUFI. Only two of the studies used different software. BSim and HAM4D_VIE. The study using BSim only simulated dynamic diffusive moisture transport for a one-dimensional whole building model [7]. HAM4D_VIE was used to simulate static convective moisture transport for a three-dimensional model [22]. The capabilities of this software cannot be determined from the literature review as these are only represented in a single article.

The other found software were COMSOL (19%), Delphin (33%) and WUFI (44%). For WUFI three different versions were found. These are WUFI plus, WUFI pro and WUFI 2D. WUFI pro and WUFI 2D are used for the simulation of building components either one- or two-dimensional. With WUFI 2D allowing for more complex simulation compared to WUFI pro. WUFI plus is designed for the simulation of whole buildings considering one-dimensional transport. [48]

The used HAM transfer methods of each study give an indication of the capabilities of the software. As mentioned before the BSim and HAM4D_VIE capabilities are not representative as they were both only used in one study. COMSOL, Delphin and WUFI all had studies that included heat conduction, heat radiation, moisture diffusion, capillary moisture transport and driving rain. This indicates that all of the models should be able to simulate these HAM transfer methods. Convective heat and moisture transport was only included in 6 out of the 45 studies. Four of these studies used COMSOL and two of these studies used Delphin. Out of the two studies which used Delphin one of them simulated convective HAM transport with an additional zone model.

The literature review also shows which dimensions are commonly used with the software. Most studies used either a one-dimensional or a two-dimensional model. Only 5 out of the 45 studies examined a three-dimensional model. None of the studies which used WUFI

examined a three-dimensional model. Most studies which examined three-dimensional models used COMSOL. One study noted an extension for Delphin 5.8 which can simulate three-dimensional models, but the HAM transfer capabilities are not reported. [6]

Some articles of the literature review used whole building simulation coupling. These studies used the output of whole building simulations as the boundary conditions for hygrothermal risk assessments of construction elements. WUFI plus and BSim already include whole building simulation with one-dimensional hygrothermal component assessment. Some of the other studies used a second model to perform whole building simulation. In two studies HAMBase was used in addition to a simulation in COMSOL. [3] [43] HAMBase is a multi-zone model built in Matlab used to simulate heat air and moisture transport in multiple zones of a building. Another whole building model that was used in combination with COMSOL is TRNSYS. This is a whole building simulation program often used to simulate transient systems [56]. Only one study used Delphin with numerical calculations to simulate the whole building [5].

All of the studies found in the literature review assessed hygrothermal risks. The method that each study used was also examined in the literature study. 22 out of 45 studies based their hygrothermal risk assessment on the found humidities and temperatures, some of these studies also used a scale to determine mold growth based on humidity and temperature (mold index). 11 out of the 45 studies used a mold growth model. The other studies used methods like the occurrence of condensation, moisture accumulation, freeze thaw assessment, time of wetness criteria or a corrosion propagation model.

## III – VI Conclusion literature review

The literature review showed that not many studies include convective moisture transport and/or simulated 3 dimensional models. Furthermore, a limited amount of studies coupled whole building simulation and hygrothermal risk assessment of construction elements. The current capabilities of hygrothermal software allow for more complex risk assessment, but this is not often utilized.

# IV: Validation study

The simulations in Delphin are validated using the measurements from a laboratory study. This laboratory study was performed at the Tampere University in Finland by Juha Vinha and Pasi Käkelä. In the study water vapor transmission was examined in different wall structures considering diffusion and convection. [53] A total of eight wall structures were tested in three pressure situations. The test started with an under pressure period followed by a period of no pressure difference and the test ended with a period of overpressure. All of the examined walls were timber frame wall structures with external wooden cladding and a vapor barrier. Holes were drilled in three of the eight wall structures to examine the effect of leaks in the external sheathing and vapor barriers. To examine the test wall structures a climate chamber was built. In the climate chamber the indoor and outdoor air were controlled and the test element was placed in the middle. Sensors were applied in the test element as well as in the warm and cold chambers. Figure 2 shows the test arrangement used in the study.

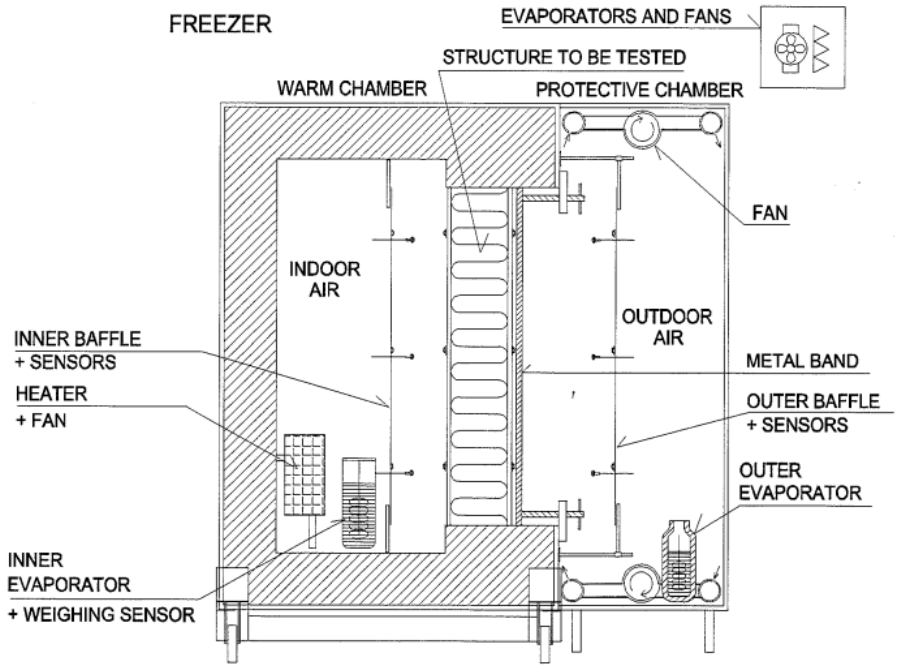


*Figure 2 Test arrangement for the test on wall structures in the building physical test equipment. Copied from Water vapour transmission in wall structures due to diffusion and convection. Publication 103 structural engineering. Vinha, J, Käkelä, P (1999). p. 42*

## IV – I Measurements and conditions

The test wall that is used to validate the simulations in Delphin is test wall 8 from the laboratory study. This test wall was chosen as it was set up to have the most permeable properties. To further increase the permeability holes were drilled through the internal sheathing and vapor barrier. As this setup is very permeable, the effect of convective moisture transport should be noticeable and can therefore be used to validate the simulation of convective moisture transport. In Figure 3 the structure of test wall 8 is shown. The specific boundary conditions used in the laboratory study are noted in Table 8 with the respective test period durations.

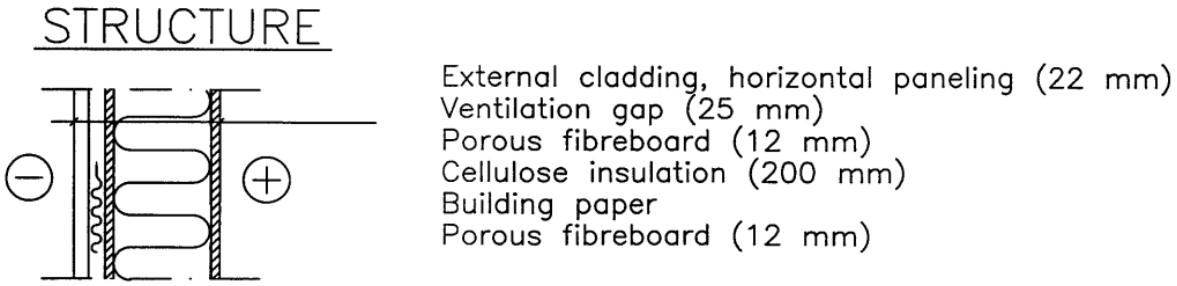


*Figure 3 Structure of test wall 8 Copied from Water vapour transmission in wall structures due to diffusion and convection. Publication 103 structural engineering. Vinha, J, Käkelä, P (1999) p. 101*

| **Test boundary conditions** | | | |
|---|---|---|---|
| Test period | Under pressure | No pressure | Overpressure |
| Duration | 297.3 h | 256.8 h | 231.8 h |
| Indoor temperature | 20 °C | 20 °C | 20 °C |
| Outdoor temperature | -10 °C | -10 °C | -10 °C |
| Indoor relative humidty | 50 % | 50 % | 50 % |
| Outdoor relative humidity | 90 % | 90 % | 90 % |
| Pressure difference | -10 Pa | 0 Pa | 10 Pa |

*Table 8 Laboratory test boundary conditions*

The test arrangement allowed for a variety of measurements. In Figure 4 positioning of some sensors in the test wall is shown. The following variables were measured in the study:

- Temperature [ °C ] – Indoor, outdoor and some surface temperatures
- Relative humidity [ % ] – Indoor, outdoor and in the porous structure
- Differential pressure across different parts of the structure [ Pa ]
- Humidity by volume [ $g/m^3$ ]
- Velocity of air flow [ m/s ] – Indoor, outdoor and in ventilation gap
- Air flow rate [ l/min ]
- Moisture flow rate [ g/day ]
- Heat flow rate [W]

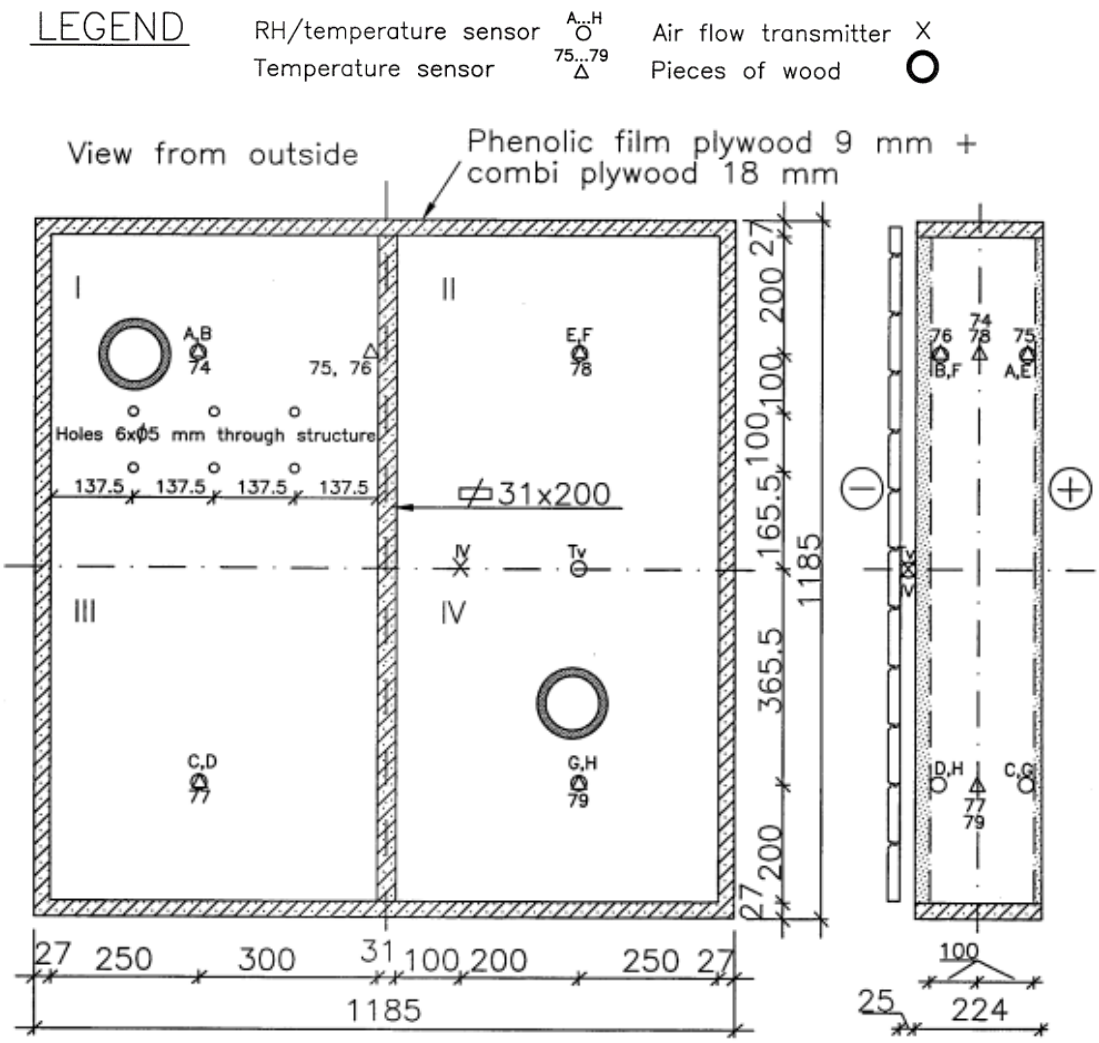


*Figure 4 Dimensions of test element 8 and positioning of measuring sensors Copied from Water vapour transmission in wall structures due to diffusion and convection. Publication 103 structural engineering. Vinha, J, Käkelä, P (1999) p. 101*

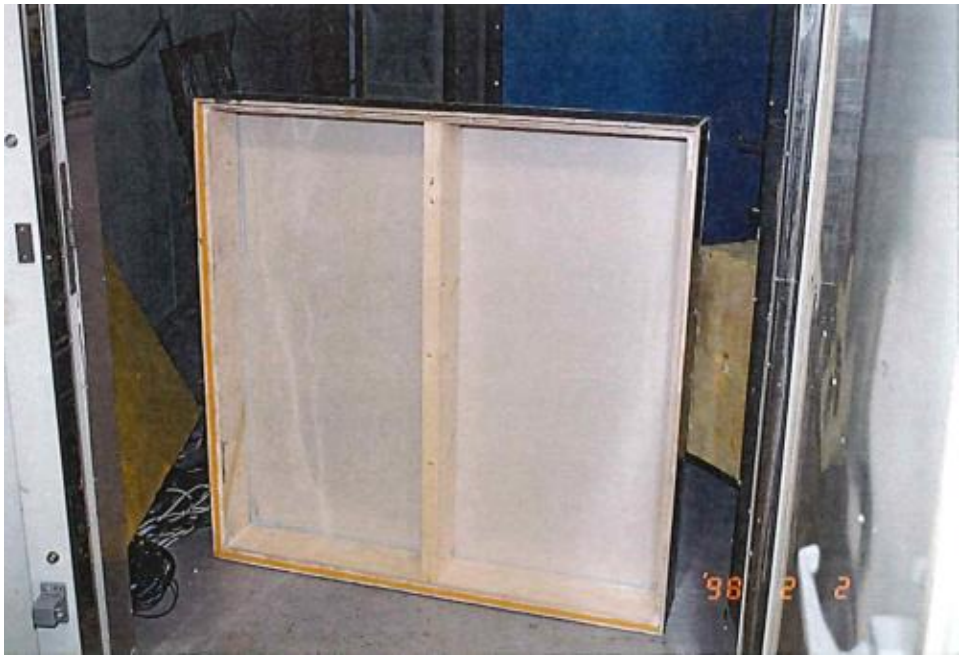


*Figure 5 Frame and bracing of the test element to which vapor barrier and inner sheet have been attached. Copied from Water vapour transmission in wall structures due to diffusion and convection. Publication 103 structural engineering. Vinha, J, Käkelä, P (1999) p. 87*


*Figure 6 Detachable horizontal paneling was used as exterior cladding in test walls. Copied from Water vapour transmission in wall structures due to diffusion and convection. Publication 103 structural engineering. Vinha, J, Käkelä, P (1999) p. 87*

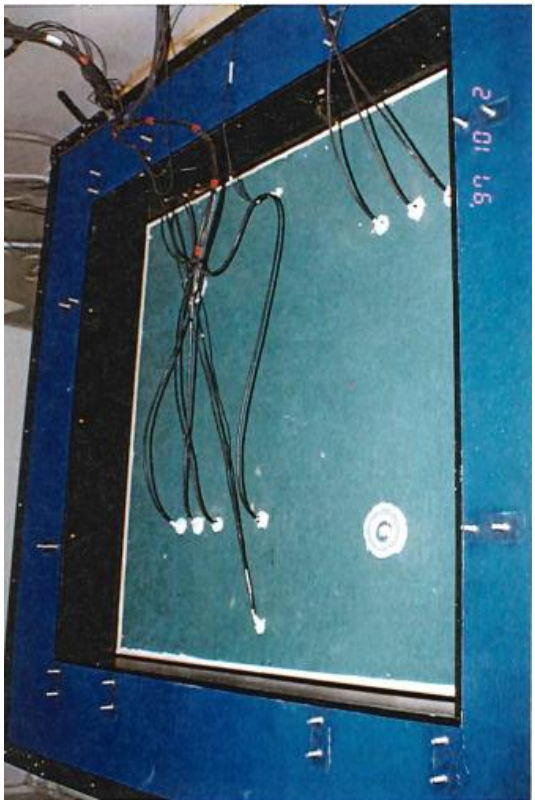


*Figure 7 (left) Test wall was installed in the opening and the edges were sealed.*
*Figure 8 (right) The external protective board with sensors was attached.*
*Copied from Water vapour transmission in wall structures due to diffusion and convection. Publication 103 structural engineering. Vinha, J, Käkelä, P (1999) p. 89*

Several conclusions were drawn from the laboratory study regarding convection. Firstly, if there is an under pressure in the building or when an air barrier is applied convection does not have to be assessed. Secondly, when there is overpressure in the building the size of holes in the structure needs to be known in order to examine the effect of convection. Lastly, in

practice it would be difficult to estimate the effect of convection as the number of air leaks in the structure is largely dependent on the built quality of the construction. [53]

The laboratory study also reported that a lack of material properties hinders the accuracy of hygrothermal modeling. For instance, the water vapor permeability, air permeability and thermal conductivity properties have to be known under varying circumstances as some are related to the temperature or relative humidity. At the time of the research, very limited material data was available and it was concluded that additional research was needed on the properties of building materials. [53]

## IV – II Balance equations in Delphin

Some of the balance equations that Delphin uses have been listed below. Delphin also has functions for the simulation of radiation, driving rain and the behavior of volatile organic compounds (VOC). These functions are not listed below as they are not relevant to the laboratory study. All of the listed equations can also be found in the Delphin 5 manual [50].

Energy balance equation

$$\frac{\partial}{\partial t}\rho_{REV}^{U} = -\frac{\partial}{\partial x}\left[ j_{diff}^{Q} + u_l \cdot j_{conv}^{m_l} + u_g \cdot j_{conv}^{m_g} + h_v \cdot j_{diff}^{m_v}\right] \quad (1$$

With:

| | | | |
|---|---|---|---|
| $\rho_{REV}^{U}$ | = | internal energy density reference volume | [ j/m$^3$ ] |
| $j_{diff}^{Q}$ | = | Heat conduction | [ W/m$^2$ ] |
| $j_{conv}^{m_l}$ | = | Capillary water flux | [ kg/m$^2$s ] |
| $j_{conv}^{m_g}$ | = | Convective flux of gas | [ kg/m$^2$s ] |
| $j_{diff}^{m_v}$ | = | Diffuse water vapor flux | [ kg/m$^2$s] |
| $u_l$ | = | Specific internal energy of liquid | [ J/kg ] |
| $u_g$ | = | Specific internal energy of gas | [ J/kg ] |
| $h_v$ | = | Specific enthalpy water vapor | [ J/kg ] |

Heat conduction flow

$$j_{diff}^{Q} = -\lambda\,(w, T)\,\frac{\partial T}{\partial x} \quad (2$$

With:

| | | | |
|---|---|---|---|
| $\lambda\,(w, T)$ | = | Thermal conductivity | [ W/mK ] |
| $T$ | = | Temperature | [ K ] |

Total internal energy density

$$\rho_{REV}^{U} = \rho_s \theta_s u_s + \rho_l \theta_l u_l + \rho_g \theta_g u_g \quad (3$$

With:

| | | | |
|---|---|---|---|
| $\rho$ | = | Density of the material | [ kg/m$^3$ ] |
| $\theta$ | = | Porosity of the material | [ - ] |
| $u$ | = | Specific internal energy | [ J/kg ] |

Moisture balance equation

$$\frac{\partial}{\partial t}\rho_{REV}^{m_{l+v+i}} = -\frac{\partial}{\partial x}\left[j_{conv}^{m_l} + j_{conv}^{m_v} + j_{diff}^{m_v}\right] \quad (4$$

With:

| | | | |
|---|---|---|---|
| $\rho_{REV}^{m_{l+v+i}}$ | = | moisture density in reference volume | [ kg/m$^3$ ] |
| $j_{conv}^{m_l}$ | = | Capillary water flux | [ kg/m$^2$s ] |
| $j_{conv}^{m_v}$ | = | Convective water vapor flux | [ kg/m$^2$s ] |
| $j_{diff}^{m_v}$ | = | Diffusive water vapor flux | [ kg/m$^2$s ] |

Capillary water flux

$$j_{conv}^{m_l} = -K_l(w)\left[\frac{\partial p_l}{\partial x} + \rho_l \cdot g\right] \quad (5$$

With:

| | | | |
|---|---|---|---|
| $K_l(w)$ | = | Liquid water conductivity | [ s ] |
| $p_l$ | = | Liquid water pressure | [ Pa ] |
| $\rho_l$ | = | Intrinsic density of liquid | [ kg/m$^3$ ] |
| $g$ | = | Gravity | [ m/s$^2$ ] |

Convective water vapor flux

$$j_{conv}^{m_v} = j_{conv}^{m_g} \cdot \left[\frac{p_v}{p_v + p_a} \cdot \frac{R_a}{R_v}\right] \quad (6$$

With:

| | | | |
|---|---|---|---|
| $p_v$ | = | Partial water vapor pressure | [ Pa ] |
| $p_a$ | = | Partial air pressure | [ Pa ] |
| $R_a$ | = | Gas constant air | [ 287.10 J/kgK ] |
| $R_v$ | = | Gas constant water vapor | [ 461.89 J/kgK ] |
| $j_{conv}^{m_g}$ | = | Convective air flux | [ kg/m$^2$s ] |

Diffuse water vapor flux

$$j_{diff}^{m_v} = -\frac{D_{v,air}(T)}{\mu \cdot R_v \cdot T} \cdot f(\theta_g) \cdot \frac{\partial p_v}{\partial x} \qquad \theta_g = \theta_{por} - \theta_l \quad (7$$

With:

| | | | |
|---|---|---|---|
| $D_{v,air}(T)$ | = | Vapor diffusivity in free air | [ m$^2$/s ] |
| $\mu$ | = | Water vapor diffusion resistance | [ - ] |
| $\theta_g$ | = | Volume fraction gas | [ m$^3$/m$^3$ ] |
| $\theta_{por}$ | = | Porosity | [ m$^3$/m$^3$ ] |
| $\theta_l$ | = | Volume fraction liquid | [ m$^3$/m$^3$ ] |
| $f(\theta_g)$ | = | Function of volume fraction gas | [ - ] |

Air balance equation

$$\frac{\partial}{\partial t}\rho_{REV}^{m_a} = -\frac{\partial}{\partial x}[\,j_{conv}^{m_a}\,] \qquad (8$$

With:

| | | | |
|---|---|---|---|
| $\rho_{REV}^{m_a}$ | = | Air density in reference volume | [ kg/m$^3$ ] |
| $j_{conv}^{m_a}$ | = | Convective air mass flux | [ kg/m$^2$s ] |

Convective air mass flux

$$j_{conv}^{m_a} = j_{conv}^{m_g} \cdot \left[\frac{p_v}{p_v+p_a} \cdot \frac{R_a}{R_v}\right] \qquad j_{conv}^{m_g} = -K_g(w)\left[\frac{\partial p_g}{\partial x} + \rho_g \cdot g\right] \qquad (9$$

With:

| | | | |
|---|---|---|---|
| $p_v$ | = | Partial water vapor pressure | [ Pa ] |
| $p_a$ | = | Partial air pressure | [ Pa ] |
| $R_a$ | = | Gas constant air | [ 287.10 J/kgK ] |
| $R_v$ | = | Gas constant water vapor | [ 461.89 J/kgK ] |
| $j_{conv}^{m_g}$ | = | Convective air flux | [ kg/m$^2$s ] |
| $K_g(w)$ | = | Gas permeability | [ kg/(msPa)] |
| $p_g$ | = | Gas pressure (air and vapor) | [ Pa ] |
| $\rho_g = \frac{p_g}{R_a \cdot T}$ | = | Intrinsic density of gas | [ kg/m$^3$ ] |

In order to solve the balance equations, one has to know which of the flux expressions are independent. For the Delphin model the water vapor diffusion flux, convective gas flux, capillary water flux and heat conduction flux are independent. Using these independent fluxes the balance equations can be solved.

## IV – III Balance equations in COMSOL

The laboratory study has once before been simulated in a study using COMSOL. The study was carried out in 2014 by C. Allué Hoyos at the Tampere University [57]. In the study the accuracy of COMSOL simulations was analyzed using measurement from the laboratory study. In the first part of the study only diffusion simulation was assessed. And in the second part of the study test wall 8 from the laboratory study was assessed considering all transfer methods. In the study it was concluded that some of the results simulated in COMSOL were close to the measurements from the laboratory study, but the overall results did not match well. The study questioned the equations and material properties used for the simulation.

The balance equations which were used in the COMSOL simulation are listed. These equations can also be found in the article of C. Allué Hoyos [57].

Heat and moisture transfer balance equation

$$d_a \frac{\partial u}{\partial t} + \nabla \cdot (-c\nabla u) + \beta \cdot \nabla u = 0 \qquad (10$$

With:

| | | | |
|---|---|---|---|
| $d_a$ | = | Damping or Mass Coefficient | [ $s^2/m^2$ ] |
| $c$ | = | Diffusion coefficient | [ - ] |
| $\beta$ | = | Convection coefficient | [ 1/m ] |

Heat and moisture storage

$$d_a \frac{\partial u}{\partial t} = \begin{bmatrix} \rho C_{p,w} + C_{p,s} w & 0 \\ 0 & \xi \end{bmatrix} \cdot \begin{bmatrix} \frac{\partial T}{\partial t} \\ \frac{\partial RH}{\partial t} \end{bmatrix}, \qquad (11$$

With:

| | | | |
|---|---|---|---|
| $\rho$ | = | Density | [ $kg/m^3$ ] |
| $C_{p,w}$ | = | Specific heat capacity water | [ J/kgK ] |
| $C_{p,s}$ | = | Specific heat capacity solid | [ J/kgK ] |
| $w$ | = | Water content | [ $kg/m^3$ ] |
| $T$ | = | Temperature | [ K ] |
| $RH$ | = | Relative humidity | [ % ] |

Heat conduction and moisture diffusivity flux

$$\nabla \cdot (-c\nabla u) = -\begin{bmatrix} \lambda + H_v \delta_p RH \cdot \frac{\partial p_{vsat}}{\partial T} & H_v \delta_p p_{vsat} \\ \delta_p RH \cdot \frac{\partial p_{vsat}}{\partial T} & \delta_p p_{vsat} \end{bmatrix} \cdot \nabla \begin{bmatrix} \nabla T \\ \nabla RH \end{bmatrix} \qquad (12$$

| | | | |
|---|---|---|---|
| $\lambda$ | = | Thermal conductivity | [ W/mK ] |
| $H_v$ | = | Latent heat of phase change | [ J/kg ] |
| $\delta_p$ | = | Water vapor diffusion coefficient | [ kg/msPa ] |
| $p_{vsat}$ | = | Partial water vapor pressure | [ Pa ] |

Convective heat and moisture flux

$$\beta \cdot \nabla u = \begin{bmatrix} \begin{bmatrix} u \cdot \frac{R_{air}}{C_{p,air} T} p_{atm} \\ v \cdot \frac{R_{air}}{C_{p,air} T} p_{atm} \end{bmatrix} & \begin{bmatrix} 0 \\ 0 \end{bmatrix} \\ \begin{bmatrix} u \cdot \frac{RH \cdot M_w}{RT} \cdot \frac{\partial p_{vsat}}{\partial t} \\ v \cdot \frac{RH \cdot M_w}{RT} \cdot \frac{\partial p_{vsat}}{\partial t} \end{bmatrix} & \begin{bmatrix} u \cdot \frac{M_w p_{vsat}}{RT} \\ v \cdot \frac{M_w p_{vsat}}{RT} \end{bmatrix} \end{bmatrix} \cdot \begin{bmatrix} \nabla T \\ \nabla RH \end{bmatrix} \qquad (13$$

| | | | |
|---|---|---|---|
| $u$ | = | Velocity vector | [ m/s ] |
| $v$ | = | vapor content of air | [ $kg/m^3$ ] |
| $R_{air}$ | = | gas constant of air | [ 287.058 J/kgK ] |
| $C_{p,air}$ | = | Specific heat capacity air | [ $J/m^3K$ ] |
| $p_{atm}$ | = | Atmosphere pressure | [ Pa ] |

| | | | |
|---|---|---|---|
| $p_{vsat}$ | = | Saturation vapor pressure | [ Pa ] |
| $M_w$ | = | mean molar mass of water | [ 0.018 kg/mol ] |
| R | = | Ideal gas constant | [ 8.314 J/molK ] |

Air transfer balance equation

$$\frac{\rho}{\epsilon_p}\left((u\cdot\nabla)\frac{u}{\epsilon_p}\right) = \nabla\cdot\left[-pI+\frac{\mu}{\epsilon_p}(\nabla u+(\nabla u)^T)-\frac{2\mu}{3\epsilon_p}(\nabla u)I\right]-\left(\frac{\mu}{k_{br}}\right)u+F \quad (14$$

$$\rho\nabla\cdot u = 0$$

| | | | |
|---|---|---|---|
| $\epsilon_p$ | = | Porosity | [ - ] |
| $p$ | = | Pressure | [ Pa ] |
| $\mu$ | = | Dynamic viscosity | [ Pa s ] |
| $I$ | = | Identity vector | [ Pa ] |
| $k_{br}$ | = | Permeability | [ $m^2$ ] |
| $F$ | = | Volume force (influenced by gravity) | [ $kg/(m^2 s^2)$ ] |
| $u$ | = | Velocity vector | [ m/s ] |
| $\rho$ | = | Density | [ $kg/m^3$ ] |

## IV – IV Comparison of balance equations in COMSOL and Delphin

The balance equations that Delphin uses can be compared to those used in the COMSOL study. One difference that can be noticed is that the study in COMSOL left out capillary water transport. In the study it is mentioned that the addition of capillary HAM transport was considered, but it was neglected as the effect was not significant and it impacted the computational speed. As can be seen in eq. 5 the model in Delphin uses a function for the liquid water conductivity related to the moisture content to calculated capillary transport. Secondly, a difference can be observed regarding vapor diffusion. The COMSOL study used the water vapor diffusion coefficient whereas the equation from Delphin mentions the water vapor diffusion resistance. However, it should be noted that Delphin also has the option to use the water vapor diffusion coefficient [50]. Another difference can be noticed when looking at the air transport equations 9 and 14. The model in Delphin makes use of Darcy's law to calculate air transport in porous materials. In the COMSOL study Darcy's law is also used, although both models use slightly different materials properties for the air permeability. Additionally to Darcy's law the COMSOL study used the brinkman equation to model fluid flow in porous materials with high porosity's. The permeability used in the COMSOL model is also different from the permeability that is used in the Delphin model. However, the permeabilities are related and can be converted using eq. 15.

$$K_g = \frac{k_{br}}{\mu}\cdot\rho \quad (15$$

| | | | |
|---|---|---|---|
| $K_g$ | = | Gas permeability | [ kg/(msPa)] |
| $k_{br}$ | = | Permeability | [ $m^2$ ] |
| $\mu$ | = | Dynamic viscosity of air | [ 1,7e-5 Pa s ] |
| $\rho$ | = | Density | [ $kg/m^3$ ] |

## IV – V Delphin model setup

The laboratory study was used to build a simulation model in Delphin 6.1.0. The material properties, boundary conditions and dimensions all followed from the laboratory study. Some parts of the model have been simplified. In Figure 9 the overview of the simulation model can be seen. It should be noted that the setup is mirrored compared to the laboratory setup. This has been done so that it would be easier to compare some of the results to a different study in which COMSOL was used to simulate.

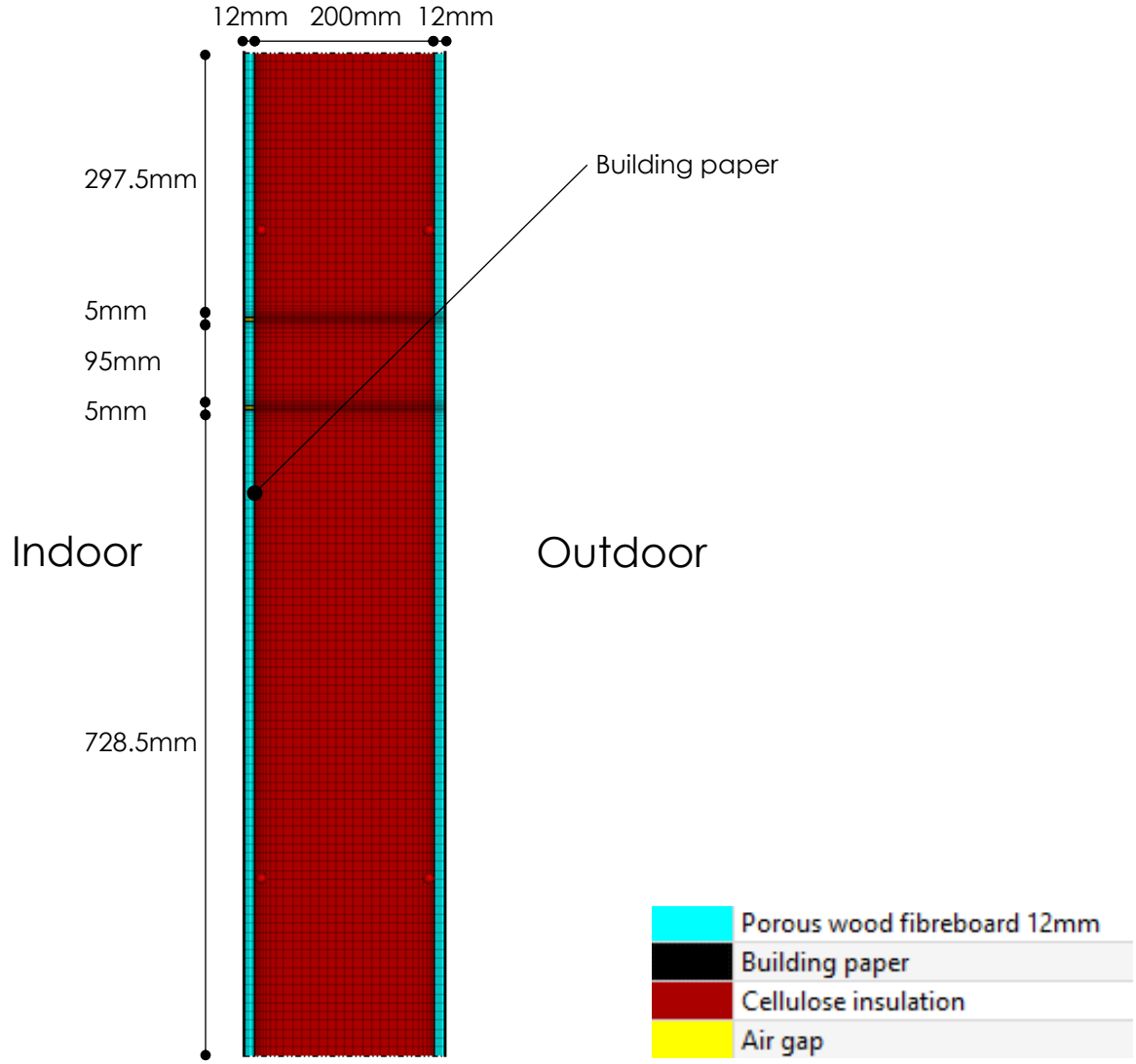


*Figure 9 Dimensions and materials simulation model*

## IV – VI Model simplifications

Comparing Figure 4 and 9 one can notice that some simplifications have been made to the simulation model.

First of all, the wooden cladding on the external side of the structure has been omitted. The reason for this is the complex nature of cavities. Many different properties would have to be known in order to properly simulate the effect of the cavity. Furthermore, extensive measurements were already performed in the cavity of the structure. Therefore, the climate conditions in the cavity can directly be used as the boundary conditions of the model which makes the modeling of the wooden cladding unnecessary.

The second simplification is the omission of the wooden framing in the structure. As can be seen in Figure 4, the distance between the wooden framing and the sensors in the structure is at least 0.2 m from all sides. This distance limits the effect of the wooden framing on the sensors. Also, the properties of the wooden framing were not clear from the laboratory study which further supports the omission of the framework.

The last simplification regards the dimension of the simulation model. Currently, it is not possible to simulate the effect of convection in Delphin using a three-dimensional model. Therefore the model has been made two-dimensional so that convection can be included. As can be seen in Figure 4, the structure largely consists of continuous layers. Except for the 6 holes that were drilled through the internal sheathing and vapor barrier. It is not possible to model the circular holes in a two-dimensional model as can be seen in Figure 9. The gap in the porous fiberboard and building paper is filled with an air layer. Because of the two-dimensional model the gap is essentially continued over the length of the structure. This would mean that instead of circular holes a linear gap across the structure is modelled. The difference between circular holes and a linear gap across the structure should have a limited impact on the thermal conduction and vapor diffusion. Mainly because the cellulose insulation is not impacted by the linear gap and is mainly responsible for the thermal resistance. The structure is also already very vapor permeable so this would not be greatly increased by the linear gaps across the structure. However, the vapor barrier and sheathing also prevent air from entering the structure so this linear gap would increase the convection through the structure. To account for this the permeability of the air gap has been increased so that the flow in the simulation is equal to the flow in the laboratory study. The permeability that is used for the air gap is 1.7e-5 kg/(msPa). Figure 10 shows the flow through the structure as determined by the laboratory study and the simulation model in Delphin. The simulated flow rate shown in Figure 10 is not fully in line with the measurements from the laboratory study. The simulated flow rate is related to the measured pressure difference across the structure and the permeability of the materials and dimensions of the model. The measured flow rate in Figure 10 is the actual flow rate measured through the element during the test period in the laboratory.

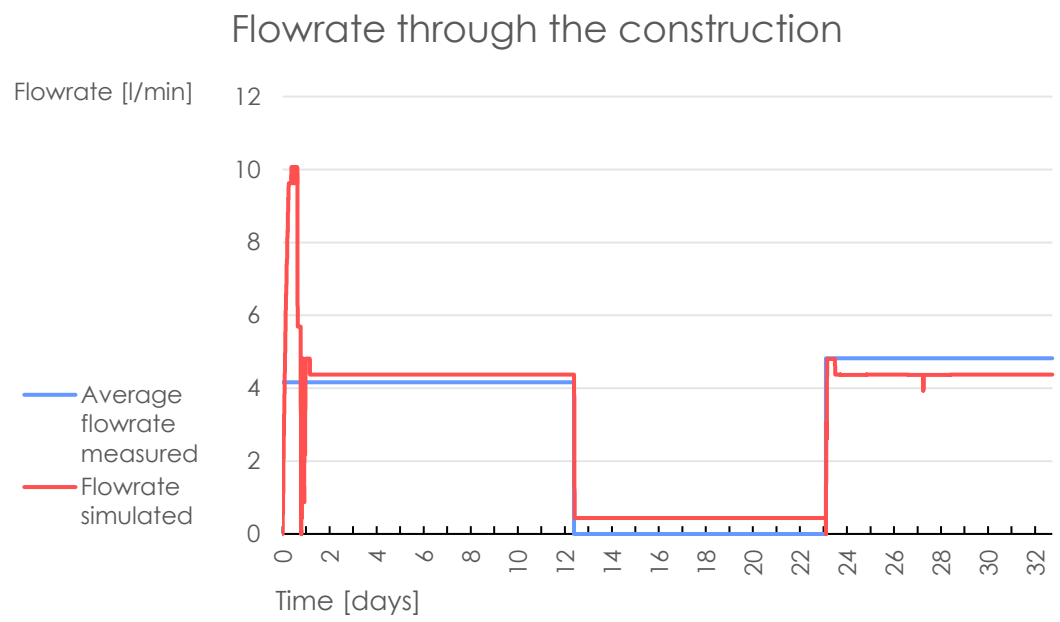


*Figure 10 Flow rate [l/min] laboratory study and simulation model*

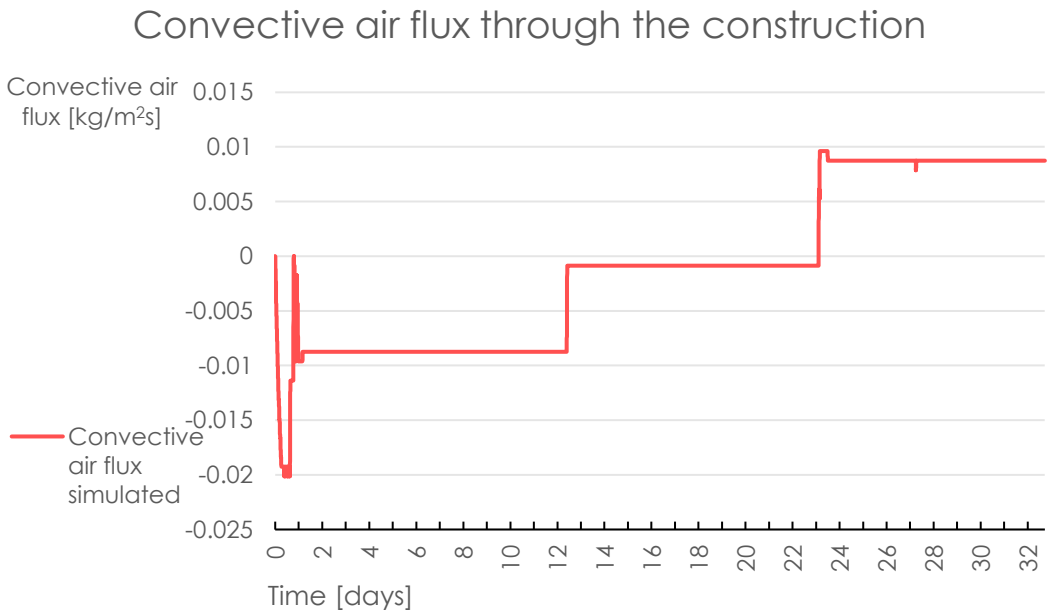


*Figure 11 Convective air flux simulated*

The flow rate in Figure 10 was calculated using the area weighted average convective air flux shown in Figure 11. The convective air flux in kg/(m²s) was simulated in Delphin over the two air gaps. Using an air density of 1.2 kg/m³ and the combined height of the gaps of 0.01 m over a length of 1 m the flow rate is converted to l/min.

Flow rate is related to the velocity of the flow and area through which the air flows. The air gaps in the simulation will have a larger surface area than the actual holes were in the laboratory study. The actual surface area of the holes in the laboratory study is 1,963e-5 m² compared to the simulated surface area of 0,01 m². Therefore, the simplification will also have a large impact on the velocity of the flow through the air gaps. In Figures 12 and 13 the velocity flow can be seen. The total velocity flow through the element is in line with the laboratory measurement, but the velocity flow through the air gaps is much lower. This should be kept in mind as it can affect the results.

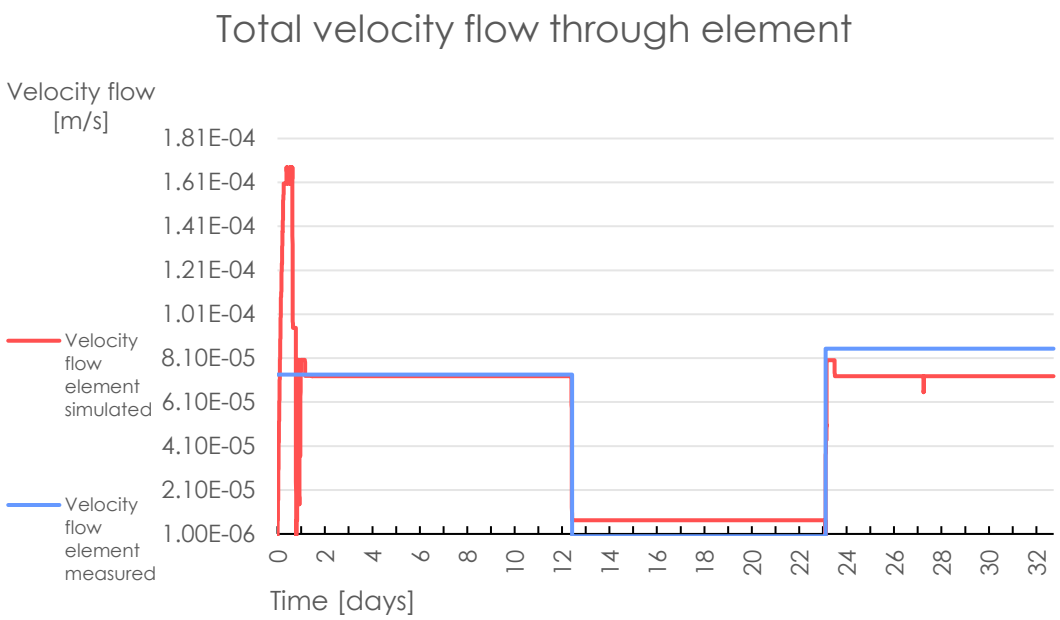


*Figure 12 Total velocity flow through the element*

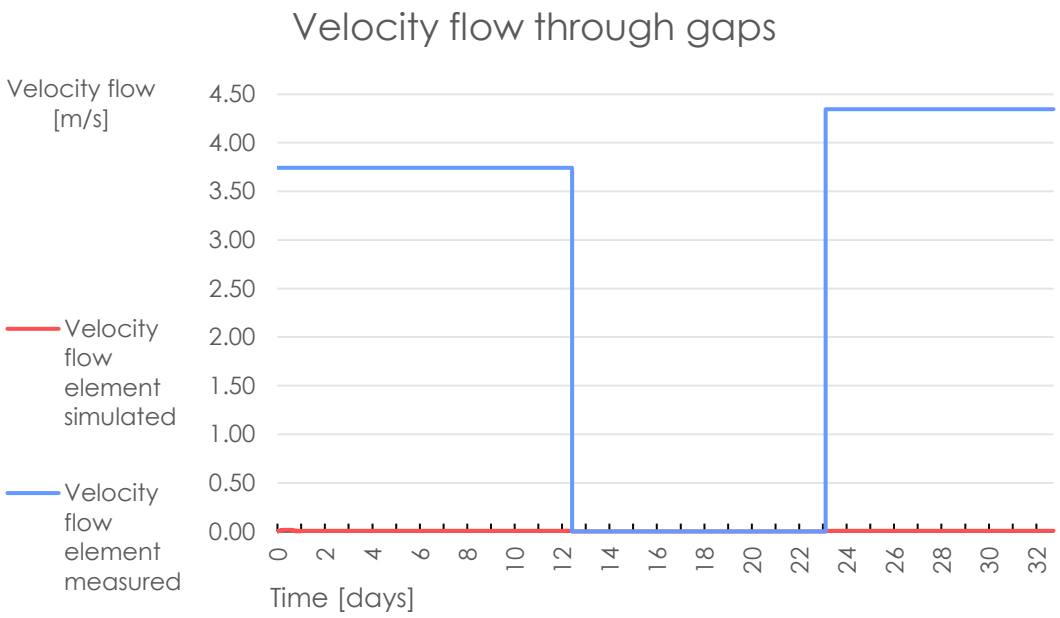


*Figure 13 Velocity flow through the air gaps*

## IV – VII Boundary conditions, material properties and solver settings

The boundary conditions used in the Delphin model are shown in Table 9. These boundary conditions are the measured values from the laboratory study. For heat conduction through the structure, a surface value is set at the external and internal sides of the structure. The boundary conditions necessary for vapor diffusion are the measured air temperatures and relative humidities. For the internal boundary the indoor air measurements are used and at the external boundary the air measurements of the cavity are used. These conditions are also used for the convective HAM transport. Additionally, convective HAM transport requires a pressure difference. This was also measured in the laboratory study. In Figure 14 the boundary conditions noted in Table 9 can also be viewed. The initial temperature of the structure is set to 20 ◦ C. The initial relative humidity of the structure is set to 55 %, except for the inner sheathing which has an initial relative humidity of 35 %.

| Boundary conditions | Kind | Temperature input | Relative humidity input | Pressure input |
|---|---|---|---|---|
| Heat conduction inner surface | Surface value | Measured internal surface temperature $T_{surf;I}$ | | |
| Vapor diffusion inner surface | Exchange coefficient 1.52e-08 s/m | Measured internal air temperature $T_{air;I}$ | Measured internal air relative humidity $RH_{air;I}$ | |
| Air convection inner surface | Exchange coefficient 2 s/m | Measured internal air temperature $T_{air;I}$ | Measured internal air relative humidity $RH_{air;I}$ | Measured pressure difference $\Delta$Pa |
| Heat conduction outer surface | Surface value | Measured surface temperature sheathing cavity $T_{surf;E}$ | | |
| Vapor diffusion outer surface | Exchange coefficient 1.22e-07 | Measured cavity air temperature $T_{air;E}$ | Measured cavity air relative humidity $RH_{air;E}$ | |
| Air convection outer surface | Exchange coefficient 2 s/m | Measured cavity air temperature $T_{air;E}$ | Measured cavity air relative humidity $RH_{air;E}$ | Constant value 101325 Pa |

*Table 9 Boundary conditions*

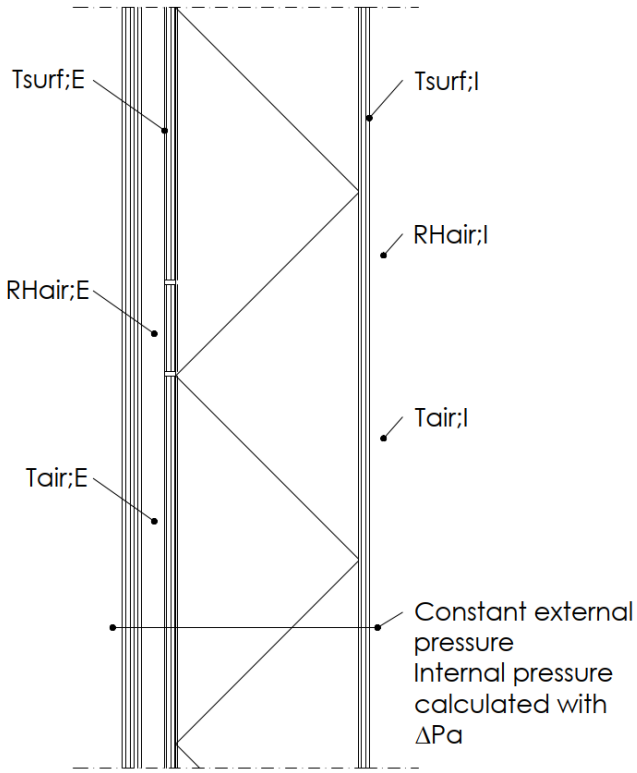


*Figure 14 Modelled boundary conditions*

The material properties that were used in the simulation are those that were measured in the laboratory study and a study published a few years after the laboratory study [53] [54]. These material properties are also listed in Appendix 2.

The used solver settings can be seen in Table 10. The integrator that was used is the CVODE with the GMRES iterative solver. A total of 785.5 hours were simulated which correspond to about 33 days which is the same length as the measurements in the laboratory study.

| **Solver settings** | |
|---|---|
| Relative tolerance | 1e-05 |
| Absolute tolerance moisture mass balance equation | 1e-06 |
| Absolute tolerance air mass balance equation | 1e-06 |

*Table 10 Delphin solver settings*

The effect of gravity on the movement of air is not enabled for this simulation. The movement of air is already driven by the pressure difference over the structure. In addition, the cellulose insulation layer is continuous over the entire structure there is only a small temperature difference over the height of the structure. This small temperature difference would have a negligible effect on the movement of air through the structure. Disabling the effect of gravity on air transport drastically increases simulation performance.

## IV – VIII Model validation indicators

In order to determine the accuracy of the simulation compared to the laboratory measurements two statistical indicators were used. These two indicators are the Mean Bias Error (MBE ; %) and the Coefficient of Variation of Root Mean Square Error (CV RMSE ; %) [55]. These indicators have been used in multiple studies to assess hygrothermal simulation models as reported in the study of [43]. In this study the ASHRAE Guideline 14 is also mentioned where standard values for the MBE and CV RMSE are noted. The simulation model can essentially be validated when a MBE of 10 % and a CV RMSE of 30 % is achieved using hourly values. The study further reports that even though these values were designed for the validation and calibration of energy performance models these are also used for the evaluation of hygrothermal models.

The MBE and CV RMSE are used to evaluate the results of the simulation in this study. The two indicators were calculated using Eq. 16 and Eq. 17.

$$\text{MBE}\ (\%) = \frac{\sum_{i=1}^{N_p}(m_i - s_i)}{\sum_{i=1}^{N_p}(m_i)} \quad (16$$

$$\text{CV RMSE}\ (\%) = \frac{\sqrt{(\sum_{i=1}^{N_p}(m_i - s_i)^2 / N_p}}{\bar{m}} \quad (17$$

With:

$m_i$ = data points measured at each interval
$s_i$ = data points simulated at each interval
$N_p$ = total amount of data points
$\bar{m}$ = average value of measured data points

The results for the MBE and CV RMSE indicators are shown in table 11 and 12.

| **MBE model validation indicator** | | | | |
|---|---|---|---|---|
| | A | B | C | D |
| Temperature | 5.38 % | 6.16 % | 3.92 % | 6.76 % |
| Relative humidity | 6.81 % | 16.93 % | 7.10 % | 18.32 % |
| Absolute humidity | 0.32 % | 20.15 % | 2.63 % | 15.26 % |

*Table 11 MBE indicator for temperature, relative humidity and absolute humidity at points A-D*

| **CV RMSE model validation indicator** | | | | |
|---|---|---|---|---|
| | A | B | C | D |
| Temperature | 7.58 % | 14.43 % | 2.78 % | 3.09 % |
| Relative humidity | 0.67 % | 2.55 % | 0.43 % | 2.92 % |
| Absolute humidity | 2.02 % | 11.62 % | 2.47 % | 4.82 % |

*Table 12 CV RMSE indicator for temperature, relative humidity and absolute humidity at points A-D*

From the results of the indicators MBE and CV RMSE, one can conclude the model cannot be fully validated. The RV RMSE shows a relatively good fit for the entire model, but the MBE indicator shows for the relative humidity and absolute humidity at point B and D an error larger than 10 %. This should be kept in mind when looking at the results further on. The indicators also show that the model has a decent fit looking at the temperatures.

# V: Results

Measurement points A-D as shown in Figure 15 were simulated and the results are compared to the laboratory data. The results are shown in Figures 16-28.

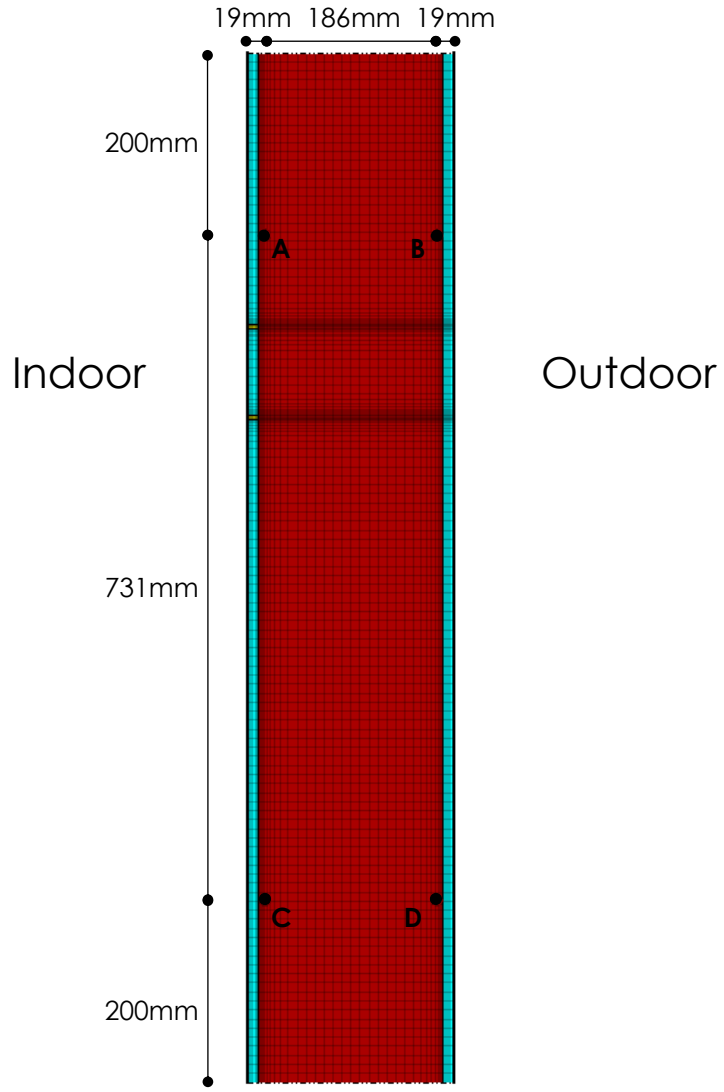


*Figure 15 Dimensions of measurement points A, B, C and D*

## V-I Pressure, temperature, humidity and vapor flux overview

Results for the pressure, temperature, humidity and diffuse/convective vapor flux can be seen in Figures 16-20. Results are shown separately for the three periods: internal under pressure, no pressure, internal over pressure.

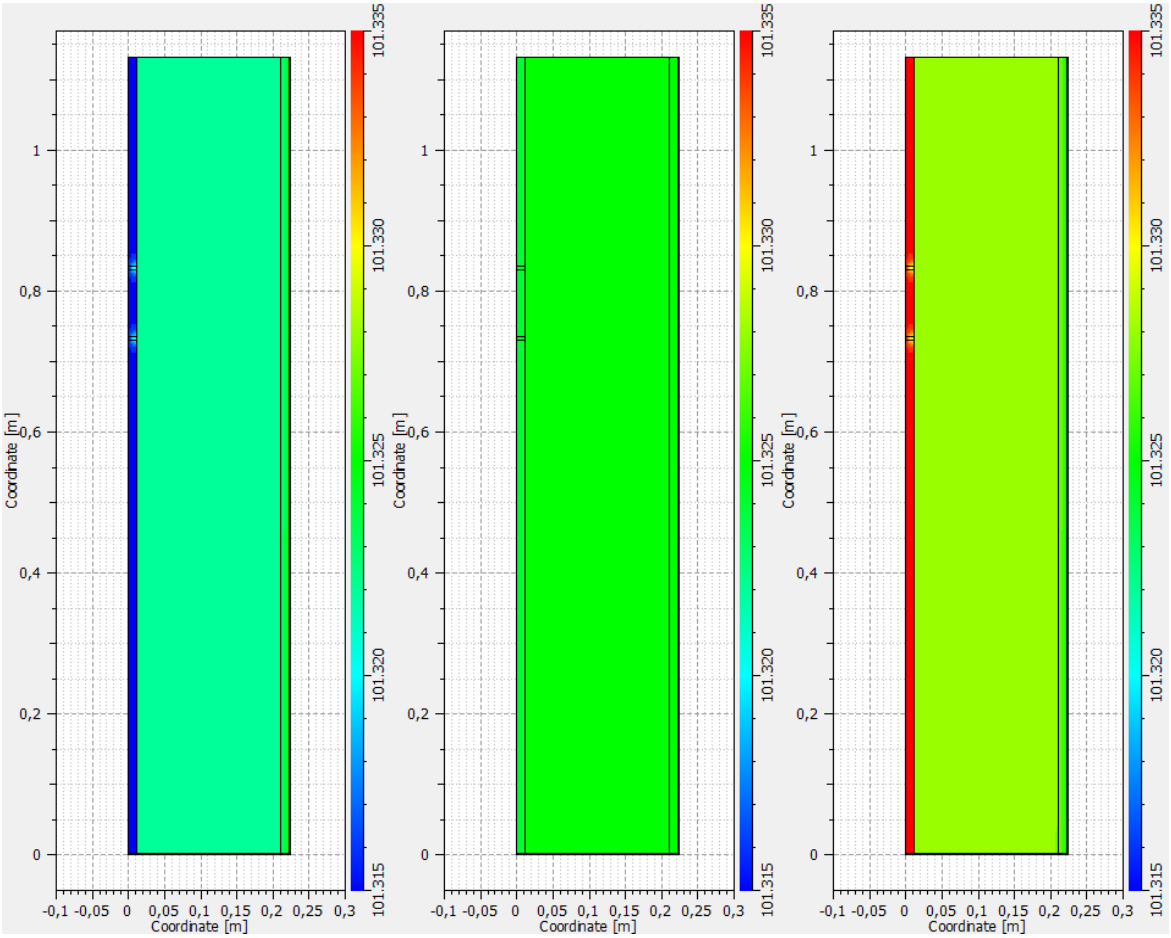


*Figure 16 Total gas pressure [Pa] - Left to right: internal under pressure, no pressure, internal over pressure*

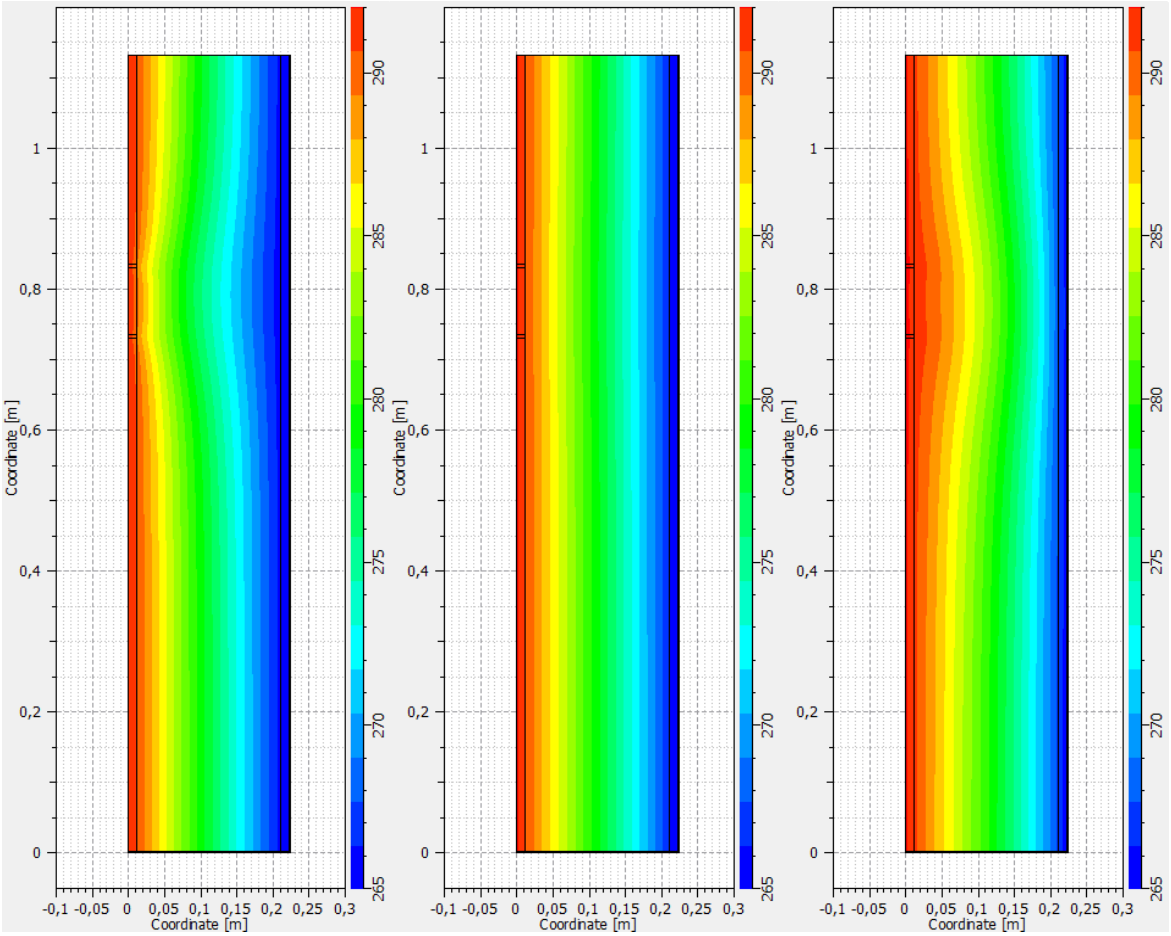


*Figure 17 Temperatures [K] - Left to right: internal under pressure, no pressure, over pressure*

The results for total gas pressure can be viewed in Figure 16. Looking at the results one can notice a large pressure difference at the internal side of the structure. This is caused by the vapor barrier as it is resistant to air transport. There is only an air flow through the gaps in the internal sheathing and building paper. This causes the pressure difference between the cellulose layer and exterior to be very small.

Results for the temperatures can be viewed in Figure 17. As can be seen, the cellulose layer is primarily responsible for the insulation of the element. The effect of convective air flow can also be noticed when looking at the internal under pressure and internal over pressure periods. Near the gaps in the internal sheathing and building paper there is a slight difference in temperatures. Cold or warm air flows through the gaps when a pressure difference is present which causes the difference in temperature. This effect cannot be noticed during the period of no pressure.

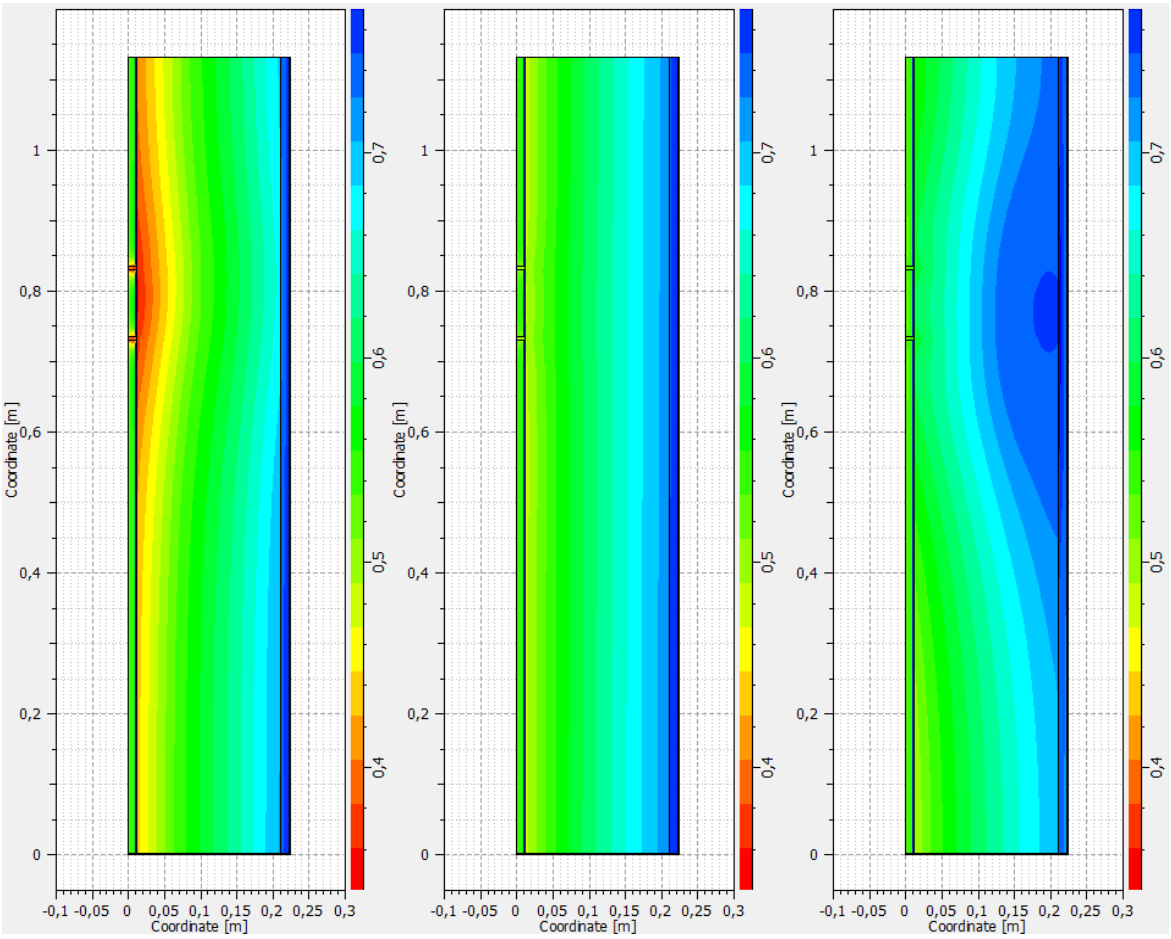


*Figure 18 Relative humidity [-] - Left to right: internal under pressure, no pressure, over pressure*

Figure 18 contains the results for relative humidity in the element. Here, the effect of the air gaps can also be observed. During the period of internal under pressure convection will cause air to move from the exterior to the interior. As the external air is drier than the internal air the air flow reduces the relative humidity in the element. The opposite can be observed during the over pressure period. During this period the humid interior air increases the relative humidity near the air gaps in the element.

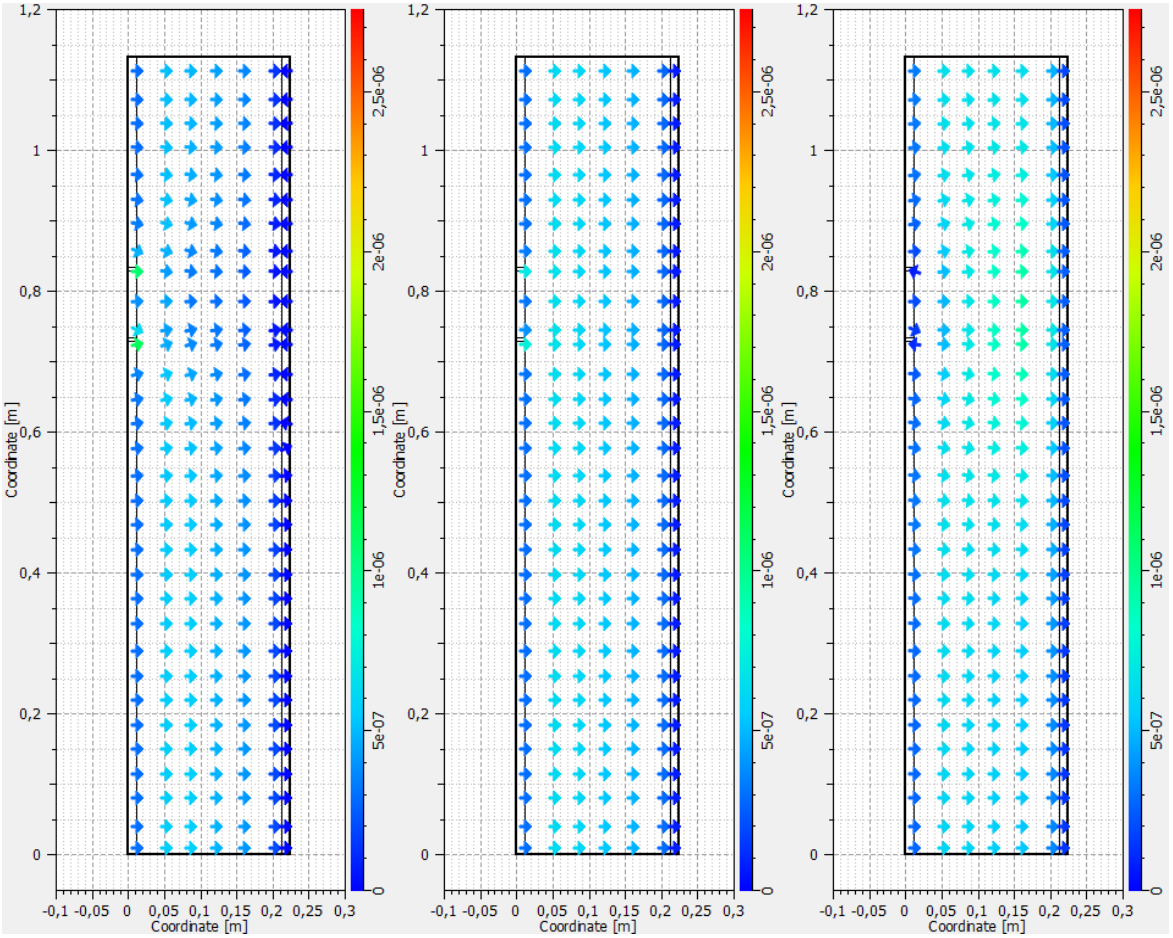


*Figure 19 Diffuse vapor flux [kg/m²s] - Left to right: internal under pressure, no pressure, over pressure*

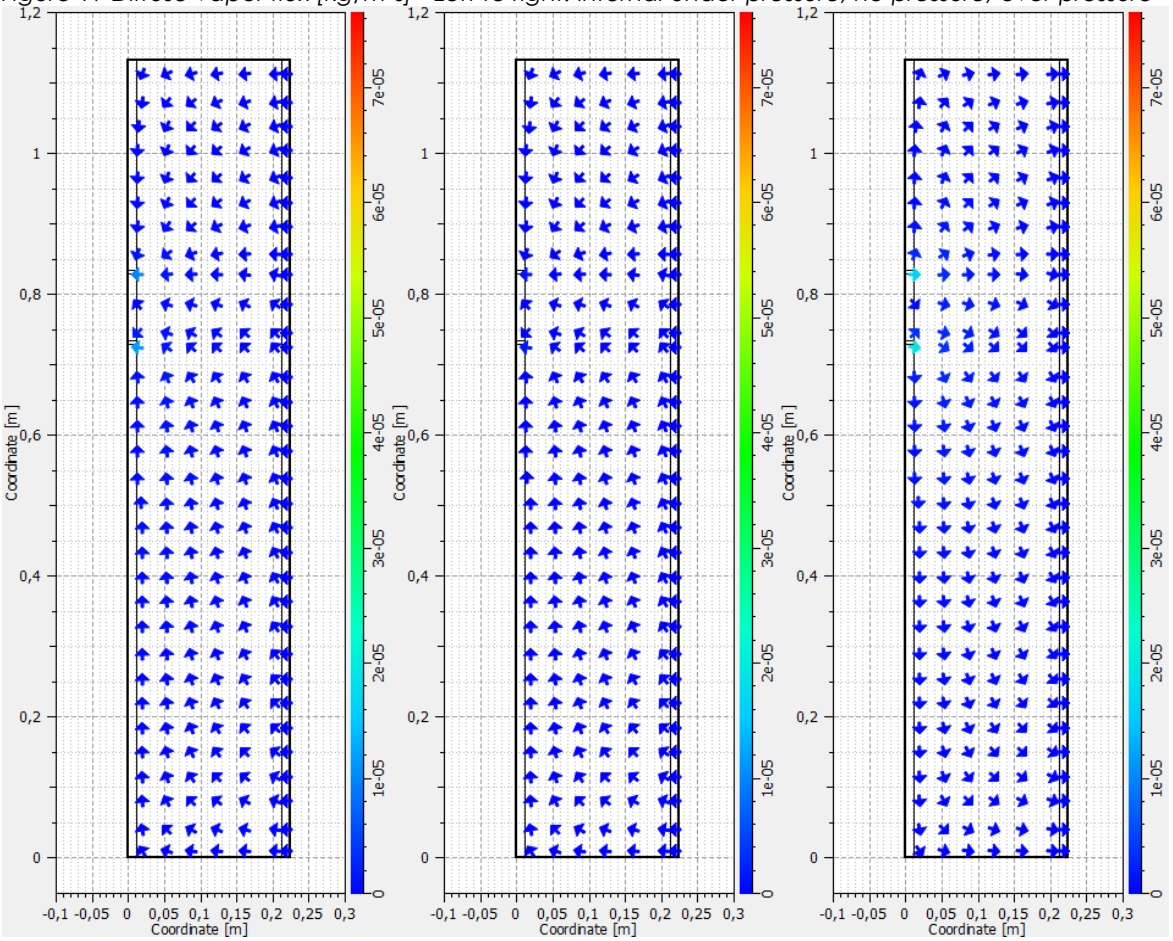


*Figure 20 Convective vapor flux [kg/m²s] - Left to right: internal under pressure, no pressure, over pressure*

In Figures 19 and 20 the convective and diffuse vapor fluxes can be viewed. It can be seen that the vapor diffuses from the interior to the exterior during all pressure periods. The convective moisture flux is dependent on the pressure difference over the element. It can be noticed that the convective moisture flux is higher near the gaps in the structure. This is caused by the building paper which prevents all air transport except the air flow through the gaps. In the period of no pressure convective air flow can also be observed as a small pressure difference was also measured in the laboratory study during the period of no pressure. Comparing the convective and diffuse vapor fluxes, one can also notice that the air convection affects the vapor diffusion. If the convection and diffusion occur in the same direction then the overall vapor diffusion increases slightly. When the convection and diffusion occur in opposite directions the overall vapor diffusion decreases slightly.
At the air gaps another interesting relation can be observed. During the internal under pressure period convection causes an air flow from the outside to the inside, but the diffusion from the interior to the exterior at the air gap increases. While during the internal over pressure period the convection causes an air flow from the inside to the outside, but diffusion at the air gap occurs from the outside to the inside. The cause of this interaction between diffusion and convection at the air gap was not found.

## V-II Temperature and humidity points A, B, C, and D

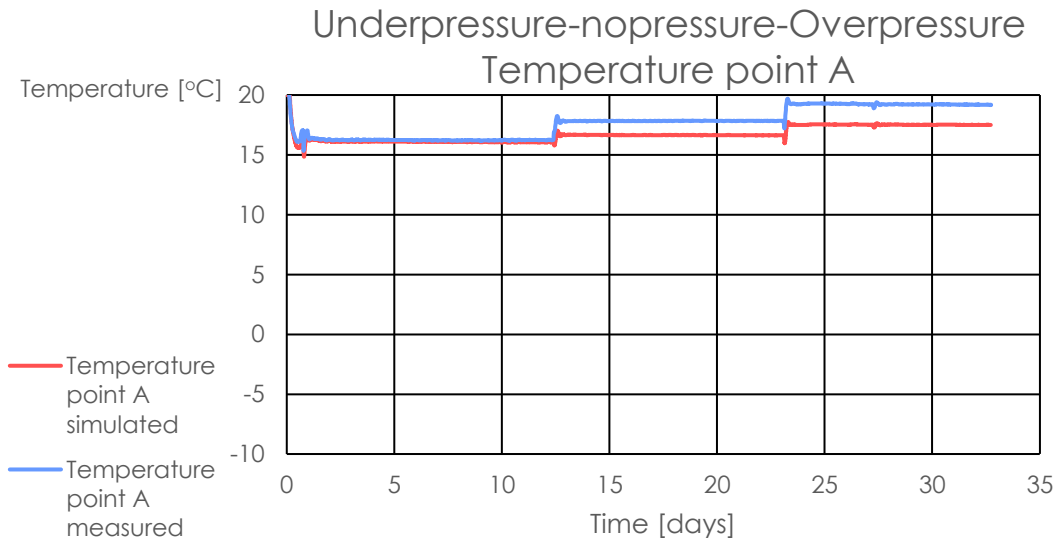


*Figure 21 Measured and simulated temperatures point A*

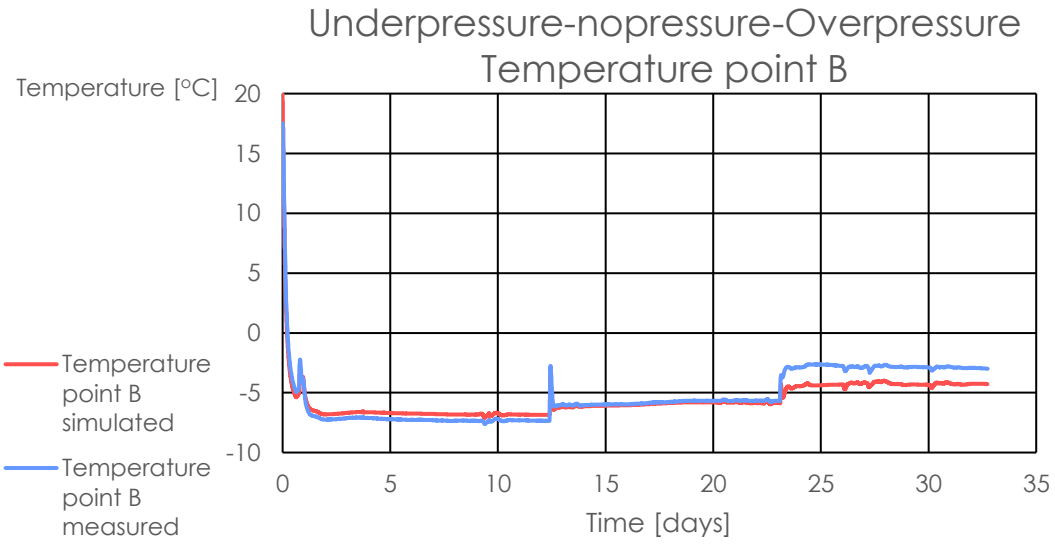


*Figure 22 Measured and simulated temperatures point B*

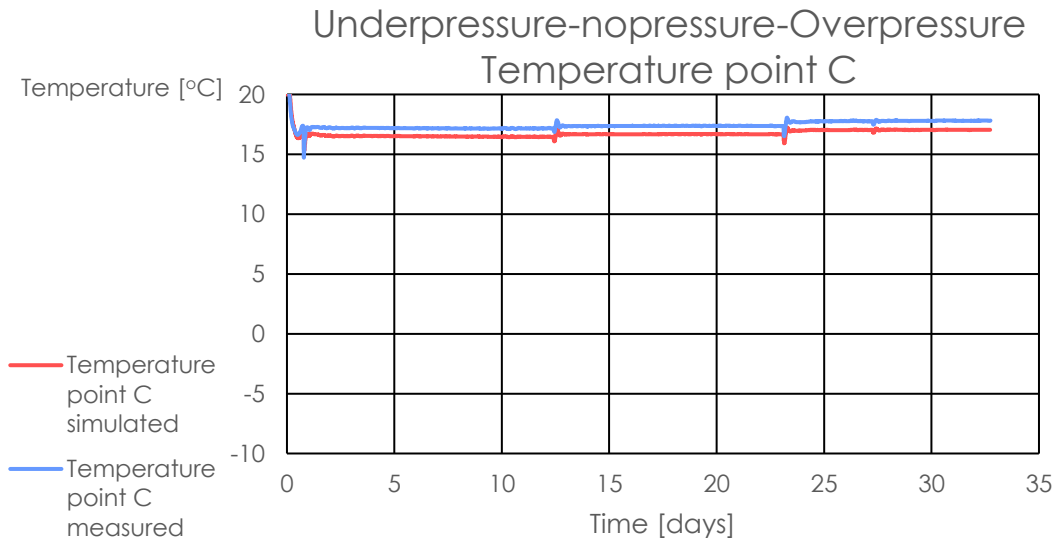


*Figure 23 Measured and simulated temperatures point C*

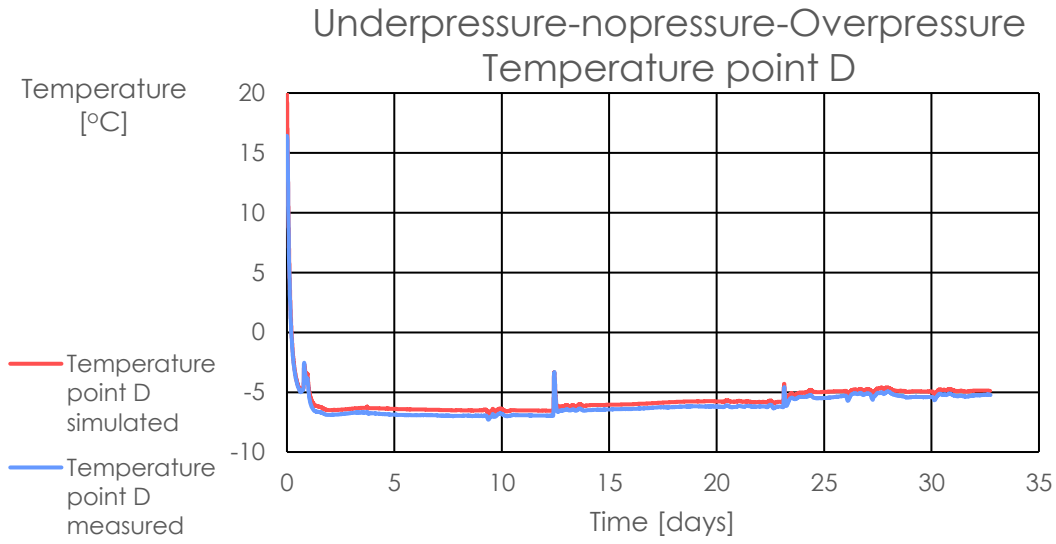


*Figure 24 Measured and simulated temperatures point D*

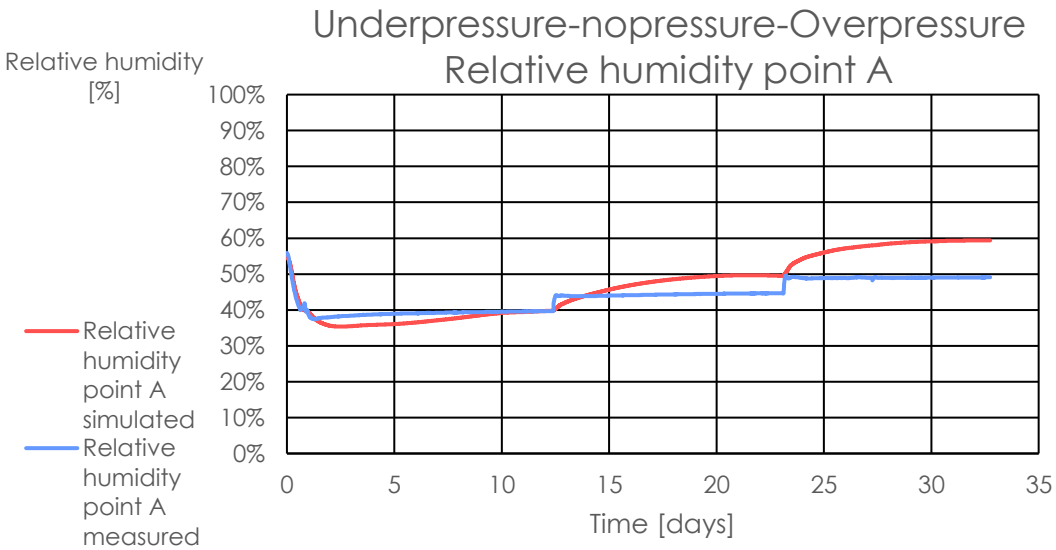


*Figure 25 Measured and simulated relative humidities point A*

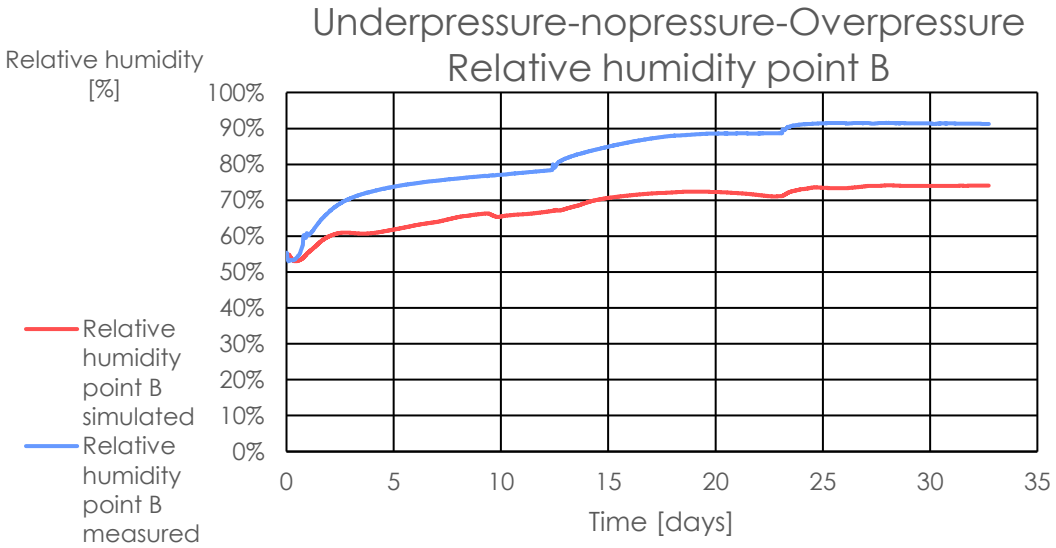


*Figure 26 Measured and simulated relative humidities point B*

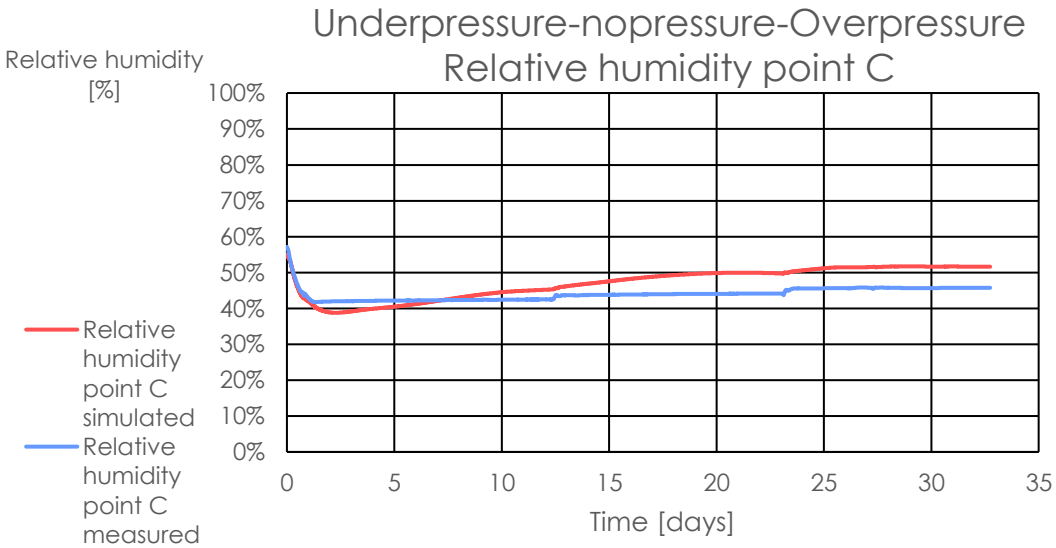


*Figure 27 Measured and simulated relative humidities point C*

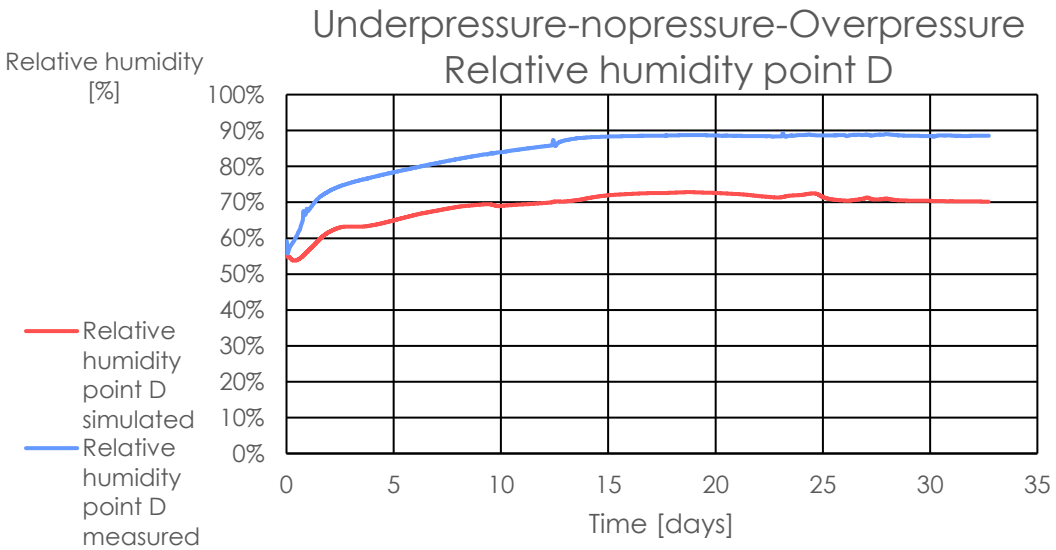


*Figure 28 Measured and simulated relative humidities point D*

In Figure 21-24 the simulated temperatures are compared to the measured temperatures. It is noticeable that the simulated temperatures are relatively in line with the measured temperatures, but there are some discrepancies. Especially during the period of over pressure the simulated temperatures at points A and B are colder than the measured values. The largest difference between measured and simulated values can be observed during the period of over pressure at point A. Here, the simulated value is about 1.7 ◦C colder than the measured value. The simulated results at point D are the closest to the measured value. Point D is also the farthest point from the holes drilled in the structure.

The simulated and measured relative humidities at each point are shown in Figure 25-28. As can be seen, the simulated and measured relative humidities deviate. For the points at the internal sheathing (points A and C) the simulated relative humidity after the under pressure period is higher than the measured values. The opposite can be noticed for the points located near the external sheathing. The difference between measured and simulated relative humidities is also larger at points B and D as supposed to points A and C. Furthermore one can notice that the results from the simulated model adapt slower to the sudden pressure changes than the measured values. This is especially true for point A show in Figure 25. The measured values show two steep jumps as the pressure difference changes. On the other hand, the simulated results show changes similar to a root function where initially the change is large and then gradually less.

It should be noted that the relative humidity is related to the temperature. In order to assess the moisture content independent of the temperature it has to be converted. Using the relative humidity and the corresponding temperature the absolute moisture content in g/kg is calculated for each of the measurement points. These results are shown in Figures 29-32.

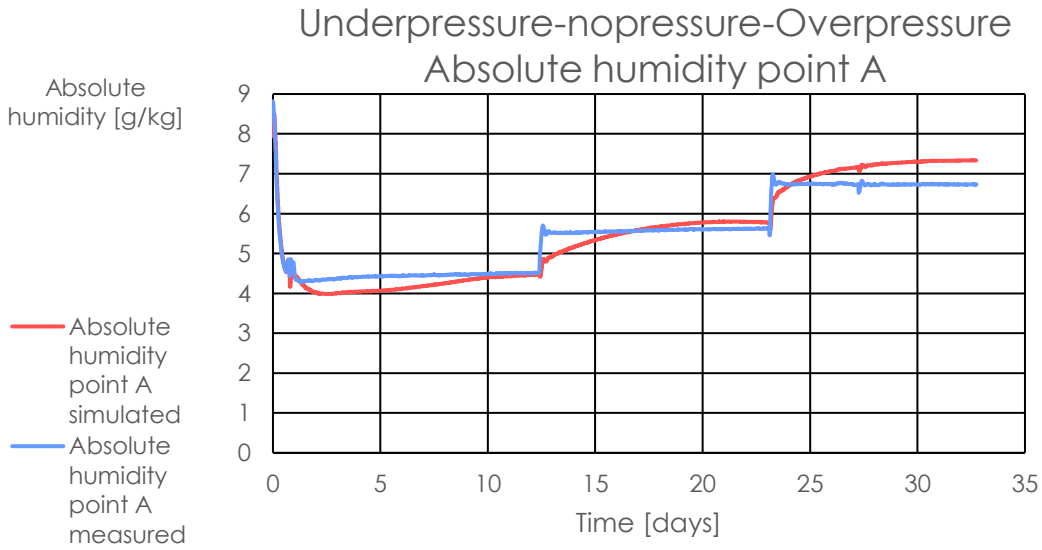


*Figure 29 Measured and simulated absolute humidities point A*

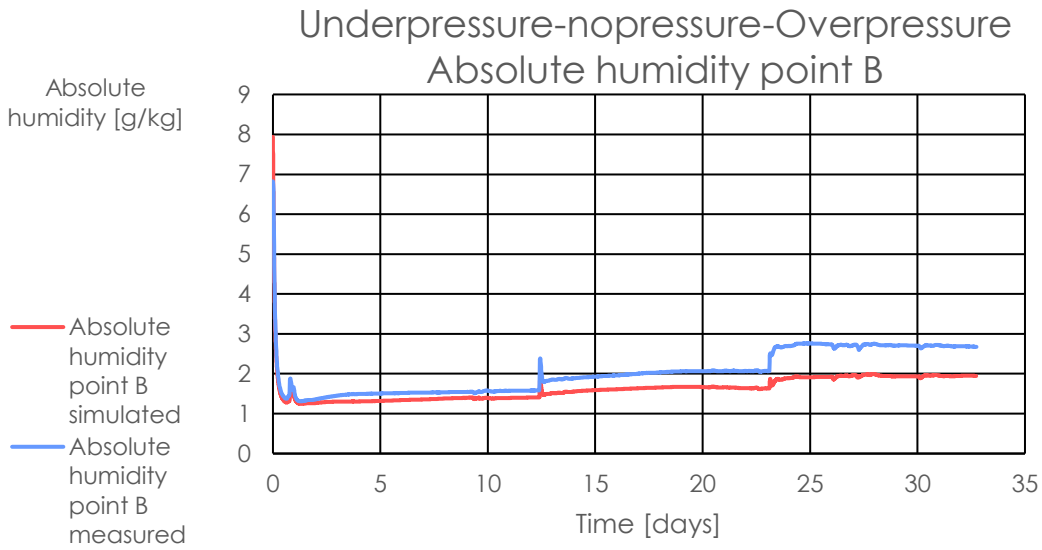


*Figure 30 Measured and simulated absolute humidities point B*

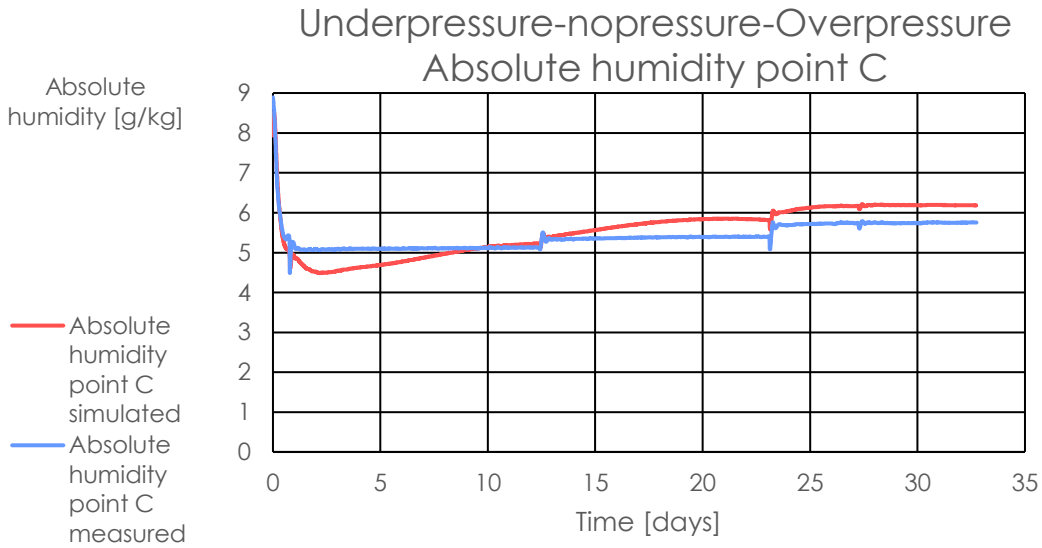


*Figure 31 Measured and simulated absolute humidities point C*

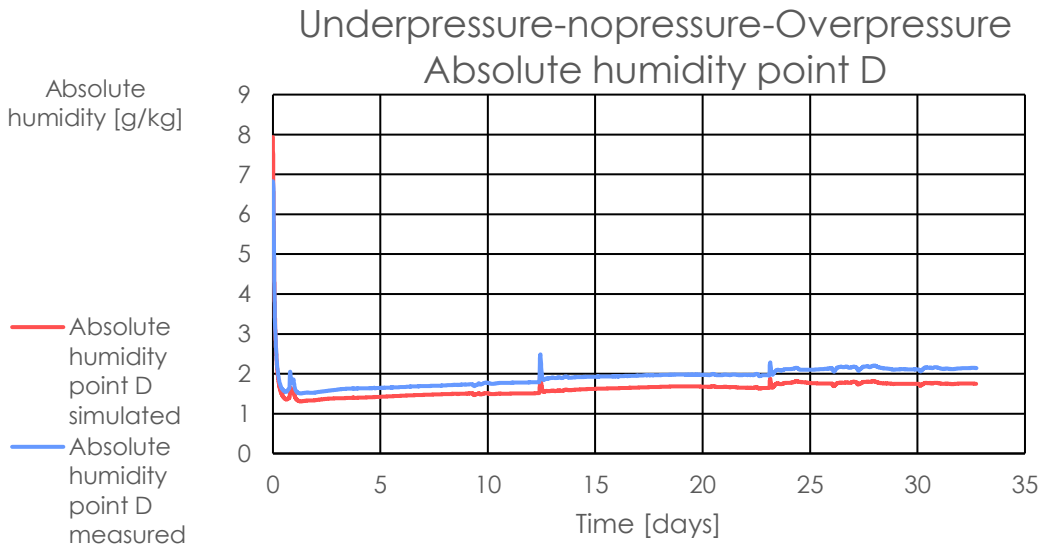


*Figure 32 Measured and simulated absolute humidities point D*

In Figure 29-32 one can see that the results for the absolute moisture content deviate less than the results for the relative humidity. The largest deviation can be observed at point B during over pressure. Here the simulated absolute moisture content is about 0.8 g/kg less than the measured values. Similar to what the results for the relative humidity showed, the points near the internal sheathing (points A and C) during no pressure and over pressure the simulated absolute moisture content is higher than the measured value. And at the points near the external sheathing the simulated moisture content is lower than the measured value. Also the results at point A show that the simulated values adapt less quickly to pressure changes than what was measured.

# VI: Comparison Delphin and COMSOL study

The results of the prior mentioned COMSOL study that also examined test wall 8 of the laboratory study were compared to the simulations in Delphin. In Figures 33-51 graphs and Figures from the study of Allué Hoyos C. (2014) have been used. The data from the Delphin simulations have been plotted onto the graphs from the study. All of the available results from the COMSOL study have been compared to the results simulated with Delphin for each of the pressure periods.

## VI-I Internal under pressure period

In Figures 33-35 the results from the COMSOL have been compared to the Delphin simulation results for the internal under pressure period. One can notice that the temperatures are comparable to the laboratory measurements. Results from Delphin and COMSOL were similar, though some differences could be noticed. These differences occur during the initial stage of the simulation and are caused by a difference in simulated boundary conditions. For Delphin measured dynamic boundary conditions were used compared to COMSOL which used static boundary conditions. The relative humidity results show a larger deviation from the laboratory measurements. Results from Delphin were closer to the measurements at the internal side (points A and C) of the construction whereas COMSOL was closer to the measurements at the external side of the construction (points B and D). Overall Delphin predicted lower relative humidities than COMSOL.

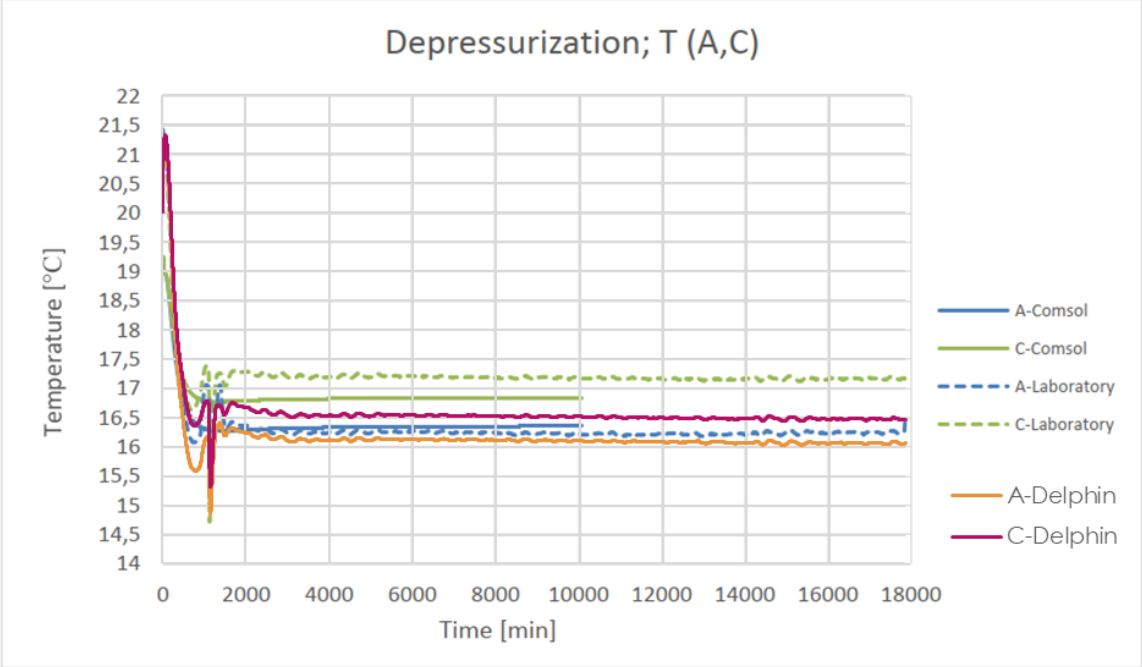


*Figure 33 Temperatures - Delphin, comsol and measured points A and C. COMSOL data copied from Applicability of COMSOL Multiphysics to combined heat, air and moisture transfer modeling in building envelopes. Cristina, Allué Hoyos (november 2014).*

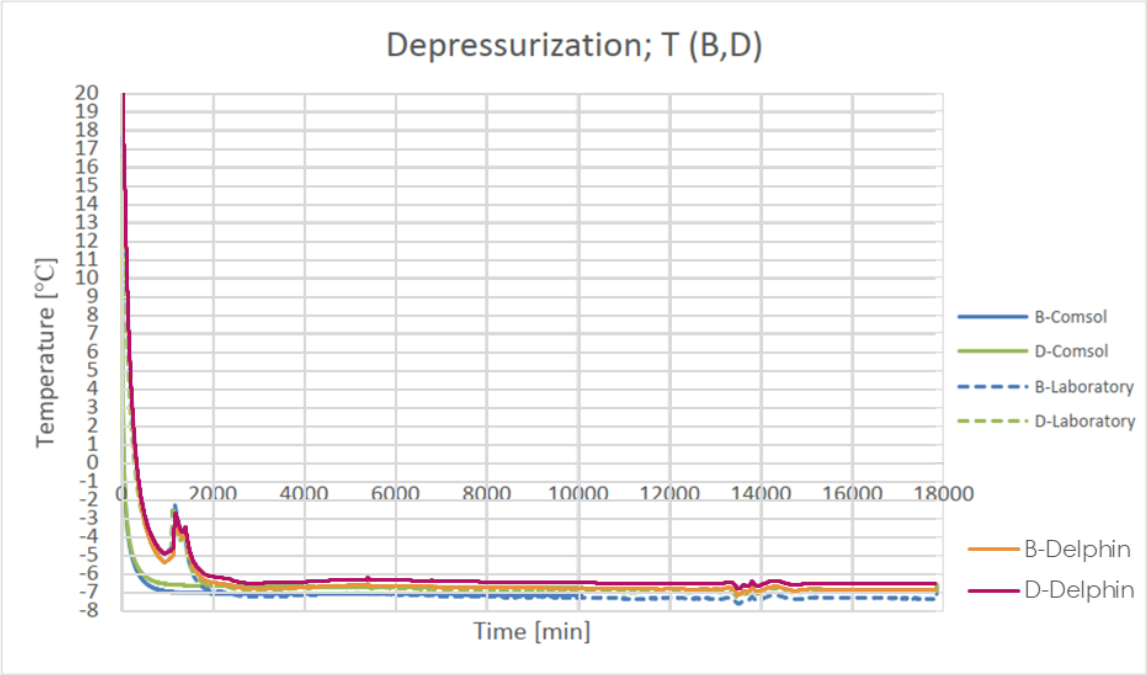


*Figure 34 Temperatures - Delphin, comsol and measured points B and D. COMSOL data copied from Applicability of COMSOL Multiphysics to combined heat, air and moisture transfer modeling in building envelopes. Cristina, Allué Hoyos (november 2014).*

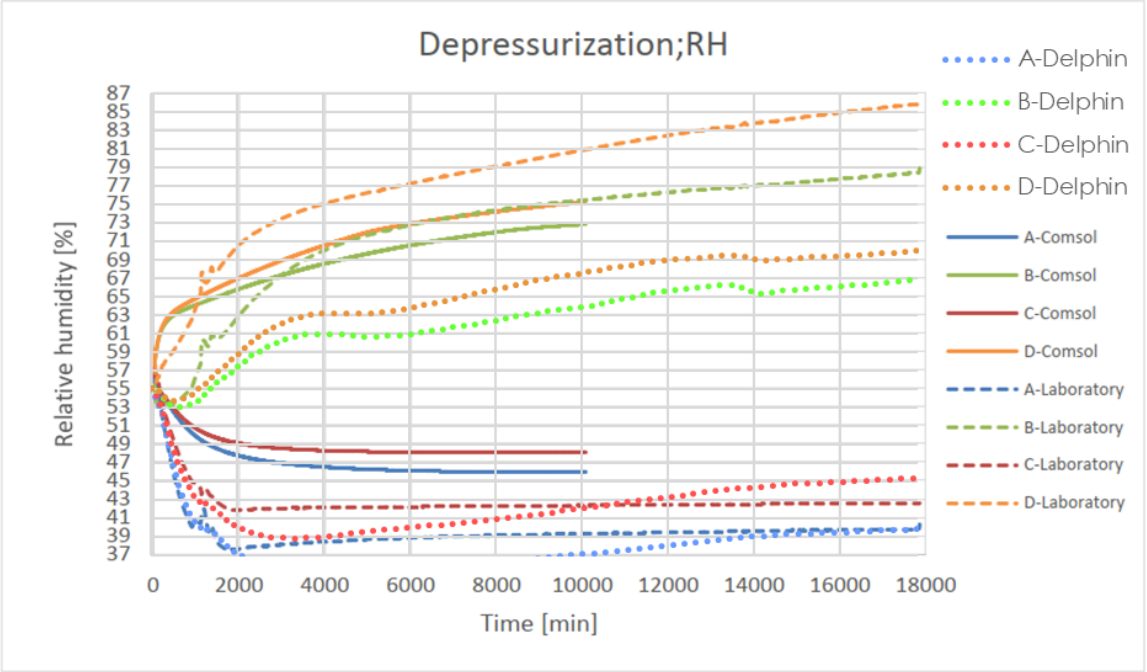


*Figure 35 Relative humidity - Delphin, comsol and measured points A, B, C and D. COMSOL data copied from Applicability of COMSOL Multiphysics to combined heat, air and moisture transfer modeling in building envelopes. Cristina, Allué Hoyos (november 2014).*

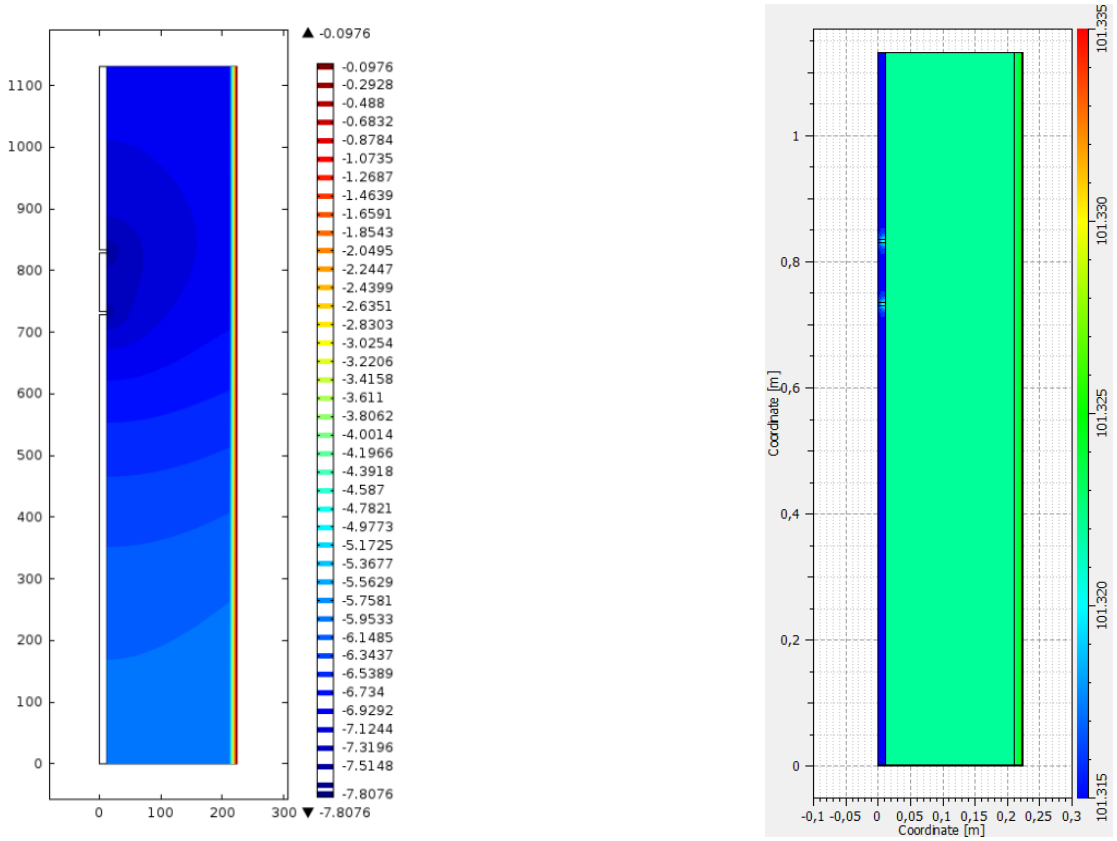


*Figure 36 Total gas pressure - COMSOL results left, Delphin results right. COMSOL image copied from Applicability of COMSOL Multiphysics to combined heat, air and moisture transfer modeling in building envelopes. Cristina, Allué Hoyos (november 2014).*

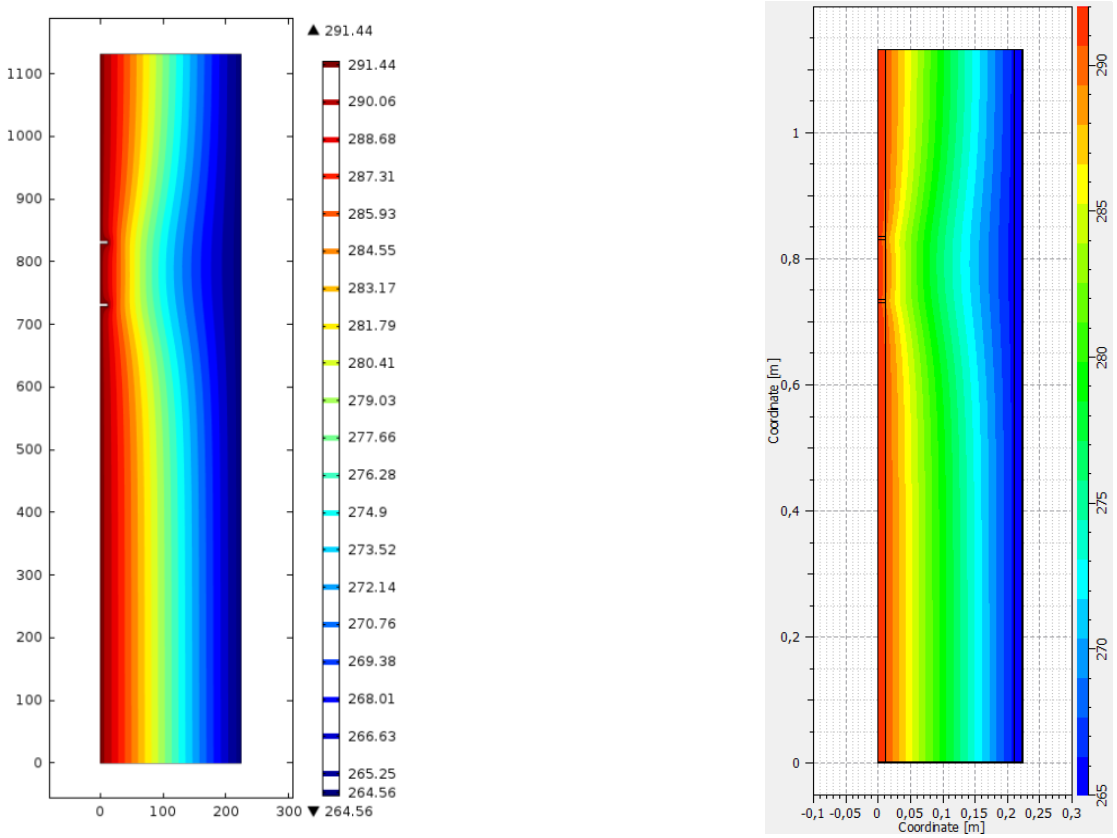


*Figure 37 Temperature - COMSOL results left, Delphin results right. COMSOL image copied from Applicability of COMSOL Multiphysics to combined heat, air and moisture transfer modeling in building envelopes. Cristina, Allué Hoyos (november 2014).*

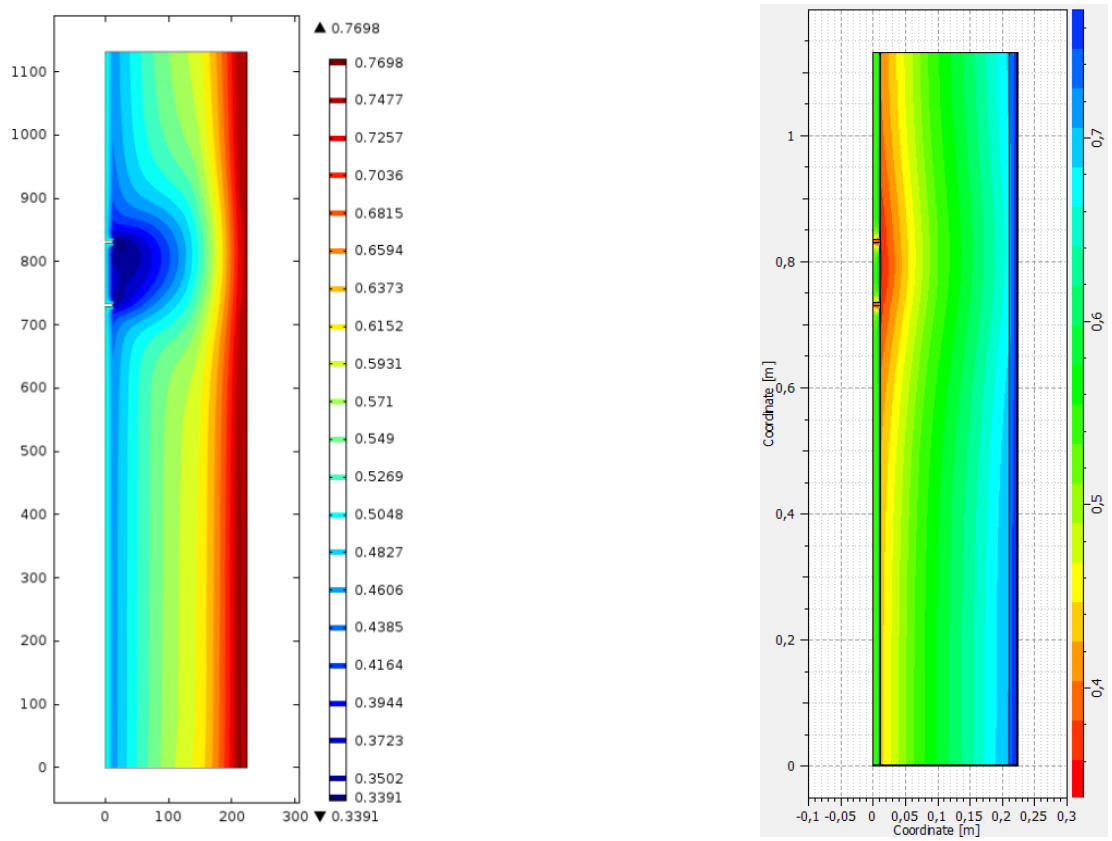


*Figure 38 Relative humidity - COMSOL results left, Delphin results right. COMSOL image copied from Applicability of COMSOL Multiphysics to combined heat, air and moisture transfer modeling in building envelopes. Cristina, Allué Hoyos (november 2014).*

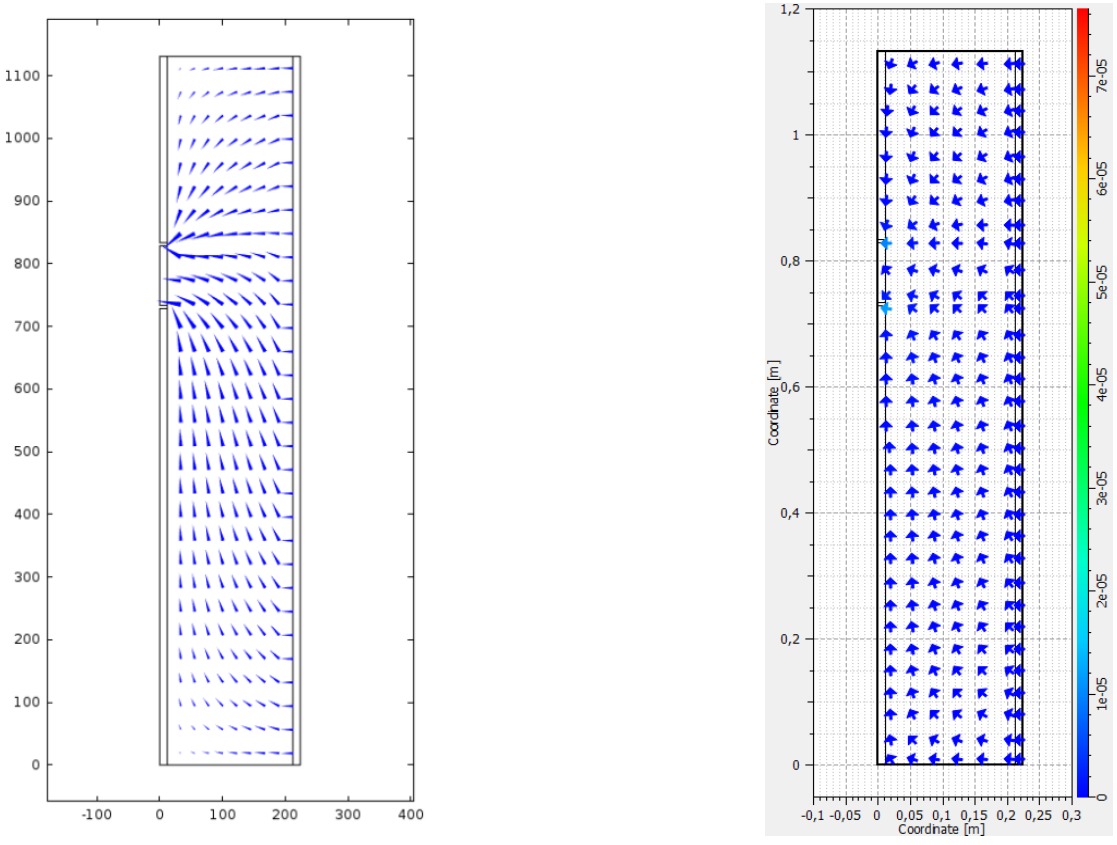


*Figure 39 Logarithmic velocity flow in COMSOL left, convective air flux in Delphin right. COMSOL image copied from Applicability of COMSOL Multiphysics to combined heat, air and moisture transfer modeling in building envelopes. Cristina, Allué Hoyos (november 2014).*

The Delphin and COMSOL results were further compared using the temperature, relative humidity, pressure and flow distribution graphics in Figures 36-39. Some differences can be observed. Firstly, in the pressure distribution graphics it can be seen that at the cellulose layer the pressure is slightly higher for the Delphin simulation. This difference is about 3 Pa and seems to be caused by the air gaps and internal sheathing. Secondly, Figures 37 and 38 show that the effect of the air gaps permeates further through the structure in the COMSOL simulations. Lastly, looking closely at the air gaps in the construction one can notice that the air in the gaps was not included in the COMSOL simulation. As the air in the gaps was included in the simulation in Delphin it could be one of the factors that cause the hygrothermal effect of the air gaps on the construction to be reduced.

## VI-II No pressure period

During the period of no pressure one can notice in Figures 40 and 41 that the temperature results of both Delphin and COMSOL are closer to the laboratory results at the external side of the constructions (points B and D). The relative humidity results in Figure 42 shows the opposite. Here, the results of the simulations are closer to the measurements at the internal side of the construction. Moreover, both simulations in Delphin and COMSOL underestimated the relative humidity at the internal side of the structure while overestimating the relative humidity at the external side of the construction.

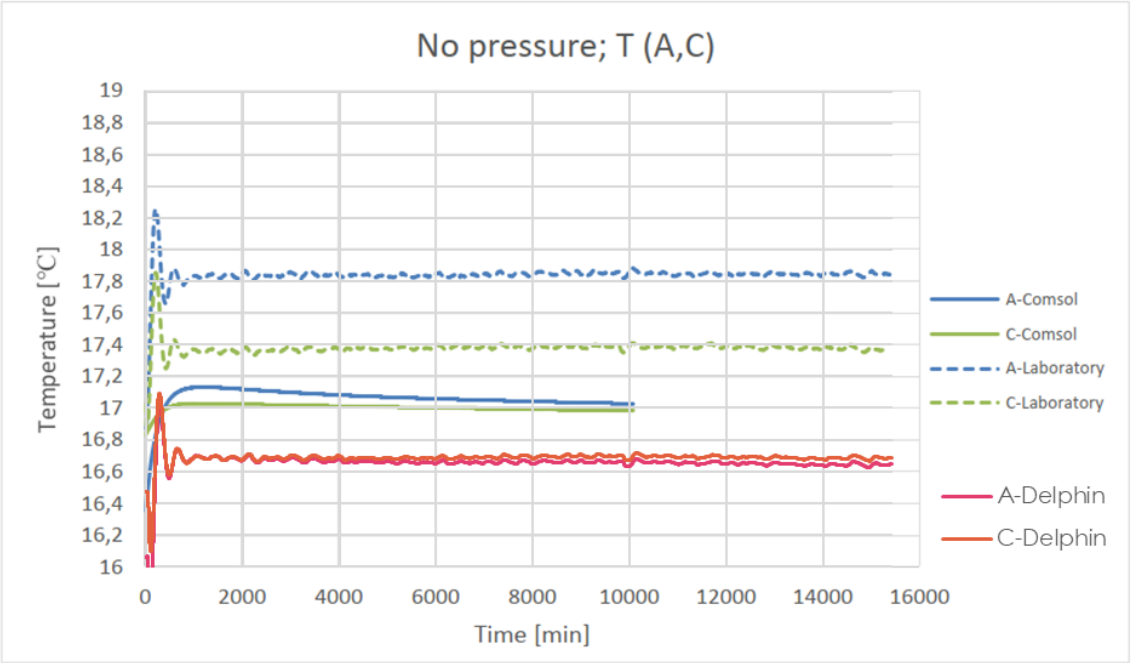


*Figure 40 Temperatures - Delphin, comsol and measured points A and C. COMSOL data copied from Applicability of COMSOL Multiphysics to combined heat, air and moisture transfer modeling in building envelopes. Cristina, Allué Hoyos (november 2014).*

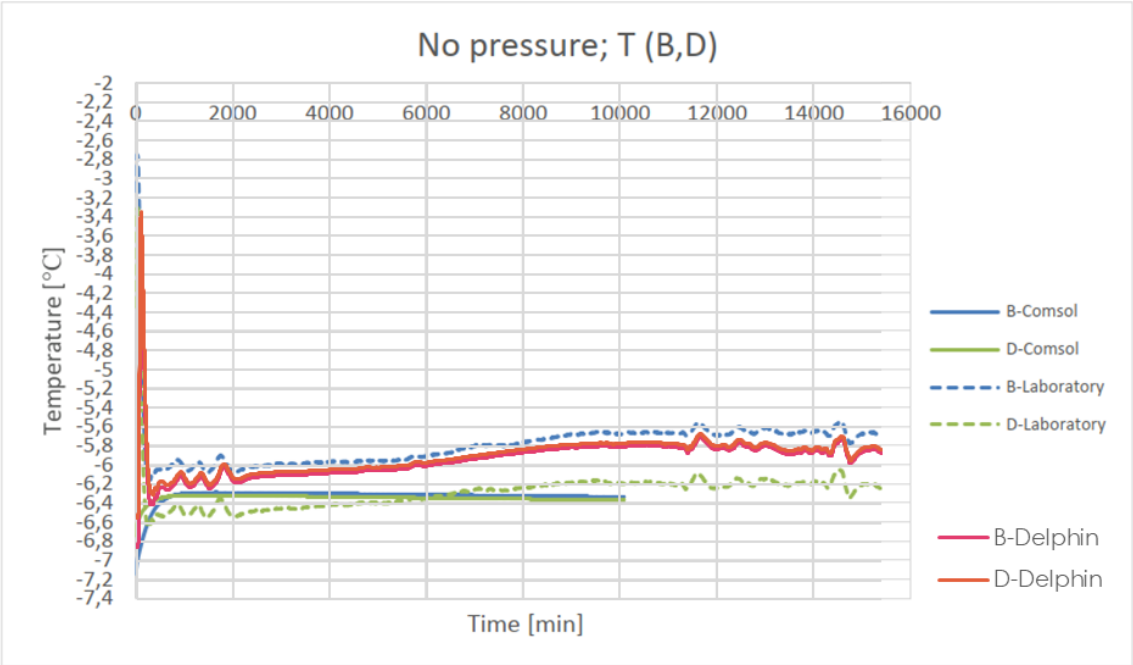


*Figure 41 Temperatures - Delphin, comsol and measured points B and D. COMSOL data copied from Applicability of COMSOL Multiphysics to combined heat, air and moisture transfer modeling in building envelopes. Cristina, Allué Hoyos (november 2014).*

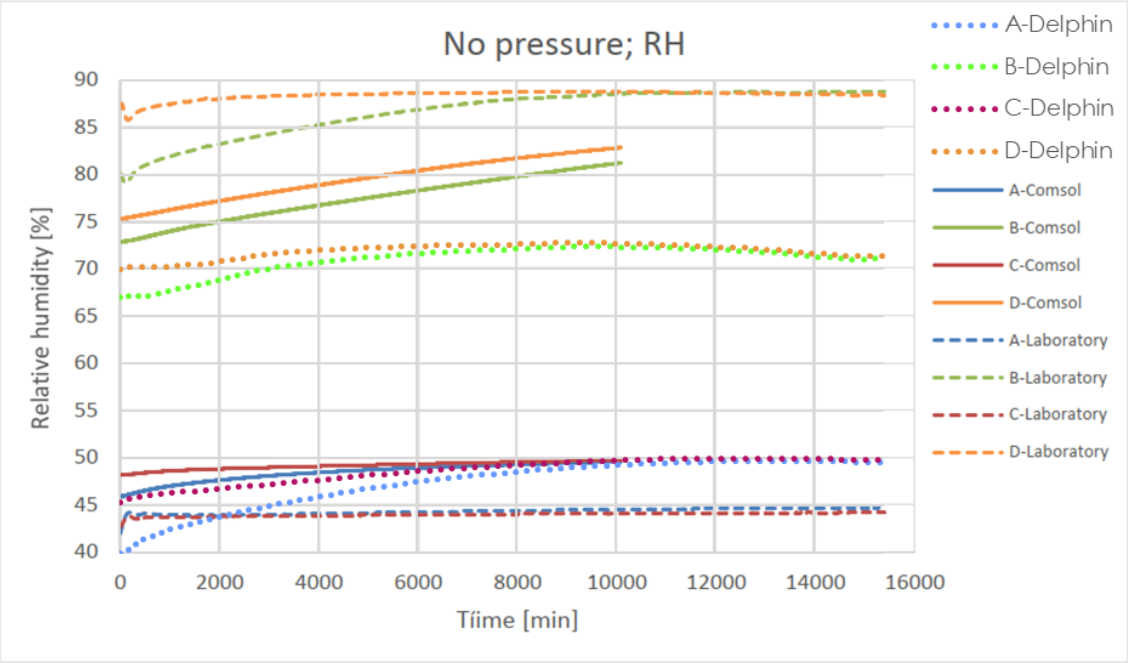


*Figure 42 Relative humidity - Delphin, comsol and measured points A, B, C and D. COMSOL data copied from Applicability of COMSOL Multiphysics to combined heat, air and moisture transfer modeling in building envelopes. Cristina, Allué Hoyos (november 2014).*

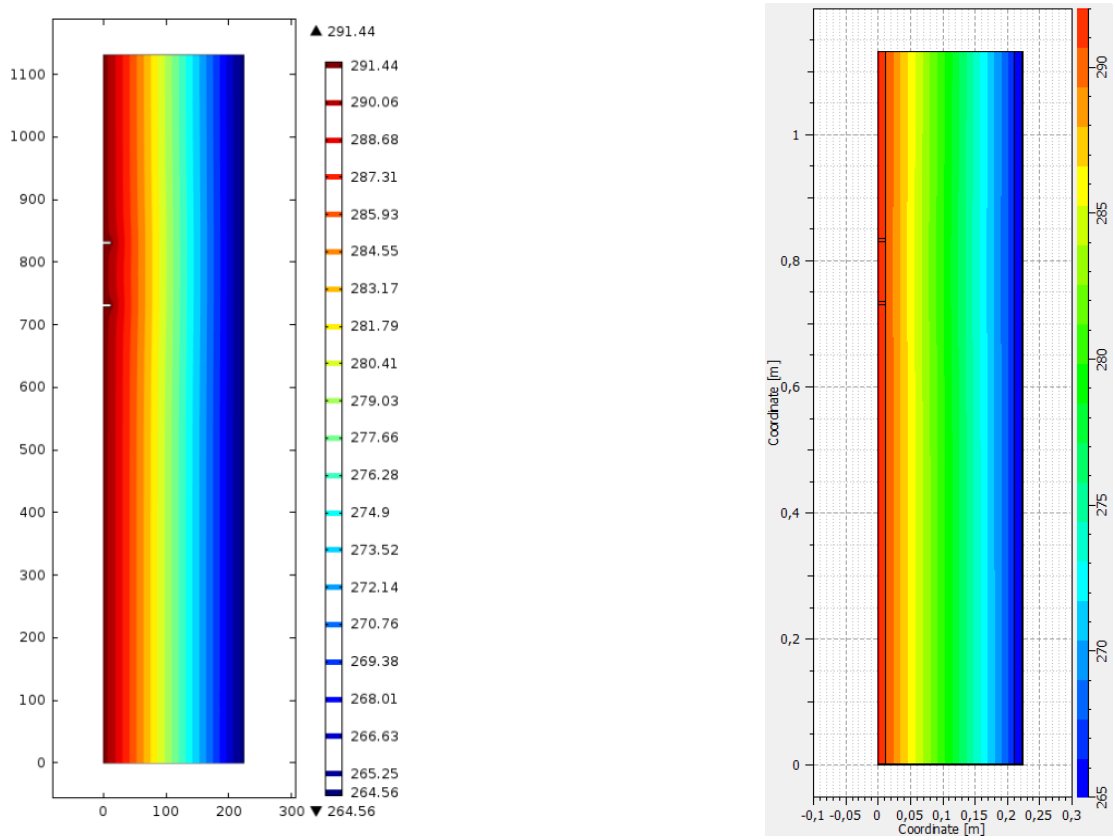


*Figure 43 Temperature - COMSOL results left, Delphin results right. COMSOL image copied from Applicability of COMSOL Multiphysics to combined heat, air and moisture transfer modeling in building envelopes. Cristina, Allué Hoyos (november 2014).*

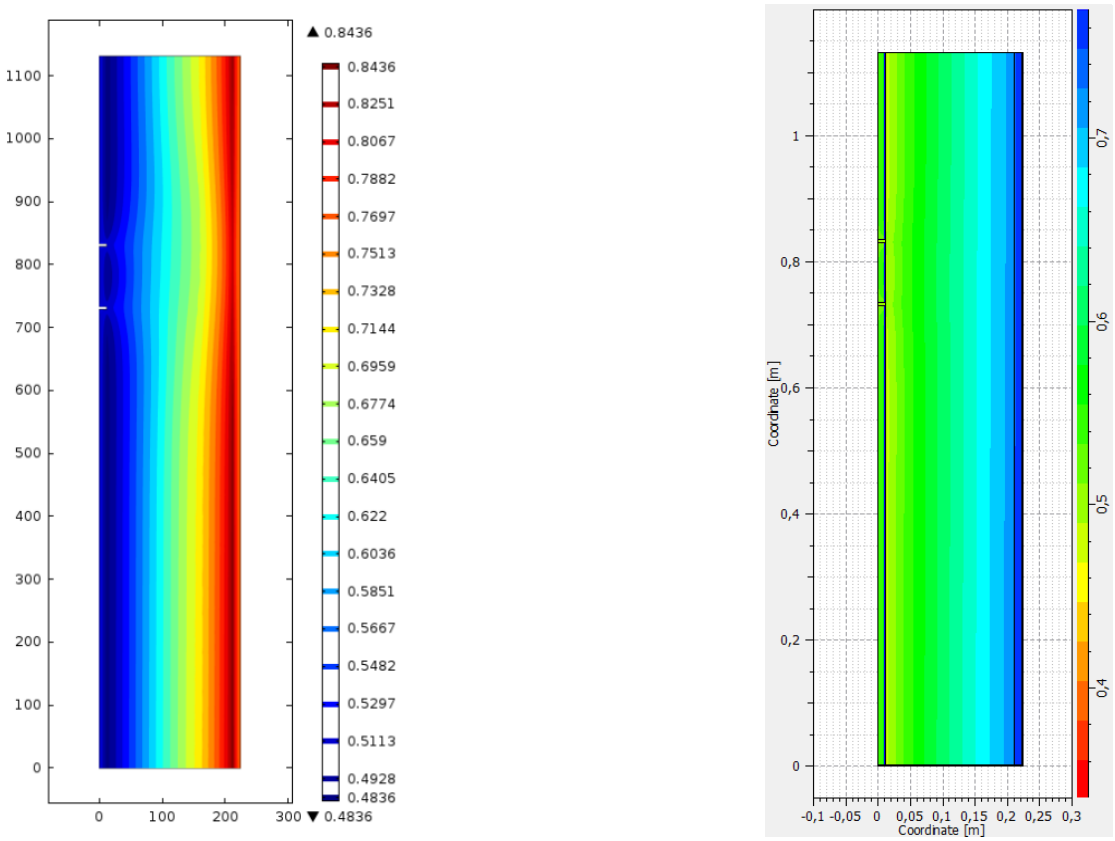


*Figure 44 Relative humidity - COMSOL results left, Delphin results right. COMSOL image copied from Applicability of COMSOL Multiphysics to combined heat, air and moisture transfer modeling in building envelopes. Cristina, Allué Hoyos (november 2014).*

The temperature and relative humidity distribution of the COMSOL and Delphin simulations in Figures 43 and 44 are similar. However, a slight difference can be noticed in the relative humidity distribution of the COMSOL simulation. Here, the effect of the air gaps can still be noticed compared to the relative humidity distribution from Delphin where the air gaps do not seem to impact the relative humidity.

## VI-III Internal over pressure period

During the period of over pressure the simulation results from Delphin and COMSOL also deviate from the laboratory measurements as can be seen in Figures 45-47. Results from the Delphin and COMSOL simulations are very similar for points A and C even though the laboratory measurements show higher temperature results. Especially point A shows a very large temperature deviation, which is interesting as it is the point closest to the air gaps. For points B and D the simulation results of COMSOL and Delphin are not in line and also deviate from laboratory results. Similar to point A, point B also shows a very large temperature deviation. Both points A and B are located behind the air gaps, therefore the air gaps could be the reason for the underestimation of the temperature in the simulations. The simulated relative humidities is also not quite in line with the measurement. For the points at the internal side of the construction (points A and C) the simulation results overestimate the relative humidity. At the points at the external side of the construction (points B and D) the relative humidity is underestimated, although COMSOL eventually reaches about the same relative humidities as the measurements for points B and D.

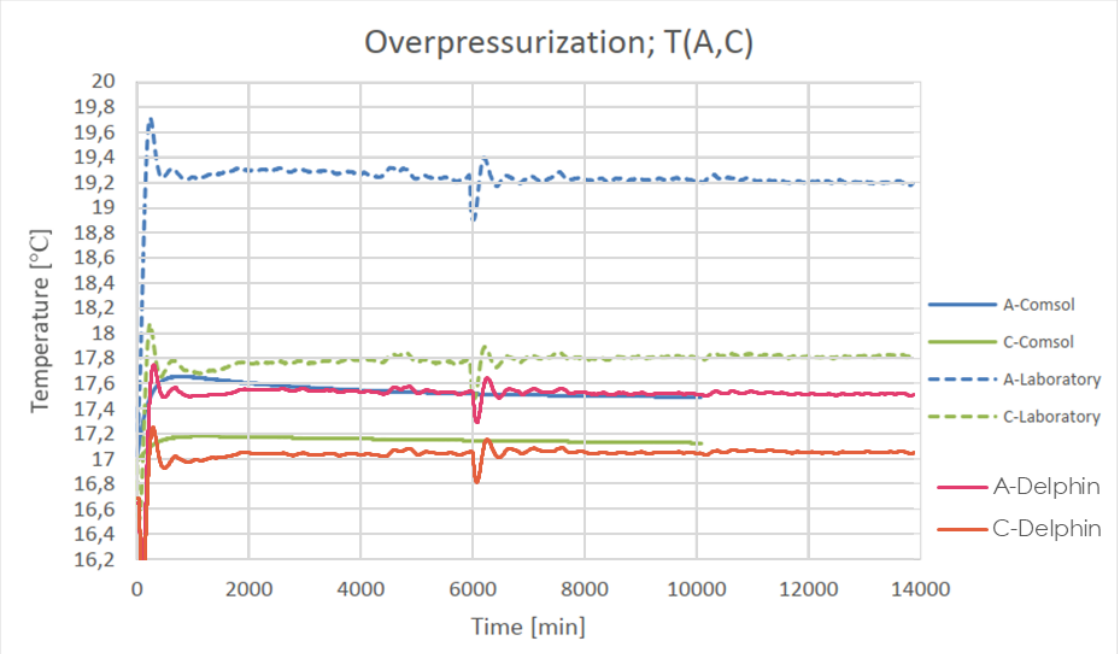


*Figure 45 Temperatures - Delphin, comsol and measured points A and C. COMSOL data copied from Applicability of COMSOL Multiphysics to combined heat, air and moisture transfer modeling in building envelopes. Cristina, Allué Hoyos (november 2014).*

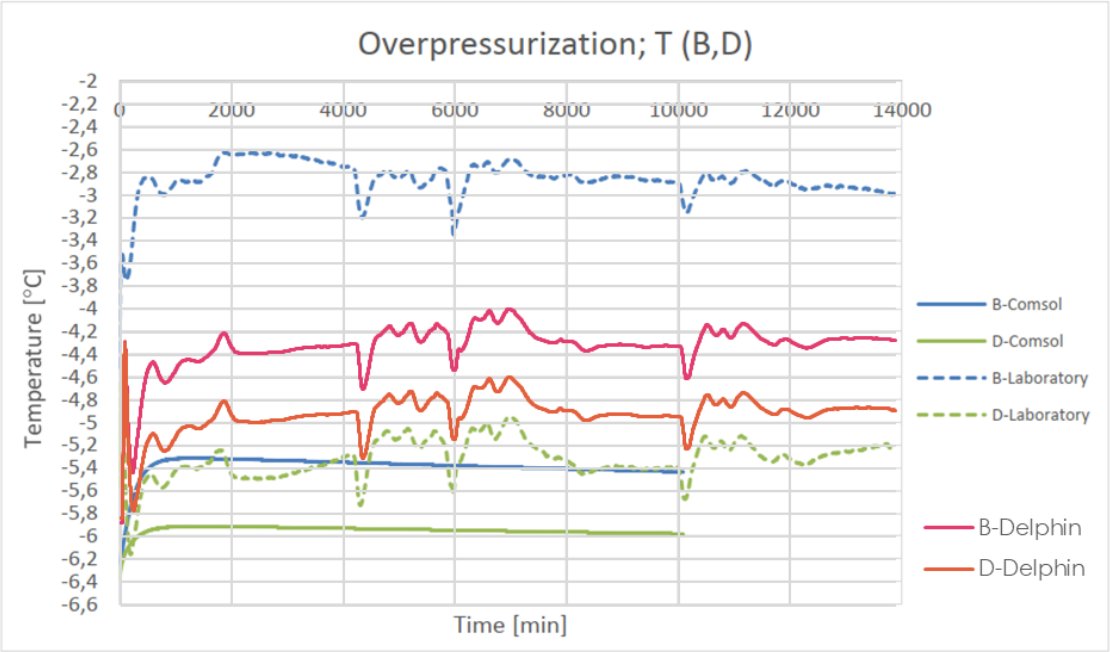


*Figure 46 Temperatures - Delphin, comsol and measured points B and D. COMSOL data copied from Applicability of COMSOL Multiphysics to combined heat, air and moisture transfer modeling in building envelopes. Cristina, Allué Hoyos (november 2014).*

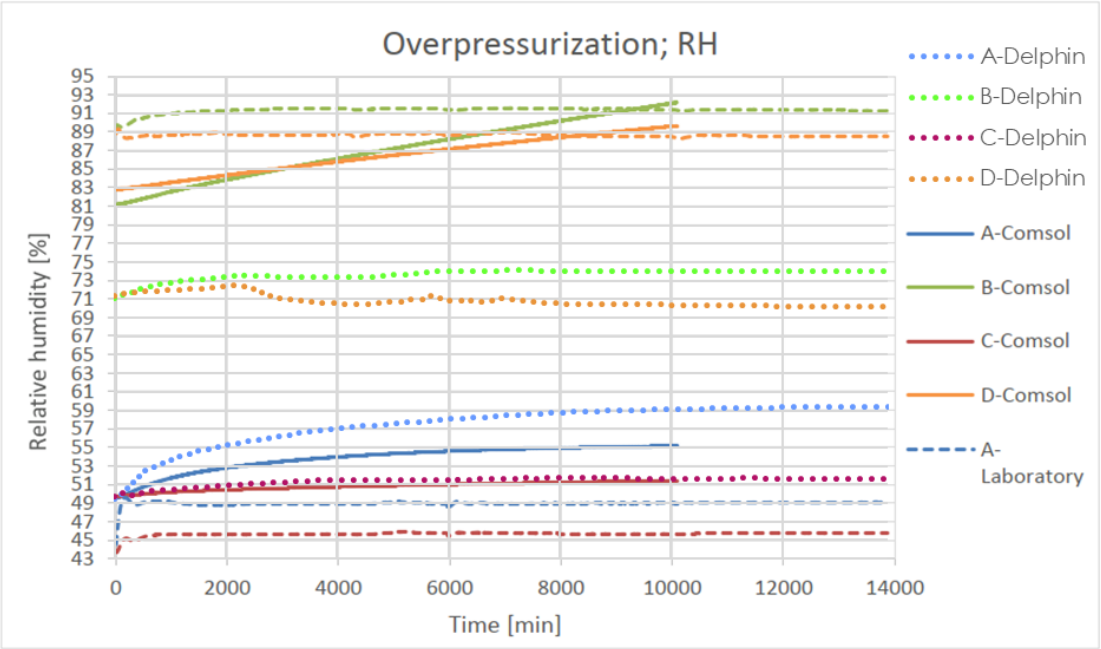


*Figure 47 Relative humidity - Delphin, comsol and measured points A, B, C and D. COMSOL data copied from Applicability of COMSOL Multiphysics to combined heat, air and moisture transfer modeling in building envelopes. Cristina, Allué Hoyos (november 2014).*

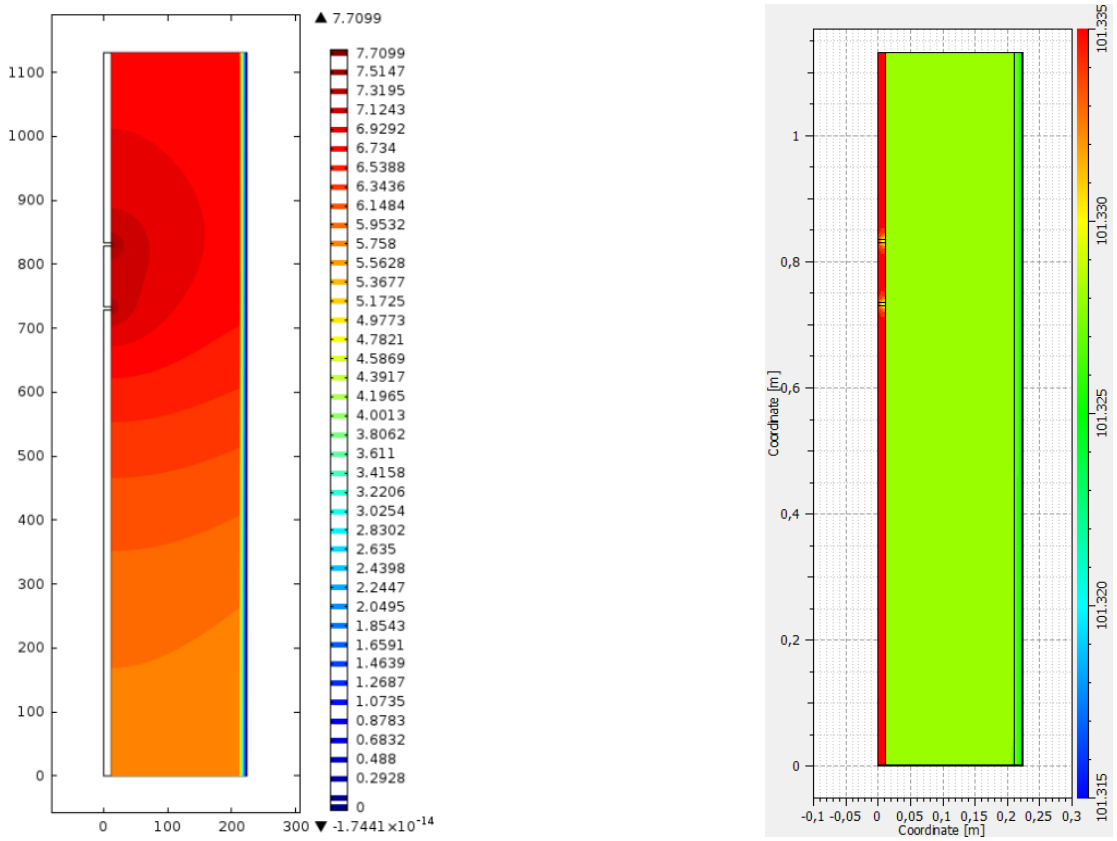


*Figure 48 Total gas pressure - COMSOL results left, Delphin results right. COMSOL image copied from Applicability of COMSOL Multiphysics to combined heat, air and moisture transfer modeling in building envelopes. Cristina, Allué Hoyos (november 2014).*

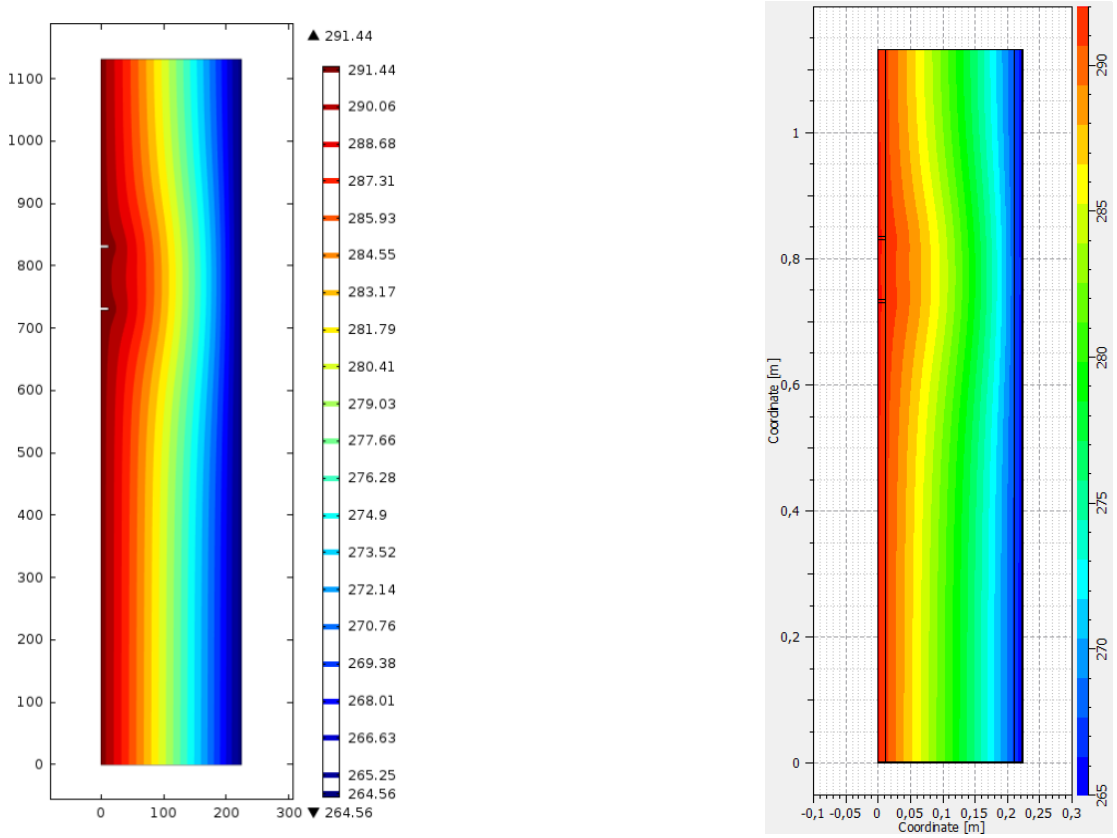


*Figure 49 Temperature - COMSOL results left, Delphin results right. COMSOL image copied from Applicability of COMSOL Multiphysics to combined heat, air and moisture transfer modeling in building envelopes. Cristina, Allué Hoyos (november 2014).*

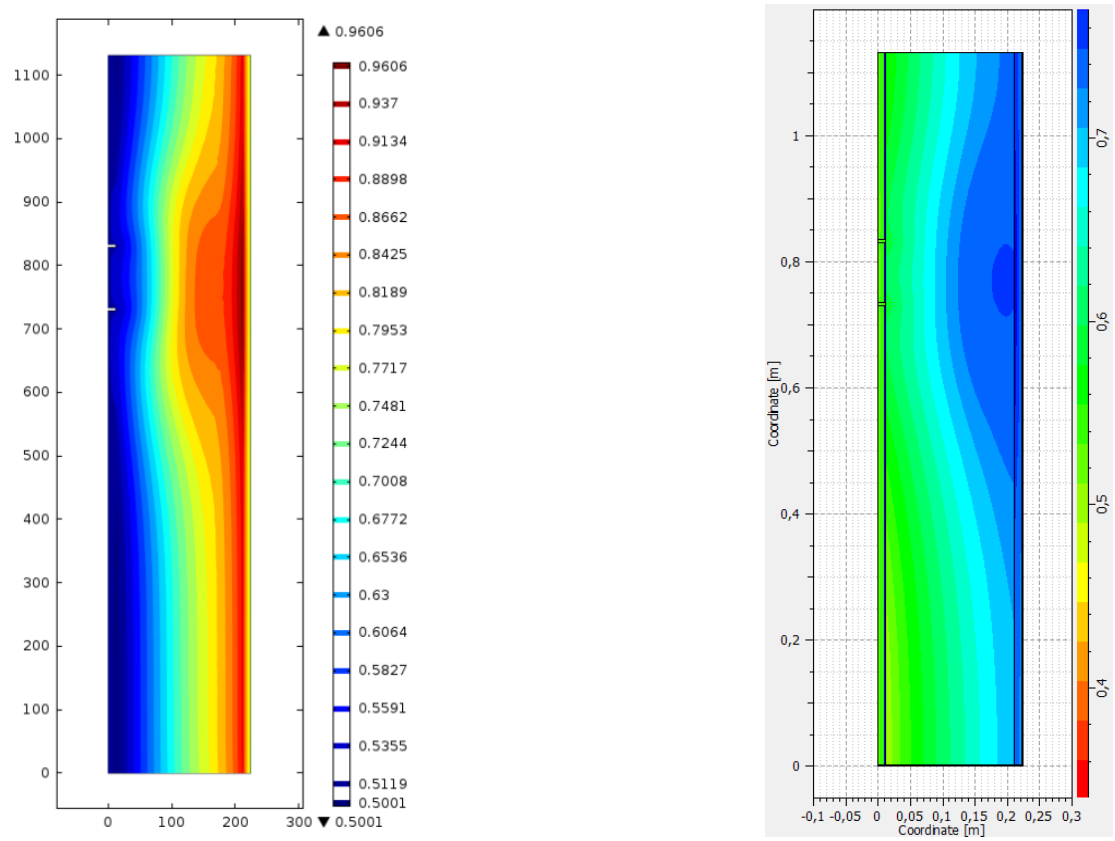


*Figure 50 Relative humidity - COMSOL results left, Delphin results right. COMSOL image copied from Applicability of COMSOL Multiphysics to combined heat, air and moisture transfer modeling in building envelopes. Cristina, Allué Hoyos (november 2014).*

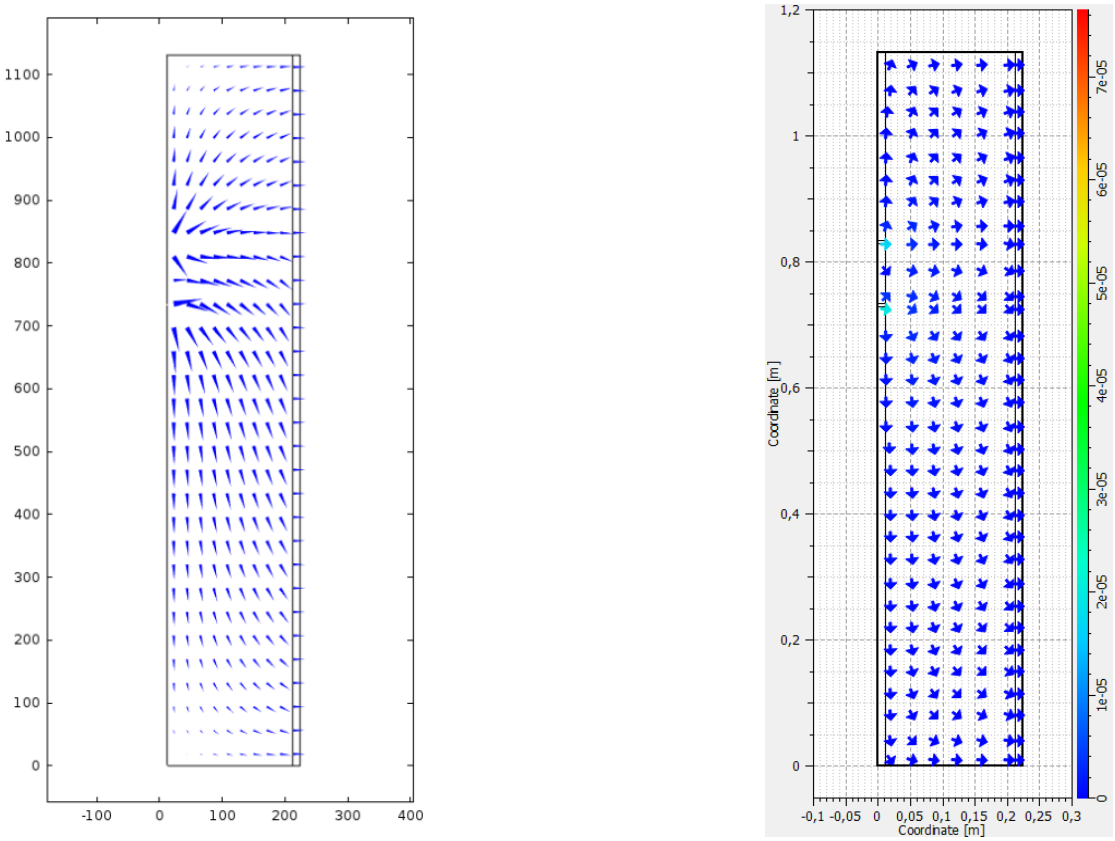


*Figure 51 Logarithmic velocity flow in COMSOL left, convective air flux in Delphin right. COMSOL image copied from Applicability of COMSOL Multiphysics to combined heat, air and moisture transfer modeling in building envelopes. Cristina, Allué Hoyos (november 2014).*

In the pressure, temperature, relative humidity and flow distribution Figures 48-51 one can notice differences. Comparable to the finding for the internal pressure period, the distribution graphic shows a different pressures in the cellulose layer. In this graphic the simulated gas pressure in COMSOL in the cellulose layer is slightly higher. Again, the sheathing and air gaps seem to have a larger impact on the pressure in the Delphin simulation than in the COMSOL simulations. The temperature and relative humidity distributions in Figures 49 and 50 show comparable results for both simulations and the flow distributions in Figure 51 are also similar.

# VII: Sensitivity analysis

In order to further investigate the effect of convective air transport sensitivity analysis was performed. First, the case study is simulated with and without air transport enabled in order to examine the added effect of convection. In addition, the effect of pressure differences was also simulated and examined. Pressure differences of 0 to 20 Pa were simulated over intervals of 5 Pa. The results show the influence of different pressures over the structure.

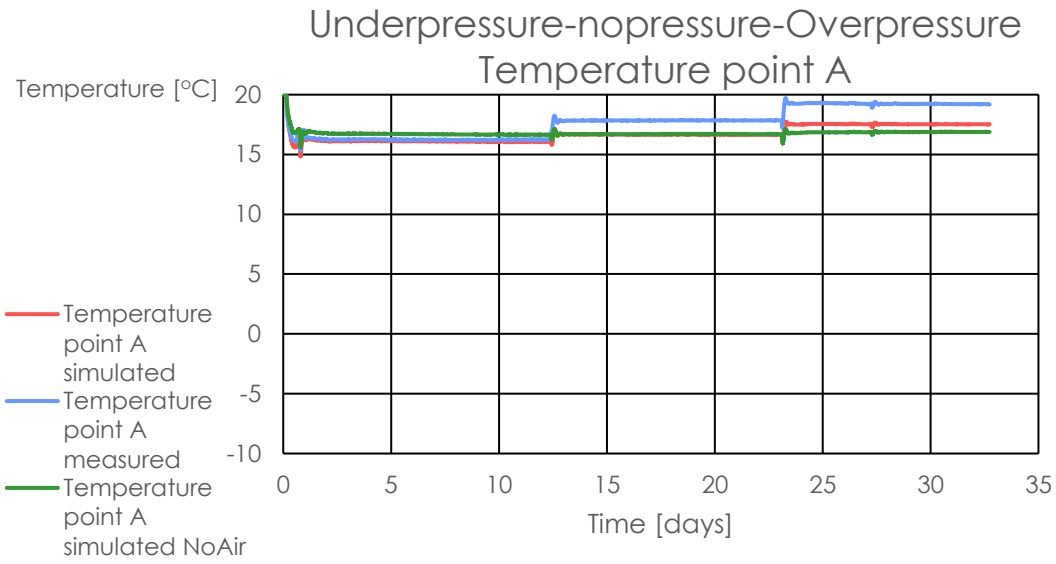


*Figure 52 Measured and simulated temperatures point A with and without convective transport*

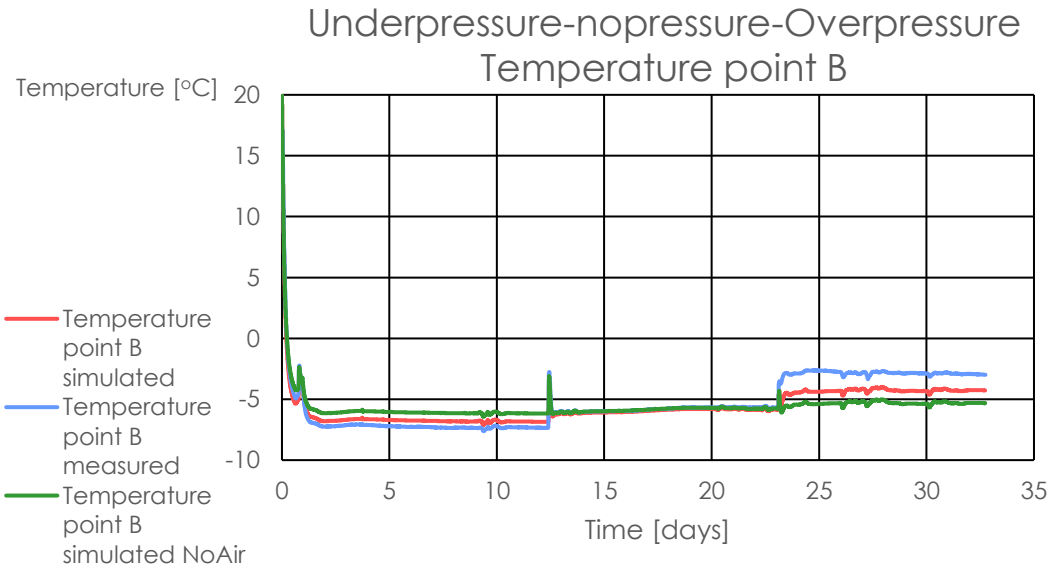


*Figure 53 Measured and simulated temperatures point B with and without convective transport*

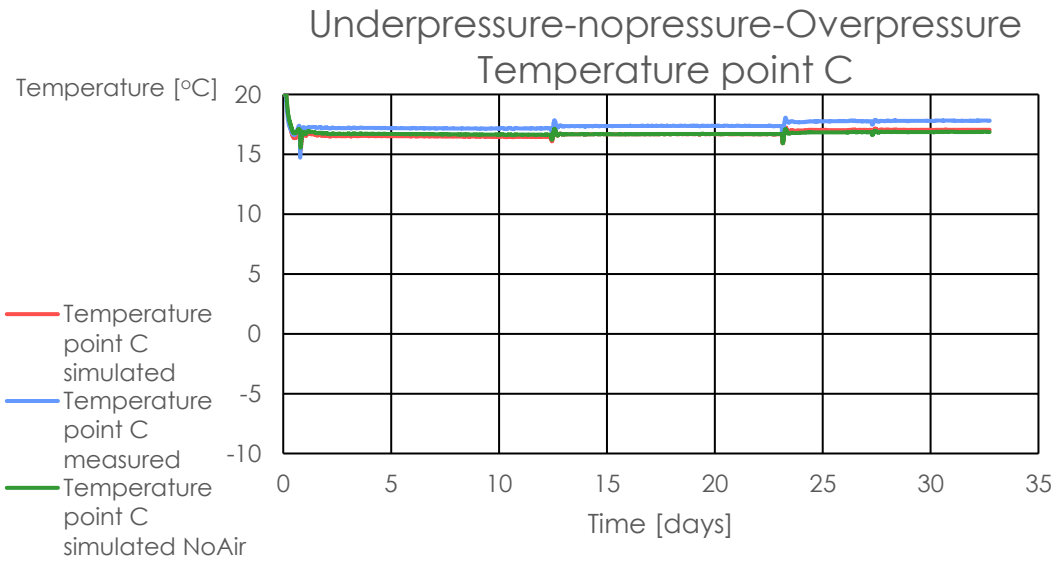


*Figure 54 Measured and simulated temperatures point C with and without convective transport*

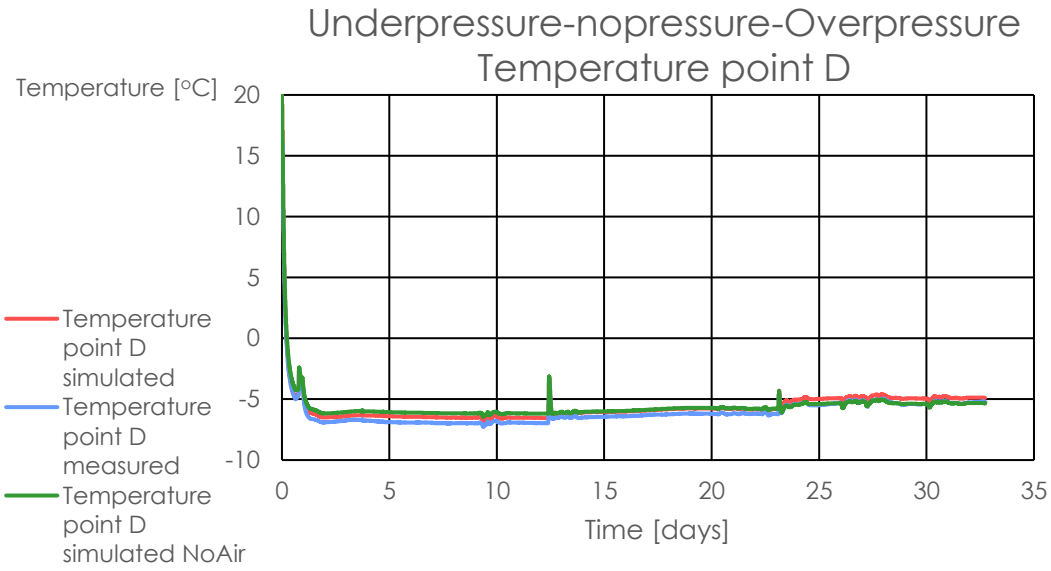


*Figure 55 Measured and simulated temperatures point D with and without convective transport*

The simulated temperatures in Figures 52-55 show a limited effect of convection. Especially points D and D which are furthest from the air gaps show almost no difference in results when air transport is excluded. Results from points A and C do show a small difference caused by convective air transport though the largest difference in temperature is only about 1 °C. Nevertheless, the results show that the simulated temperatures are closer to the measured results when convective air transport is included.

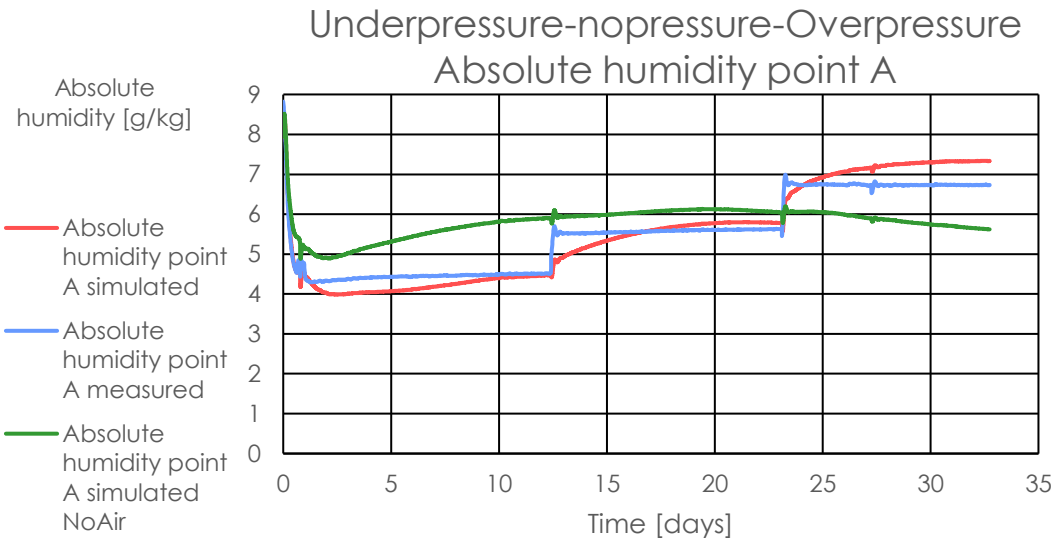


*Figure 56 Measured and simulated absolute humidities point A with and without convective transport*

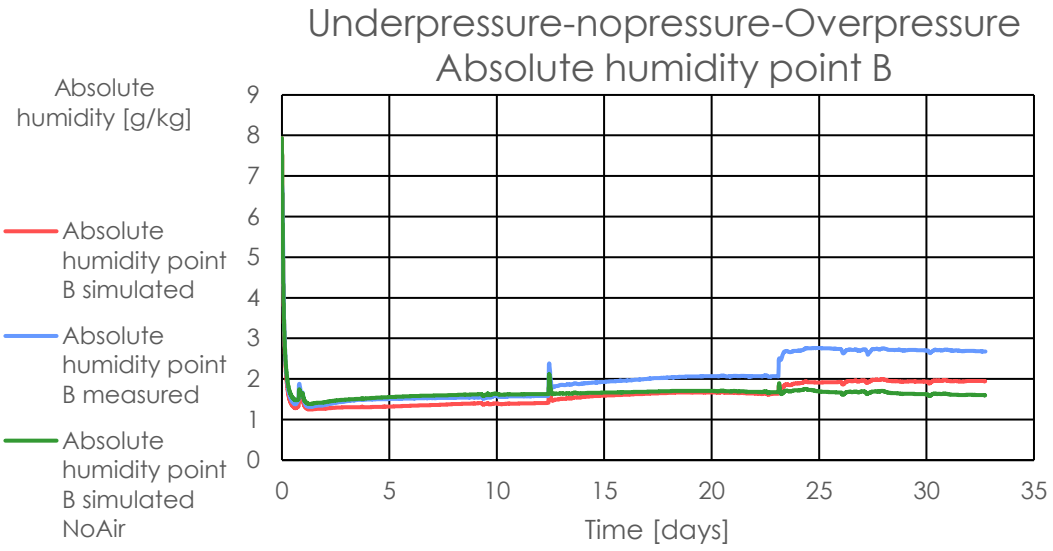


*Figure 57 Measured and simulated absolute humidities point B with and without convective transport*

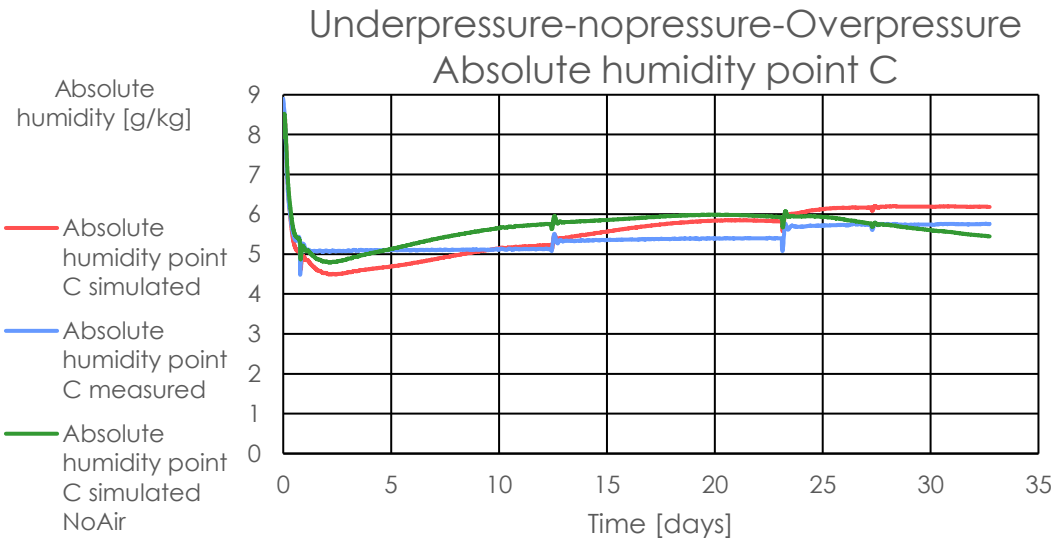


*Figure 58 Measured and simulated absolute humidities point C with and without convective transport*

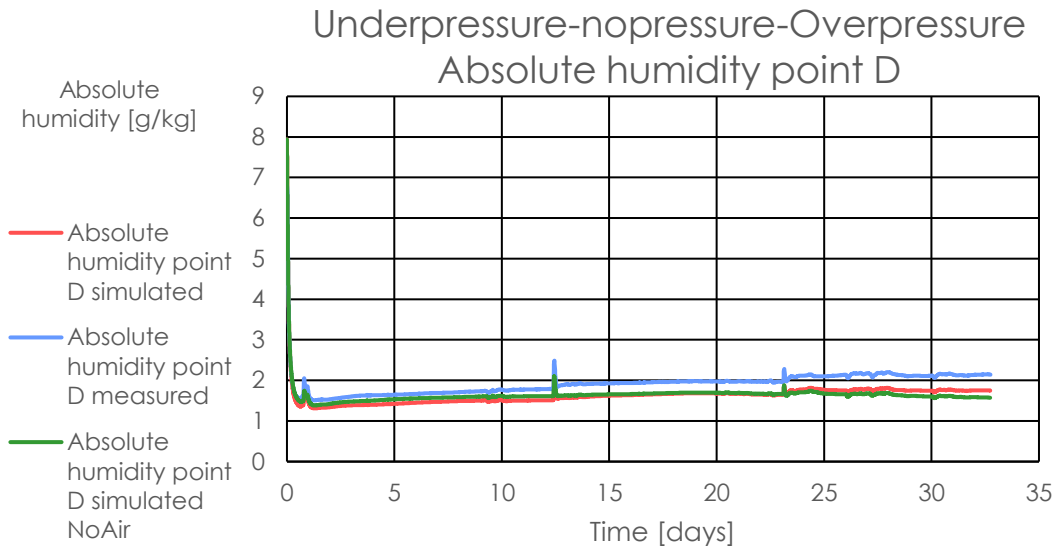


*Figure 59 Measured and simulated absolute humidities point D with and without convective transport*

In Figures 56-59 the simulated absolute humidities are shown. One can easily notice the influence of convective air transport as the results in points A and C are much closer when convective air transport is included. The impact of convective air transport is the largest near point A which is closest to the air gaps and the convective air transport has the least impact near point D which is furthest from the air gaps. It can also be noticed that the convective air transport reduces the absolute humidity during the internal under pressure phase, while it increases the absolute humidity during the internal over pressure phase. During the under pressure phase the drier air from the outside is forced by convection to flow through the structure and during the over pressure phase the humid internal air is forced to flow through the structure. Overall the convective air transport brings the simulated results closer to the measurements.

In Figures 60-63 the same case study has been simulated multiple times. In the simulations only one parameter was changed. Multiple pressure differences across the structure have been simulated between 0 – 20 Pa in intervals of 5 Pa. The previous simulations showed that air convection did not really impact the temperatures. This is why only the absolute humidities are shown in the graphs below.

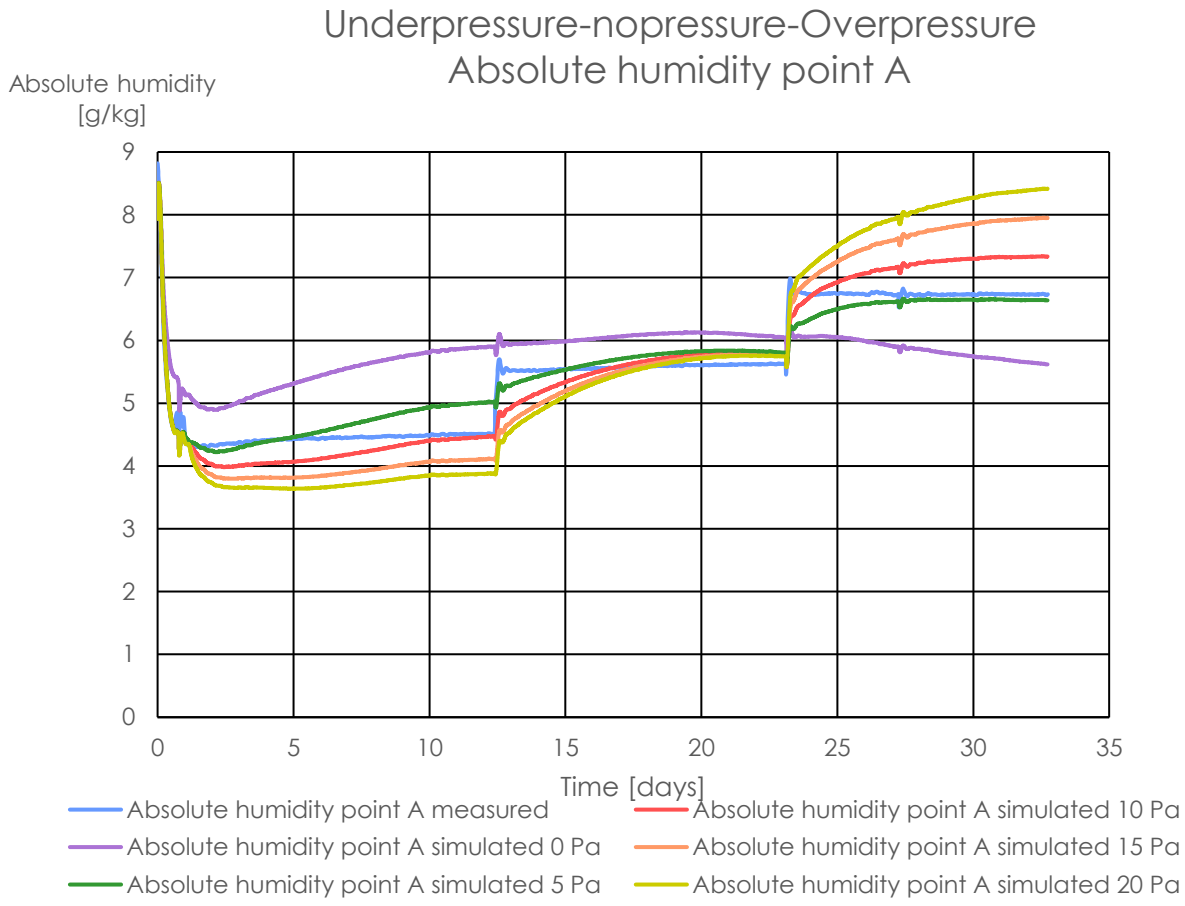


*Figure 60 Measured and simulated absolute humidities at point A for multiple pressure differences*

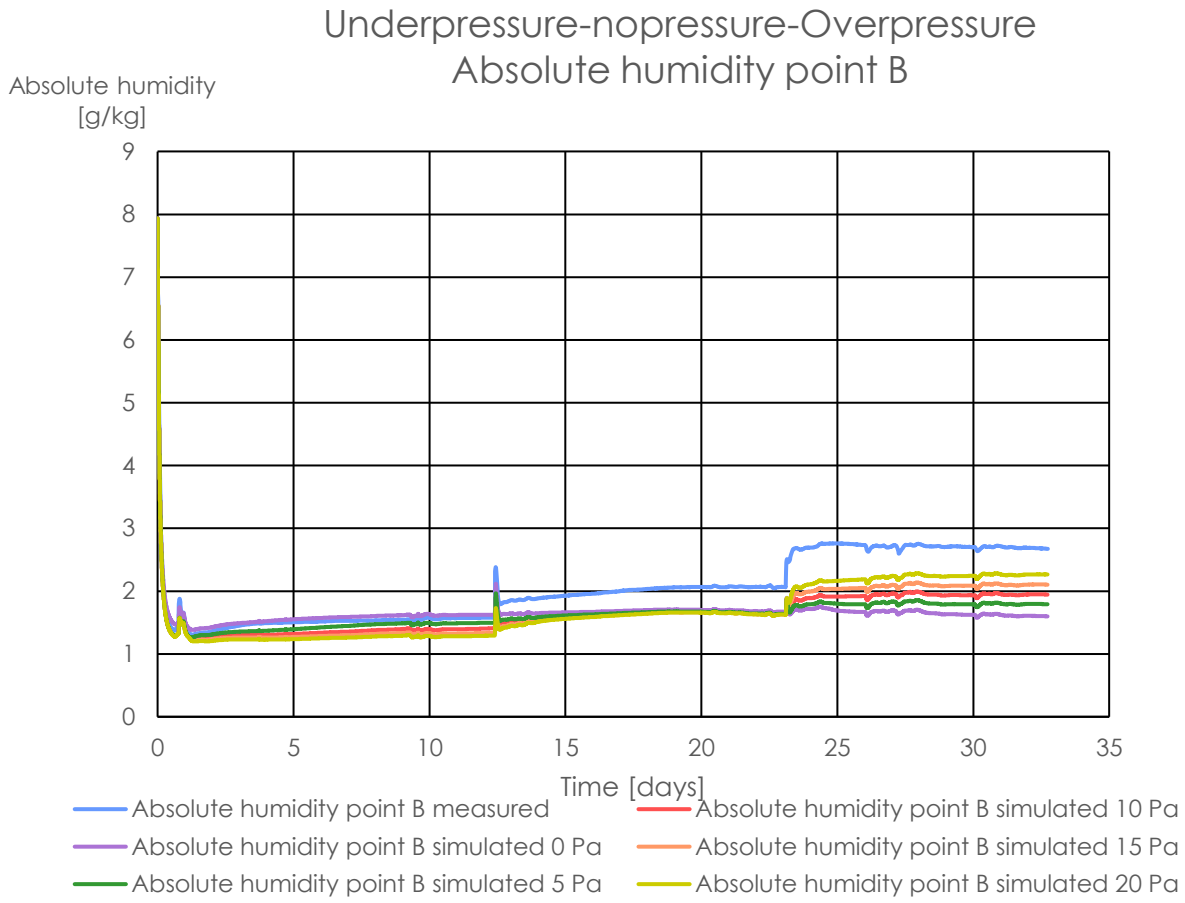


*Figure 61 Measured and simulated absolute humidities at point B for multiple pressure differences*

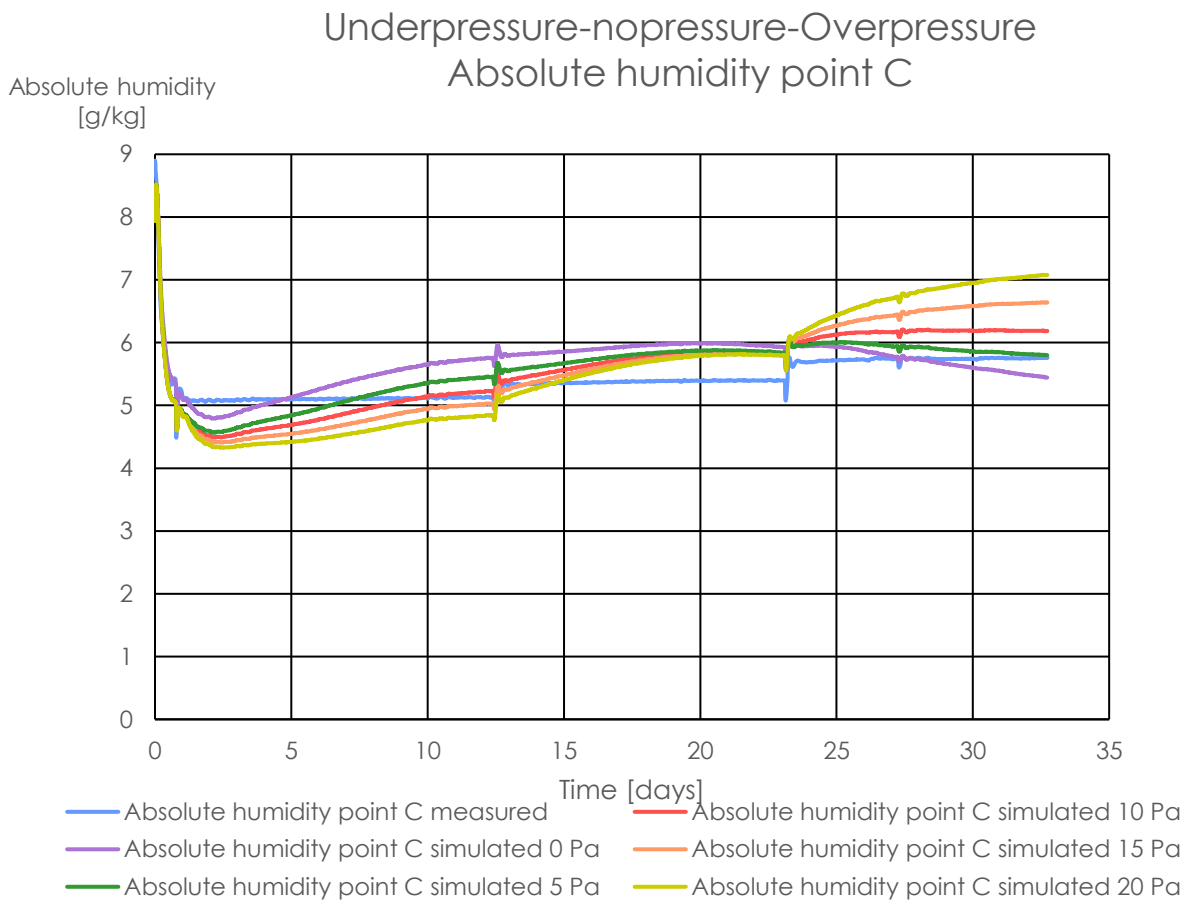


*Figure 62 Measured and simulated absolute humidities at point C for multiple pressure differences*

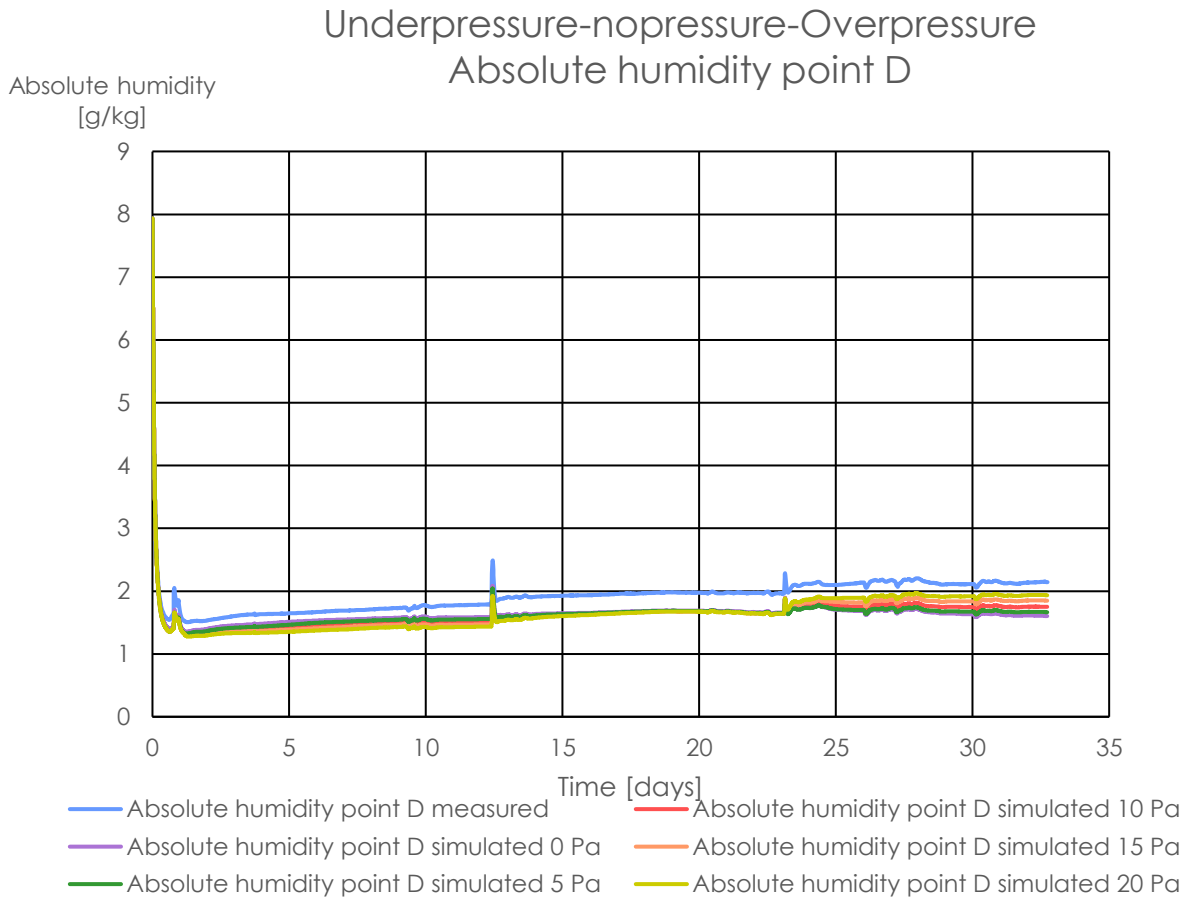


*Figure 63 Measured and simulated absolute humidities at point D for multiple pressure differences*

Looking at Figures 60-63 one can notice that overall the impact of different pressures across the structure is much less for points B and D as compared to points A and C. The reason for this might be that points B and D are located at the external side of the structure and the convective air does not permeate as far through the structure. Another interesting finding is the difference in results comparing different pressures at point A. Looking closely one can see that the difference between a 0 Pa and 5 Pa pressure over the structure shows a larger change than 5 Pa and 10 Pa. It seems that the gradual increase of pressure over the structure has a decreasing effect on the convective moisture transport the further it increases. This is especially clear comparing the difference of absolute humidity for 0 Pa - 5 Pa and 15 Pa - 20 Pa.

# VIII: Conclusion

From the literature study it was concluded that there are limited studies which include convection, three dimensional modeling or whole building simulation coupling in hygrothermal risk assessment. Even though programs such as Delphin or COMSOL offer the possibility, it is not often utilized. The addition of these aspects in hygrothermal risk assessment increases the complexity and computational need and may not always be necessary. Nevertheless the effect of these aspects on hygrothermal risk assessment is not clear as very few cases have been assessed. This emphasizes the need for additional research. It was also found that currently COMSOL, Delphin and WUFI are most often used in hygrothermal risk assessment. Both Delphin and COMSOL include all methods of HAM transport and have an option to model in 3D. Based on these capabilities, Delphin and COMSOL both would be suited to evaluate hygrothermal risk assessment of refurbished buildings. However, it should be noted that during the study it was found that there were some issues when modeling convective air transport in 3D using Delphin. This is further explained in the limitations of this study.

In this study, convection simulation has been assessed using measurement data from laboratory measurements. The study regarded a timber frame wall structure where holes were drilled through the internal sheathing and vapor barrier. This allowed for convective transport through the construction. The wall structure was measured during a period of under pressure, no pressure and over pressure. Using Delphin the wall structure was simulated. Model validation indicators have been used to assess the fit of the simulation model. The indicators showed a good fit for all of the simulated temperatures, but they also showed that the model could not be fully validated regarding the relative and absolute humidities. At the external sheathing (points B and D) an underestimation for the relative and absolute humidity could be observed. On the other hand near the internal sheathing the results were more in line and only showed a slight overestimation regarding the humidity. Another interesting finding is that the convective and diffuse vapor flux results show that diffusion is impacted by convection through the structure. During internal over pressure the diffusive vapor flow is reduced by the convective vapor flow as they move in opposite directions. On the other hand during internal under pressure the diffusive vapor flow is increased by convection as they move in the same direction.

From the convection study one can conclude that the hygrothermal risk was not accurately simulated using the Delphin model with a dynamic indoor climate and convective HAM transport. The simulated results are relatively close to the measured values which indicates that it should be possible to accurately simulate convection, but this was not achieved in this study. One of the reasons for this could be the simplification of using a two-dimensional model for a construction where three-dimensional modeling is necessary as the holes drilled in the construction could not be modelled in 2D. Because of the 2 dimensional modeling the gaps in de construction are much larger than in the laboratory study which impacts the velocity of the flow through the structure. As the area of the air gaps is much larger while the flow rate remains the same the velocity of the flow rate will be greatly decreased. This might also be the reason as to why the results from Delphin take longer to adapt to sudden changes of conditions. A second reason could be the limited availability of material properties. More detailed materials properties could lead to different simulation results. One

can conclude that three-dimensional modeling is essential when looking at the effect of convection through leaks in the construction. Also, a lot of different material properties are needed to model convection and there is a limited availability. Additional material measurements of material properties would be necessary to help with convection modeling.

The results of the simulation in Delphin were also compared to the results of a study carried out by C. Allué Hoyos (2014). In this study the laboratory setup was simulated using COMSOL. In the comparison it was found that some of the simulated results were very close, but there were also large differences. One of the reasons for these differences is the use of static boundary conditions in the COMSOL study whereas measured boundary conditions from the laboratory study were used in the Delphin simulation. Furthermore, the pressure distribution graphics also showed a pressure difference at the cellulose layer which might have led to a difference in convective air transport. Regarding the results, it could be noticed that the simulated temperature results for both Delphin and COMSOL were closest to the measurement data during the under pressure phase. During the other two phases both COMSOL and Delphin underestimated the temperature results compared to the measured values. For the relative humidity the results from COMSOL and Delphin deviated more for the points at the external side of the construction (points B and D). At the internal side of the construction (points A and C) the simulated relative humidity results were closer to the measured values, but those did also not fully align. These deviations might be caused by the reduced velocity of the flow through the air gaps for the simulations as noted before.

Sensitivity analysis was performed aimed at the effect of convective moisture transport and pressure differences across the structure. Based on this analysis some conclusions can be made. Firstly, when convection is included it drastically improves the accuracy of the hygrothermal simulation results near the air gaps. Secondly, the air convection has a limited effect on the temperature results in the construction, though the laboratory measurements show a much larger effect. This might again be caused by the difference of flow velocity through the air gaps. Finally, the different pressures across the structure showed that even small pressure differences can have a large impact on the absolute humidity in the structure and a gradual increase of pressure over the structure has a decreasing effect on the convective moisture transport the further it increases.

# IX: Discussion

In this study, there are some uncertainties regarding the simulation results. One of the uncertainties is that during the period of no pressure there was still a pressure difference across the element measured of 0.9 Pa. In the laboratory study, this resulted in a flow over the element of 0 l/min whereas the model in Delphin still accounted for a flow of 0.43 l/min. The second uncertainty is the effect of reduced flow velocity through the air gaps caused by the simplification of modeling in 2D. The last uncertainty regards the findings of the laboratory study. In that study they noticed that freezing occurred in the test wall during the period of no pressure and internal over pressure. For the simulation in Delphin this freezing effect was not taken into account. The reason for this is that Delphin uses an equilibrium ice model that requires the capillary conductivity as a function of the moisture content. For the material properties only the liquid water diffusivity as a function of the moisture content was available. The effect that the ice model would have had on the results is not clear.

It should be noted that the case study considered a very permeable test wall in order to assess convective air transport. Most walls will be less permeable than the one examined in this study so the effect of convective air transport through those walls would also be lower. However, air leaks can still be a risk and this study shows that this is definitely something to keep in mind during the assessment of hygrothermal risks.

The study also shows how sensitive convection simulations can be. Small errors can have a large impact on the results of humidity in the construction. Especially when considering an hygrothermal risks this could be problematic. It is therefore also important that validated exemplary calculations become available so that it is clear what is needed to properly simulate convective moisture transport.

# X: Limitations

The original intention of the study was to model convective air transport in 3D. During the study there was chosen to make use of Delphin as the literature review showed that Delphin had these capabilities. However, the option in Delphin to build a 3D model is still very new and during the simulations it turned out that there were issues with simulating convective air transport in 3D. Because of the limited time, the choice had to be made to continue with a 2D model even though this was not preferred.

If time was not an issue then the choice to model the case study in 3D using COMSOL would have been made. In hindsight 2D modeling is definitely not enough when considering 3D air leaks. And as COMSOL is a Multiphysics program it should have been possible to model the case study in 3D. With a 3D model the results will not be influenced by the greatly reduced flow rate through the gaps and the larger surface area for the air gaps.

Continuing this convective air study it would be important to simulate more case studies with 3D modelled leaks. However, the amount of case studies is very limited as not many studies include the pressure difference across the wall as a measurement value. Therefore, research towards laboratory measurements and air convection in practice is also necessary. Another option to continue the convection study would be to examine the case in this study with a 3D model to make sure that the simulated results are improved using a 3D model. It is advisable to make use of COMSOL for the continuation. The issues regarding convection and 3D modeling in Delphin have to be resolved in order to make use of Delphin for these studies.

[1] Hall, M. R., Casey, S. P., Loveday, D. L., & Gillott, M. (2013). Analysis of UK domestic building retrofit scenarios based on the E.ON Retrofit Research House using energetic hygrothermics simulation - Energy efficiency, indoor air quality, occupant comfort, and mould growth potential. Building and Environment, 70, 48–59. https://doi.org/10.1016/j.buildenv.2013.08.015

[2] Flynn, M. A., Richman, R., Gorgolewski, M., Saunders, K., & Race, C. (2017). An Investigation into the Hygrothermal Performance of a Mineral Wool Based Externally Insulated Enclosure in a Cold Climate. Energy Procedia, 132, 345–350. https://doi.org/10.1016/j.egypro.2017.09.746

[3] Havinga, L., & Schellen, H. (2018). Applying internal insulation in post-war prefab housing: Understanding and mitigating the hygrothermal risks. Building and Environment, 144(August), 631–647. https://doi.org/10.1016/j.buildenv.2018.08.035

[4] Gradeci, K., Labonnote, N., Time, B., & Köhler, J. (2017). A probabilistic-based approach for predicting mould growth in timber building envelopes: Comparison of three mould models. Energy Procedia, 132, 393–398. https://doi.org/10.1016/j.egypro.2017.09.641

[5] Tijskens, A., Janssen, H., & Roels, S. (2017). A simplified dynamic zone model for a probabilistic assessment of hygrothermal risks in building components. Energy Procedia, 132, 717–722. https://doi.org/10.1016/j.egypro.2017.10.012

[6] Freudenberg, P., Ruisinger, U., & Stöcker, E. (2017). Calibration of Hygrothermal Simulations by the Help of a Generic Optimization Tool. Energy Procedia, 132, 405–410. https://doi.org/10.1016/j.egypro.2017.09.645

[7] Vanhoutteghem, L., Morelli, M., & Sørensen, L. S. (2017). Can crawl space temperature and moisture conditions be calculated with a whole-building hygrothermal simulation tool? Energy Procedia, 132, 688–693. https://doi.org/10.1016/j.egypro.2017.10.007

[8] Zhao, J., & Plagge, R. (2015). Characterization of hygrothermal properties of sandstones - Impact of anisotropy on their thermal and moisture behaviors. Energy and Buildings, 107, 479–494. https://doi.org/10.1016/j.enbuild.2015.08.033

[9] Knarud, J. I., & Geving, S. (2017). Comparative study of hygrothermal simulations of a masonry wall FILLIN. Energy Procedia, 132, 771–776. https://doi.org/10.1016/j.egypro.2017.10.027

[10] Silva, P. C. P., Almeida, M., Bragança, L., & Mesquita, V. (2013). Development of prefabricated retrofit module towards nearly zero energy buildings. Energy and Buildings, 56, 115–125. https://doi.org/10.1016/j.enbuild.2012.09.034

[11] Hradil, P., Toratti, T., Vesikari, E., Ferreira, M., & Häkkinen, T. (2014). Durability considerations of refurbished external walls. Construction and Building Materials, 53, 162–172. https://doi.org/10.1016/j.conbuildmat.2013.11.081

[12] Klõšeiko, P., Varda, K., & Kalamees, T. (2017). Effect of freezing and thawing on the performance of "capillary active" insulation systems: A comparison of results from climate chamber study to HAM modeling. Energy Procedia, 132, 525–530. https://doi.org/10.1016/j.egypro.2017.09.714

[13] Coupillie, C., Steeman, M., Van Den Bossche, N., & Maroy, K. (2017). Evaluating the hygrothermal performance of prefabricated timber frame façade elements used in building renovation. Energy Procedia, 132, 933–938. https://doi.org/10.1016/j.egypro.2017.09.727

[14] Zhao, J., Grunewald, J., Ruisinger, U., & Feng, S. (2017). Evaluation of capillary-active mineral insulation systems for interior retrofit solution. Building and Environment, 115, 215–227. https://doi.org/10.1016/j.buildenv.2017.01.004

[15] Bottino-Leone, D., Larcher, M., Herrera-Avellanosa, D., Haas, F., & Troi, A. (2019). Evaluation of natural-based internal insulation systems in historic buildings through a holistic approach. Energy, 181, 521–531. https://doi.org/10.1016/j.energy.2019.05.139

[16] Ferroukhi, M. Y., Belarbi, R., Limam, K., & Bosschaerts, W. (2017). Experimental validation of a HAM-BES co-simulation approach. Energy Procedia, 139, 517–523. https://doi.org/10.1016/j.egypro.2017.11.247

[17] Cascione, V., Marra, E., Zirkelbach, D., Liuzzi, S., & Stefanizzi, P. (2017). Hygrothermal analysis of technical solutions for insulating the opaque building envelope. Energy Procedia, 126, 203–210. https://doi.org/10.1016/j.egypro.2017.08.141

[18] De Mets, T., Tilmans, A., & Loncour, X. (2017). Hygrothermal assessment of internal insulation systems of brick walls through numerical simulation and full-scale laboratory testing. Energy Procedia, 132, 753–758. https://doi.org/10.1016/j.egypro.2017.10.022

[19] Pihelo, P., Kikkas, H., & Kalamees, T. (2016). Hygrothermal Performance of Highly Insulated Timber-frame External Wall. Energy Procedia, 96(October), 685–695. https://doi.org/10.1016/j.egypro.2016.09.128

[20] Ibrahim, M., Sayegh, H., Bianco, L., & Wurtz, E. (2019). Hygrothermal performance of novel internal and external super-insulating systems: In-situ experimental study and 1D/2D numerical modeling. Applied Thermal Engineering, 150(September 2018), 1306–1327. https://doi.org/10.1016/j.applthermaleng.2019.01.054

[21] Bagarić, M., Banjad Pečur, I., & Milovanović, B. (2020). Hygrothermal performance of ventilated prefabricated sandwich wall panel from recycled construction and demolition waste – A case study. Energy and Buildings, 206. https://doi.org/10.1016/j.enbuild.2019.109573

[22] Wegerer, P., & Bednar, T. (2017). Hygrothermal performance of wooden beam heads in inside insulated walls considering air flows. Energy Procedia, 132, 652–657. https://doi.org/10.1016/j.egypro.2017.09.710

[23] Ilomets, S., Kalamees, T., Lahdensivu, J., & Klõšeiko, P. (2016). Impact of ETICS on Corrosion Propagation of Concrete Facade. Energy Procedia, 96(October), 67–76. https://doi.org/10.1016/j.egypro.2016.09.101

[24] Sehizadeh, A., & Ge, H. (2016). Impact of future climates on the durability of typical residential wall assemblies retrofitted to the PassiveHaus for the Eastern Canada region. Building and Environment, 97, 111–125. https://doi.org/10.1016/j.buildenv.2015.11.032

[25] Fedorik, F., Heiskanen, R., Laukkarinen, A., & Vinha, J. (2019). Impacts of multiple refurbishment strategies on hygrothermal behaviour of basement walls. Journal of Building Engineering, 26(July), 100902. https://doi.org/10.1016/j.jobe.2019.100902

[26] Bastien, D., & Winther-Gaasvig, M. (2018). Influence of driving rain and vapour diffusion on the hygrothermal performance of a hygroscopic and permeable building envelope. Energy, 164, 288–297. https://doi.org/10.1016/j.energy.2018.07.195

[27] Zhou, X., Carmeliet, J., & Derome, D. (2018). Influence of envelope properties on interior insulation solutions for masonry walls. Building and Environment, 135(November 2017), 246–256. https://doi.org/10.1016/j.buildenv.2018.02.047

[28] Evrard, A., Flory-Celini, C., Claeys-Bruno, M., & De Herde, A. (2014). Influence of liquid absorption coefficient on hygrothermal behaviour of an existing brick wall with Lime-Hemp plaster. Building and Environment, 79, 90–100. https://doi.org/10.1016/j.buildenv.2014.04.031

[29] Pihelo, P., Lelumees, M., & Kalamees, T. (2016). Influence of Moisture Dry-out on Hygrothermal Performance of Prefabricated Modular Renovation Elements. Energy Procedia, 96(October), 745–755. https://doi.org/10.1016/j.egypro.2016.09.137

[30] Johansson, P., Geving, S., Hagentoft, C. E., Jelle, B. P., Rognvik, E., Kalagasidis, A. S., & Time, B. (2014). Interior insulation retrofit of a historical brick wall using vacuum insulation panels: Hygrothermal numerical simulations and laboratory investigations. Building and Environment, 79, 31–45. https://doi.org/10.1016/j.buildenv.2014.04.014

[31] Ibrahim, M., Bianco, L., Ibrahim, O., & Wurtz, E. (2018). Low-emissivity coating coupled with aerogel-based plaster for walls' internal surface application in buildings: Energy saving potential based on thermal comfort assessment. Journal of Building Engineering, 18(April), 454–466. https://doi.org/10.1016/j.jobe.2018.04.008

[32] Hansen, T., Peuhkuri, R. H., Møller, E. B., Bjarløv, S. P., & Odgaard, T. (2017). Material characterization models and test methods for historic building materials. Energy Procedia, 132, 315–320. https://doi.org/10.1016/j.egypro.2017.09.738

[33] Piironen, J., Vinha, J., & Kiviste, M. (2017). Modeling hygrothermal performance of roof and floor structures with an energy-efficient constant output heating. Energy Procedia, 132, 694–699. https://doi.org/10.1016/j.egypro.2017.10.008

[34] Grynning, S., Schlemminger, C., & Uvsløkk, S. (2017). Moisture robustness assessment of a window with integrated solar screen using numerical and experimental methods. Energy Procedia, 132, 381–386. https://doi.org/10.1016/j.egypro.2017.09.637

[35] Abdul Hamid, A., Wallentén, P., & Johansson, D. (2015). Moisture supply Set Point for avoidance of moisture damage in Swedish multifamily houses. Energy Procedia, 78, 901–906. https://doi.org/10.1016/j.egypro.2015.11.016

[36] Robert, W., & Piotr, K. (2017). On rehabilitation of buildings with historical façades. Energy Procedia, 132, 927–932. https://doi.org/10.1016/j.egypro.2017.09.724

[37] Paepcke, A., & Nicolai, A. (2017). Performance analysis of coupled quasi-steady state air flow calculation and dynamic simulation of hygrothermal transport inside porous materials. Energy Procedia, 132, 759–764. https://doi.org/10.1016/j.egypro.2017.10.024

[38] Arumägi, E., Pihlak, M., & Kalamees, T. (2015). Reliability of interior thermal insulation as a retrofit measure in historic wooden apartment buildings in cold climate. Energy Procedia, 78, 871–876. https://doi.org/10.1016/j.egypro.2015.11.010

[39] Zhou, X., Derome, D., & Carmeliet, J. (2016). Robust moisture reference year methodology for hygrothermal simulations. Building and Environment, 110, 23–35. https://doi.org/10.1016/j.buildenv.2016.09.021

[40] Van Schijndel, A. W. M., Goesten, S., & Schellen, H. L. (2017). Simulating the complete HAMSTAD benchmark using a single model implemented in Comsol. Energy Procedia, 132, 429–434. https://doi.org/10.1016/j.egypro.2017.09.651

[41] Wang, L., & Ge, H. (2018). Stochastic modeling of hygrothermal performance of highly insulated wood framed walls. Building and Environment, 146(July), 12–28. https://doi.org/10.1016/j.buildenv.2018.09.032

[42] Pihelo, P., & Kalamees, T. (2016). The effect of thermal transmittance of building envelope and material selection of wind barrier on moisture safety of timber frame exterior wall. Journal of Building Engineering, 6, 29–38. https://doi.org/10.1016/j.jobe.2016.02.002
[43] Havinga, L., & Schellen, H. (2019). The impact of convective vapour transport on the hygrothermal risk of the internal insulation of post-war lightweight prefab housing. Energy and Buildings, 204. https://doi.org/10.1016/j.enbuild.2019.109418
[44] Biseniece, E., Žogla, G., Kamenders, A., Purviņš, R., Kašs, K., Vanaga, R., & Blumberga, A. (2017). Thermal performance of internally insulated historic brick building in cold climate: A long term case study. Energy and Buildings, 152, 577–586. https://doi.org/10.1016/j.enbuild.2017.07.082
[45] Hema, C. M., Van Moeseke, G., Evrad, A., Courard, L., & Messan, A. (2017). Vernacular housing practices in Burkina Faso: Representative models of construction in Ouagadougou and walls hygrothermal efficiency. Energy Procedia, 122, 535–540. https://doi.org/10.1016/j.egypro.2017.07.398
[46] Bouwbesluit 2012 (2021-05-19). *Retrieved from https://www.briswarenhuis.nl/*
[47] NEN 2778:2015 Vochtwering in gebouwen. (2015-06-01). *Retrieved from https://www.briswarenhuis.nl/*
[48] Fraunhofer IBP. (n.d.). WUFI Product overview. *Retrieved from* https://wufi.de/en/software/product-overview/
[49] Bauklimatik dresden. (n.d.) 3D modeling in Delphin. *Retrieved from https://bauklimatik-dresden.de/delphin/2nd/doc/DELPHIN6_3D-Tutorial_en.pdf*
[50] Bauklimatik dresden. (n.d.) Delphin 5 manual. *Retrieved from Delphin 5 software files*
[51] COMSOL. (n.d.). COMSOL Reference manual. *Retrieved from https://doc.comsol.com/5.5/doc/com.comsol.help.comsol/COMSOL_ReferenceManual.pdf*
[52] Goesten, A. J. P. M. (2016) Hygrothermal simulation model: damage as a result of insulating historical buildings.
[53] Vinha, J, Käkelä, P. (1999). Water vapour transmission in wall structures due to diffusion and convection. Publication 103 structural engineering.
[54] Vinha, J. (2007). Hygrothermal Performance of Timber-Framed External Walls in Finnish Climatic Conditions: A method for Determining the Suffiicient Water Vapour Resistance of the Interior Lining of a Wall Assembly.
[55] Coakley, D., Raftery, P., Keane, M. (2014) A review of methods to match building energy simulation models to measured data.
[56] TRNSYS. (n.d.) Transient System Simulation Tool product information. *Retrieved from http://www.trnsys.com/index.html*
[57] Allué Hoyos, C. (2014). Applicability of COMSOL Multiphysics to combined heat, air and moisture transfer modeling in building envelopes.

APPENDIX 1

# Literature study comparison overview

| | Heat transfer method | | | Moisture transfer methods | | | |
|---|---|---|---|---|---|---|---|
| **Model** | Conduction | Convection | radiation | Convection | diffusion | capilary | driving rain |
| WUFI plus | [26] [45] | | | | [26] [45] | [26] | [26] |
| WUFI pro | [2] [17] [20] [21] [28] [31] [33] [38] | | [2] [11] [17] [20] [28] | | [2] [17] [21] [24] [28] [31] [33] [35] [38] | | [11] [17] [20] [24] [28] [31] [35] |
| WUFI 2D | [9] [30] [34] | | [30] | | [9] [30] [34] | [9] [30] | [9] [30] |
| Comsol | [9] [16] [27] [40] [43] | [3] [16] [40] [43] | [3] [27] [40] | [3] [16] [40] [43] | [9] [16] [40] [43] | [9] [16] [27] [40] | [9] [27] [40] |
| Delphin no version noted | [14] [19] [23] [29] [37] [42] [44] | [*37*] [42] | [14] | [*37*] [42] | [14] [19] [23] [29] [37] [42] [44] | [14] [19] [29] [42] [44] | [14] [23] [29] [44] |
| Delphin 5 | [8] [32] | | [8] [32] | | [8] [32] | [32] | [32] |
| Delphin 5.8 | [5] [6] [18] [25] [36] [41] [12] | | [5] | | [5] [12] [18] [25] [36] [41] | [36] | [18] [25] [36] [41] |
| Delphin 6 | [15] | | [15] | | [15] | [15] | [15] |
| Bsim | | | | | [7] | | |
| HAM4D_VIE | | | | [22] | | | |

In the overview results are only included when an article explicitly mentions a certain criterea. It is therefore possible that a study does include a criterea, but is not included in the overview as the criteria is not clearly mentioned.

Additional notes
[*6*] notes an extension for Delphin 5.8 which can simulate 3d models, but the HAM tranfer method capabilities are not reported.
[*15*] Study 21 notes that the chosen hygrothermal model used the study should include liquid water convective transport. Delphin 6 is chosen which could mean that delphin 6 includes convective moisture transport. But it is not really mentioned in the study.
[*37*] In this study heat and moisture convection is simulated in Delphin using additional air flow model
Delphin 6, Bsim and HAM4D_VIE are only represented in a single article so the overview will not be representative for the capabilities of the models

# Literature study comparison overview

| Model | HAM transfer methods | Dimension | | | Moisture buffering | |
|---|---|---|---|---|---|---|
| | Not reported | 1D | 2D | 3D | Simplified in numerical zone model | HAMBase modelled internal and partition |
| WUFI plus | [1] | [1] [26] [45] | | | | |
| WUFI pro | [10] [13] | [2] [11] [17] [20] [21] [24] [28] [31] [33] [35] | [10] [13] [20] | | | |
| WUFI 2D | [4] [13] | [4] | [9] [13] [30] [34] | | | |
| Comsol | [39] | [27] [39] [40] | [9] [16] | [3] [16] [43] | | [43] |
| Delphin no version noted | | [14] [19] [23] | [14] [29] [37] [42] [44] | | | |
| Delphin 5 | | [8] [32] | | | | |
| Delphin 5.8 | | [5] [12] [18] [25] [41] | [6] [25] [36] | [*6*] | [5] | |
| Delphin 6 | | | [15] | | | |
| Bsim | | [7] | | | | |
| HAM4D_VIE | | | | [22] | | |

# Literature study comparison overview

| | Coupled whole building simulation | | | | | |
|---|---|---|---|---|---|---|
| **Model** | Hambase | TRNSYS | WUFI | Bsim | Simplified numerical zone model | Not coupled |
| WUFI plus | | | [1] | | | [26] [45] |
| WUFI pro | | | | | | [10] [11] [13] [17] [20] [21] [24] [28] [31] [33] |
| WUFI 2D | | | | | | [4] [9] [13] [30] [34] |
| Comsol | [3] [43] | [16] | | | | [9] [27] [39] [40] |
| Delphin no version noted | | | | | | [14] [19] [23] [29] [37] [42] [44] |
| Delphin 5 | | | | | | [8] [32] |
| Delphin 5.8 | | | | | [5] | [6] [12] [18] [25] [36] [41] |
| Delphin 6 | | | | | | [15] |
| Bsim | | | | [7] | | |
| HAM4D_VIE | | | | | | [22] |

# Literature study comparison overview

| | Moisture analysis | | | Risk assessment | | | |
|---|---|---|---|---|---|---|---|
| **Model** | RH | Moisture content | Not reported | Mold growth model WUFI BIO | Mold growth model isopleth system | Mold growth method VTT model, MRD model, | Mold growth model Viitanen |
| WUFI plus | [1] [26] [45] | [1] [26] | | [1] | | | |
| WUFI pro | [10] [11] [13] [17] [20] [21] [28] [31] [33] [35] | [2] [10] [13] [17] [24] [28] | | | | [13] [20] | [11] |
| WUFI 2D | [9] [13] [30] [34] | [9] [13] [30] [34] | [4] | | | [4] [13] | |
| Comsol | [3] [9] [16] [27] [39] [40] [43] | [9] [27] [40] | | | [3] | | |
| Delphin no version noted | [14] [19] [23] [29] [42] [44] | [14] [29] | [37] | | [14] | | |
| Delphin 5 | [32] | [8] | | | | | |
| Delphin 5.8 | [5] [6] [12] [18] [25] [36] | [5] [12] [18] [36] [41] | | | | | |
| Delphin 6 | [15] | [15] | | | | | |
| Bsim | [7] | [7] | | | | | |
| HAM4D_VIE | [22] | | | | | | |

# Literature study comparison overview

| | Risk assessment | | | | | | |
|---|---|---|---|---|---|---|---|
| **Model** | Condensation | Based on relative humidity and | Moisture accumulation | Freeze-thaw assessment | Time of wetness TOW criterea by Viitanen | Corrosion propagation model | Not reported |
| WUFI plus | | [26] | | | | | [45] |
| WUFI pro | [2] [17] [20] | [20] [21] [24] [31] [33] [35] [38] | [10] [24] [28] | | [13] | | |
| WUFI 2D | | [34] | [9] | [30] | [13] | | |
| Comsol | [3] | [27] [39] | [9] | | | | [16] [40] [43] |
| Delphin no version noted | | [19] [29] [42] [44] | | [14] [44] | | [23] | [37] |
| Delphin 5 | | [32] | | | | | [8] |
| Delphin 5.8 | [6] | [18] [25] [41] | [36] | [12] | | | [5] |
| Delphin 6 | | [15] | | | | | |
| Bsim | | [7] | | | | | |
| HAM4D_VIE | | [22] | | | | | |

APPENDIX 2 Material properties

| Property | | Unit | Porous wooden fiberboard | Cellulose insulation | Building paper | Air gap |
|---|---|---|---|---|---|---|
| Density | ρ | kg/m$^3$ | 270 | 37 | 750 | 1,3 |
| Specific heat capacity | c | J/(kgK) | 1500 | 2000 | 1500 | 1050 |
| Open porosity | $\theta_{por}$ | m$^3$/m$^3$ | 0,85 | 0,97 | 0,6 | 1 |
| Effective saturation moisture content | $\theta_{eff}$ | m$^3$/m$^3$ | 0,21 | 0,43 | - | 1 |
| Hygroscopic moisture content at 80 % Relative humidity | $\theta_{80}$ | m$^3$/m$^3$ | 0,0366 | 0,0061 | - | 1e-5 |
| Thermal conductivity of dry material | λ | W/(mK) | 0,055 | 0,041 | 0,12 | 0,067 |
| Water uptake coefficient | $A_w$ | kg/(m$^2$s$^{1/2}$) | 0,004 | 0,074 | - | 1e-7 |
| Water vapor diffusion resistance factor | μ | - | 5,5 | 1,3 | 23 | 1 |
| Liquid water diffusivity at effective saturation | $D_{l;eff}$ | m$^2$/s | 1,38e-9 | 1,07e-7 | - | - |
| Air permeability of dry material | $K_g$ | kg/(msPa) | 3,888e-7 | 2,83e-4 | - | *1,7e-5* |

*The air permeability of the air gap was not measured in the laboratory studies, but determined in simulations. Using this value the flow through the simulated element matched with the flow measured in the laboratory study. Note paragraph V – III Model simplification for further explanation.

| Sorption curve | Moisture content | m$^3$/m$^3$ |
|---|---|---|
| Relative humidity RH | Porous wooden fiberboard | Cellulose insulation |
| 0 | 0 | 0 |
| 0,33 | 0,0124 | 0,0019 |
| 0,55 | 0,0196 | 0,0031 |
| 0,65 | 0,0224 | 0,004 |
| 0,75 | 0,0252 | 0,0048 |
| 0,80 | 0,0336 | 0,0061 |
| 0,83 | 0,0387 | 0,0068 |
| 0,86 | 0,0459 | 0,0086 |
| 0,93 | 0,0627 | 0,0129 |
| 0,97 | 0,0713 | 0,0152 |
| 1 | 0,21 | 0,43 |

| Liquid moisture diffusivity | log10($m^2/s$) |
|---|---|
| Moisture content $m^3/m^3$ | Porous wooden fiberboard |
| 0,0336 | -11,3799 |
| 0,21 | -8,86012 |

| Liquid moisture diffusivity | log10($m^2/s$) |
|---|---|
| Moisture content $m^3/m^3$ | Cellulose insulation |
| 0,0061 | -9,92812 |
| 0,43 | -6,97062 |

| Thermal conductivity function | Porous wooden fiberboard | | Cellulose insulation |
|---|---|---|---|
| Moisture content | Thermal conductivity W/(mK) | Moisture content | Thermal conductivity |
| 0 | 0,048 | 0 | 0,038 |
| 0,0124 | 0,049 | 0,0019 | 0,038 |
| 0,0224 | 0,05 | 0,004 | 0,038 |
| 0,0459 | 0,052 | 0,0086 | 0,039 |
| 0,0713 | 0,055 | 0,0152 | 0,042 |
| 0,21 | 0,6 | 0,43 | 0,6 |